

Virus Inactivation by Homogeneous and Heterogeneous Fenton-like Processes

THÈSE N° 5295 (2012)

PRÉSENTÉE LE 20 AVRIL 2012

À LA FACULTÉ DE L'ENVIRONNEMENT NATUREL, ARCHITECTURAL ET CONSTRUIT
LABORATOIRE DE CHIMIE ENVIRONNEMENTALE
PROGRAMME DOCTORAL EN ENVIRONNEMENT

ÉCOLE POLYTECHNIQUE FÉDÉRALE DE LAUSANNE

POUR L'OBTENTION DU GRADE DE DOCTEUR ÈS SCIENCES

PAR

Jessica Ivana NIETO JUAREZ

acceptée sur proposition du jury:

Prof. F. Golay, président du jury
Prof. T. Kohn, directrice de thèse
Prof. K. McNeill, rapporteur
Dr A. Sienkiewicz, rapporteur
Prof. V. Slaveykova, rapporteur



ÉCOLE POLYTECHNIQUE
FÉDÉRALE DE LAUSANNE

Suisse
2012

Acknowledgements

This thesis was carried out in the Laboratory of Environmental Chemistry (LCE) at the EPFL and supported by Swiss National Science Foundation (Project No. 200021-118077 and 200020-131918).

I would like to express my gratitude to several people. First of all, to Tamar Kohn, my advisor who has always supported me. Her patience, help, scientific discussions and guidance during thesis have been fundamental for the good development of my work. From her I learned a lot and I am deeply grateful.

To the reviewers of the thesis, Prof. Andrzej Sienkiewicz, Prof. Kristopher McNeill and Prof. Vera Slaveykova and Prof. Francois Golay, president of jury, for accepting to read and evaluate my work.

To Isabelle Worms, for performing the aFIFFF-ICP-MS measurements in Chapter 2.

To Laurin Wissmeier, for the assistance with PHREEQC-2 in Chapter 2.

To Katarzyna Pierzchała and Andrzej Sienkiewicz for their collaboration in the quantitative determination of HO• production in the homogeneous Fenton-like processes by Electronic Spin Resonance (ESR) measurements in Chapter 2.

To Brian Pecson and Thérèse Sigstam, for performing the quantitative Polymerase Chain Reaction (qPCR) measurements in Chapter 3.

To Michael Stuer and Dr. Paul Bowen for performing the isoelectric points (IEP) measurements of iron particles by AcoustoSizer II in Chapter 3.

To Thérèse Sigstam, for performing the protein mass spectrometry measurements by MALDI-TOF-MS in Chapter 4.

To Karine Maritz, for her support in administrative and logistics affairs during my stay in the group, and for her enthusiasm and good humor.

Acknowledgements

To Julien Omilien and Karine Maritz, for reading and correcting my thesis's summary in French and friendship.

To all my friends, in particular, Paula Osorio, María Laura Molina and her husband Julian Rengifo, Fanny Della Puppa and her husband Claudio, Cara Tobin and her husband William, Amalin Sad and her husband Eric, Lucía Perez and her husband Marco, Laetitia Grosjean, Dalila Ellafi, Lisbeth Suarez, Marie Vasquez, Otoniel Carranza, Sandra Angarita, Pilar Gomis and Pedro Bandim, for their supporting in the daily work and life, and friendship.

Finally, to my lovely parents: Gonzalo and Irma, my exceptional siblings: Kelly, Hector and Gary, my beautiful nephews: David and Carolina, and all my wonderful family, for the continuous support, confidence and love; without these key individuals this thesis would not have been possible.

J. N.

Summary

Human enteric viruses in water sources cause a great public health risk. Conventional disinfection treatments are not able to completely inactivate viruses. However, advanced oxidation processes (AOPs) have recently been shown to effectively inactivate pathogens. One of the most promising AOPs is the Fenton process.

In the framework of this work, the main objective was to characterize the fate of viruses upon inactivation by homogeneous and heterogeneous Fenton and Fenton-like processes, as well as to elucidate the mechanisms governing virus inactivation by these processes. MS2 coliphage, a commonly used surrogate for human enteric viruses, was used as the model organism.

Virus inactivation by homogeneous, Cu- or Fe-catalyzed Fenton(-like) reactions, were studied at neutral pH. The effect of the metal (1-10 μM) and H_2O_2 (3-50 μM) concentrations, HO^\bullet production and sunlight on virus inactivation was investigated. Virus inactivation followed first-order kinetic with respect to the H_2O_2 concentration for both treatments. The influence of the metal concentrations was more complex. For the Cu/ H_2O_2 system, it was found that inactivation was governed by soluble Cu. In contrast, for the Fe/ H_2O_2 system, the colloidal Fe was involved in inactivation rather than dissolved iron. Sunlight only affected the Fe/ H_2O_2 system. HO^\bullet production rates measured by electron spin resonance (ESR), could not account for the observed inactivation in Fe/ H_2O_2 system. Other oxidants, such as ferryl species, must therefore play a role. Overall, our results have shown that virus inactivation by Cu- and Fe- catalyzed Fenton reaction may serve as an efficient disinfection method.

Virus inactivation by the heterogeneous Fenton process was carried out via iron(hydr)oxide particles, such as hematite ($\alpha\text{-Fe}_2\text{O}_3$), goethite ($\alpha\text{-FeOOH}$), magnetite (Fe_3O_4) and amorphous iron ($\text{Fe}(\text{OH})_3$), in batch reactors at circumneutral pH. The influence of adsorption and sunlight exposure on the survival of MS2 was investigated. Both mass-based and surface-area normalized pseudo-second order adsorption rate constants followed the same trend of $\alpha\text{-FeOOH} > \alpha\text{-Fe}_2\text{O}_3 > \text{Fe}_3\text{O}_4 \approx \text{Fe}(\text{OH})_3$. Virus adsorption onto all particles was only partly reversible. In addition to irreversible adsorption, adsorption to three of the particles studied ($\alpha\text{-FeOOH}$, Fe_3O_4 , $\text{Fe}(\text{OH})_3$) caused slight virus inactivation (85%, 77%, 97%, respectively). Exposure of particle-adsorbed viruses

to sunlight and H_2O_2 resulted in efficient inactivation, whereas inactivation was negligible for suspended viruses. The observed first-order inactivation rate constants were 1.44×10^{-3} , 1.09×10^{-3} , 0,58, 1.48 min^{-1} for $\alpha\text{-Fe}_2\text{O}_3$, $\alpha\text{-FeOOH}$, Fe_3O_4 and $\text{Fe}(\text{OH})_3$, respectively. Our results showed that in the heterogeneous Fenton system, inactivation was mainly attributed to a particle-mediated photo-Fenton-like reaction.

Finally, the extent of genome and protein damage of MS2 coliphage during inactivation by the homogeneous $\text{Cu}/\text{H}_2\text{O}_2$ and $\text{Fe}/\text{H}_2\text{O}_2$ /sunlight systems were studied. The results showed that both damage to the genome and the capsid protein may contribute on virus inactivation by both treatments. The patterns of damage were different, even though the same oxidant (HO^\bullet) was present in both systems, indicating the source of the oxidant is important. For the Cu system, the extent of genome damage was similar to that of inactivation, indicating that inactivation may occur via single-hit kinetics. In contrast, for the Fe system, genome damage was very extensive in comparison to inactivation, consistent with multi-hit inactivation kinetics. For both systems, the most susceptible region of the capsid protein was peptide segment 84-106, which is located on the capsid outer surface. The other regions of the protein are not likely to be involved in inactivation. Overall, our findings suggested that both genome and protein oxidation by Cu and Fe systems may play a role in inactivation, and that the determination of molecular-level mechanisms governing inactivation can be assessed by MALDI-TOF-MS and qPCR.

Keywords: *Advanced oxidation processes, virus disinfection, homogeneous Fenton process, heterogeneous Fenton process, sunlight, genome damage, protein oxidation*

Résumé

Les virus entériques humains dans les sources d'eau provoquent un grand risque pour la santé publique. Les traitements de désinfection conventionnels ne sont pas capables d'inactiver complètement les virus. Cependant, les procédés d'oxydation avancée (POA) ont récemment montré leurs capacités à inactiver efficacement les agents pathogènes. Le plus prometteur POA est le procédé Fenton.

Dans le cadre de ce travail, l'objectif principal était de caractériser le devenir des virus sur l'inactivation par les procédés Fenton et type-Fenton homogènes et hétérogènes, ainsi que d'élucider les mécanismes qui régissent l'inactivation des virus par ces procédés. Le coliphage MS2, un substitut usuellement utilisé pour les virus entériques humains, a été utilisé comme organisme modèle.

L'inactivation du virus par les processus (de type-) Fenton homogènes catalysés par Cu et Fe ont été étudiés à pH neutre. L'effet des concentrations du métal (1-10 μM) et du peroxyde d'hydrogène (H_2O_2 ; 3-50 μM), la production des HO^\bullet et la lumière solaire sur l'inactivation du virus ont été étudiés. Les résultats ont montré que l'inactivation du virus suit un modèle cinétique de premier ordre pour ce qui est de la concentration de H_2O_2 pour les deux traitements. L'influence des concentrations de métaux était plus complexe. Pour le système Cu/ H_2O_2 , il a été constaté que l'inactivation a été régie par le Cu soluble. Par contre, pour le système Fe/ H_2O_2 , le fer colloïdal est impliqué dans l'inactivation contrairement au fer dissous. La lumière solaire a seulement affecté le système Fe/ H_2O_2 . Les taux de production des HO^\bullet mesurés par résonance de spin électronique (RSE), ne pouvaient pas tenir compte de l'inactivation observée dans le système Fe/ H_2O_2 . D'autres oxydants, comme les espèces ferryl, doivent par conséquent jouer un rôle. Globalement, nos résultats ont montré que l'inactivation du virus par la réaction catalysée par Cu et Fe peut servir comme une méthode de désinfection efficace.

L'inactivation du virus par le procédé Fenton hétérogène a été effectuée par des particules d'(hydr-)oxyde de fer, telles que l'hématite ($\alpha\text{-Fe}_2\text{O}_3$), la goethite ($\alpha\text{-FeOOH}$), la magnétite (Fe_3O_4) et le fer amorphe ($\text{Fe}(\text{OH})_3$), dans les réacteurs discontinus à des pH proches de la neutralité. L'influence de l'adsorption et l'exposition à la lumière solaire sur la survie des coliphages MS2 ont été étudiées. Quelles soient basées sur la masse ou la surface normalisée, les constantes de vitesse de pseudo-deuxième ordre d'adsorption

ont suivi la même tendance: $\alpha\text{-FeOOH} > \alpha\text{-Fe}_2\text{O}_3 > \text{Fe}_3\text{O}_4 \approx \text{Fe}(\text{OH})_3$. L'adsorption de virus sur les particules n'a été que partiellement réversible. En plus de l'adsorption irréversible, l'adsorption de trois des particules étudiées ($\alpha\text{-FeOOH}$, Fe_3O_4 , $\text{Fe}(\text{OH})_3$) a produit une légère inactivation des virus (85%, 77%, 97%, respectivement). L'exposition des virus adsorbés sur les particules de la lumière solaire et du peroxyde d'hydrogène (H_2O_2) a conduit à une inactivation efficace, alors que l'inactivation des virus a été négligeable en suspension. Les constantes de vitesse d'inactivation de premier ordre observées étaient 1.44×10^{-3} , 1.09×10^{-3} , 0,58, 1.48 min^{-1} pour $\alpha\text{-Fe}_2\text{O}_3$, $\alpha\text{-FeOOH}$, Fe_3O_4 et $\text{Fe}(\text{OH})_3$ respectivement. Nos résultats ont montré que dans les systèmes Fenton hétérogènes, l'inactivation était principalement attribuée aux particules qui produisent la réaction photo-type-Fenton.

Enfin, l'étendue des dommages du génome et de la protéine du coliphage MS2 pendant l'inactivation a été étudiée par les systèmes homogènes $\text{Cu}/\text{H}_2\text{O}_2$ et $\text{Fe}/\text{H}_2\text{O}_2$ /lumière solaire. Les résultats ont démontré que les dommages du génome et de la protéine de capsid pouvaient contribuer à l'inactivation du virus par les deux traitements. Les types de dommages ont été différentes, même si le même oxydant ($\text{HO}\bullet$) était présent dans les deux systèmes, indiquant que la source de l'oxydant est importante. Pour le système Cu , l'étendue des dommages du génome a été similaire à celui de l'inactivation, indiquant que l'inactivation pourrait se produire par cinétique single-hit. Par contre, pour le système Fe , le dommage du génome était très étendu en comparaison à l'inactivation générée par la cinétique d'inactivation multi-hit. Pour les deux systèmes, la région la plus vulnérable de la protéine de la capsid du virus a été le segment peptidique 84-106, qui est situé sur la surface externe de la capsid du virus. Les autres régions de la protéine ne sont pas susceptibles d'être impliquées dans l'inactivation. Globalement, nos résultats ont suggéré que les deux oxydations du génome et de la protéine par les systèmes Fe et Cu pourraient jouer un rôle dans l'inactivation. Ainsi la détermination des mécanismes au niveau moléculaire en régissant l'inactivation pourrait être évaluée par MALDI-TOF-MS et qPCR.

Mots clés: *Procédés d'oxydation avancée, désinfection des virus, processus de Fenton homogène, processus de Fenton hétérogène, lumière solaire, dommage du génome, oxydation de la protéine.*

Contents

Acknowledgements	i
Summary	iii
Résumé	v
Contents	vii
List of Symbols	x
List of Figures	xii
List of Tables	xv
1 Introduction	1
1.1 Rationale	1
1.2 Background	3
1.2.1 Enteric waterborne viruses and coliphages as their surrogates	3
1.2.2 Advanced oxidation processes	5
1.2.3 Fenton process	5
1.2.4 Effect of the Fenton reaction on biological systems	9
1.3 Knowledge gaps	10
1.4 Objectives and hypotheses	10
Bibliography	13
2 Inactivation of MS2 coliphage in Fenton and Fenton-like systems: influence of transition metals, hydrogen peroxide and sunlight	18
2.1 Introduction	18
2.2 Experimental section	20
2.2.1 Reagents and Organisms	20
2.2.2 Phage quantification	21
2.2.3 Experimental setup	21
2.2.4 Inactivation experiments	21
2.2.5 Electron spin resonance (ESR) measurements	22

2.2.6	Asymmetrical Flow Field-Flow Fractionation connected to inductively coupled plasma/mass spectrometry (aFIFFF-ICP-MS) analyses	23
2.2.7	Metal solubility calculations	23
2.2.8	Data analysis	23
2.3	Results and Discussion	24
2.3.1	Effect of H ₂ O ₂	25
2.3.2	Effect of metal concentrations	27
2.3.3	Dependence of inactivation on HO• production	30
2.3.4	Influence of sunlight	34
2.4	Conclusions	38
	Bibliography	39
3	Virus removal and inactivation by heterogeneous Fenton-like processes under sunlight and in the dark	43
3.1	Introduction	43
3.2	Experimental Section	45
3.2.1	Reagents and Organisms	45
3.2.2	Virus adsorption experiments	46
3.2.3	Adsorption-mediated inactivation experiments	47
3.2.4	(Photo-) Fenton-mediated inactivation experiments	47
3.2.5	Light screening correction and surface area normalization	48
3.3	Results and Discussion	49
3.3.1	Virus adsorption onto iron particles	49
3.3.2	Contribution of virus adsorption to inactivation	53
3.3.3	Contribution of the heterogeneous (photo-)Fenton-like process to virus inactivation	54
3.3.4	Importance of adsorption in the Fenton-mediated inactivation process	58
3.4	Conclusions	59
	Bibliography	60
4	Protein and genome damage in MS2 coliphage upon inactivation by Fenton like-systems	64
4.1	Introduction	64
4.2	Experimental Section	66
4.2.1	Reagents and Organisms	66
4.2.2	Inactivation experiments	67
4.2.3	Measurements of genome damage by qPCR	67
4.2.4	Measurements of protein damage by MALDI-TOF-MS	68
4.3	Results and Discussion	72
4.3.1	MS2 genome damage upon virus inactivation	72
4.3.2	MS2 protein damage upon virus inactivation	76
4.4	Conclusions	81

Bibliography	82
5 General conclusions and perspectives	85
Curriculum Vitae	88

List of Symbols

q_t	Adsorption capacity at any time
k_e	Adsorption rate constant
AOP	Advanced oxidation process
aFIFFF	Asymmetrical Flow-Field-Flow Fractionation
$\alpha_{(\lambda)}$	Absorbance of the suspension at each wavelength (λ)
BEEF solution	Solution of beef extract and glycine
BET surface area	Brunauer-Emmett-Teller surface area
CBS	Carbonate-buffered saline
DB	Dilution buffer
DMPO	5,5,-dimethylpyrroline N-oxide
EDTA	Ethylenediaminetetraacetic acid
ESR	Electron spin resonance
r_{OH}	Hydroxyl radical production rate
ICP	Inductively coupled plasma
ID	Inside diameter
IEP	Isoelectric point
k_{obs}^o	Light screening corrected rate constant
LB	Liquid broth

LMCT	Ligand-to-metal charge transfer
MALDI	Matrix-Assisted Laser Desorption/Ionisation
q_e	Maximum adsorption capacity
MCO	Metal catalyzed oxidation
MOI	Multiplicity of infection
MS	Mass spectrometry
k_{obs}	Observed rate constant
OD	Outside diameter
PFU	Plaque forming units
qPCR	Quantitative polymerase chain reaction
ROS	Reactive oxygen species
k_{obs}^1	Surface area normalized rate constant
ρ_a	Surface concentration
SF	Screening factor
TOF	Time-of-flight
z	Total depth of irradiated solution

List of Figures

1.1	Images of capsid protein for the a) Poliovirus; b) Echovirus; c) Coxsackievirus; d) Adenovirus and e) Hepatitis B virus.	4
1.2	Generation of HO• radicals by different advanced oxidation processes (AOPs).	6
1.3	Proposed mechanism for the hydrogen peroxide activation by Cu(II) [48]. L=glycine, alanine or lysine.	10
2.1	MS2 inactivation by Cu- and Fe- catalyzed Fenton process in CBS (0.1 mM NaHCO ₃ , 15 mM NaCl, pH= 6.8). Initial MS2= 10 ⁷ PFU mL ⁻¹ , metal concentrations= 1.0 μM, H ₂ O ₂ = 50 μM. The plots correspond to: Cu (hollow blue circle), Fe (hollow red square), H ₂ O ₂ + 0.1 μM EDTA (hollow black triangle), Cu + H ₂ O ₂ (solid blue circle), Fe+H ₂ O ₂ (solid red square).	25
2.2	Effect of H ₂ O ₂ concentration activated by (a)1 μM Cu(II) and (b) 1 μM Fe(III) on MS2 inactivation in bicarbonate-buffered saline. MS2= 10 ⁷ PFU mL ⁻¹ in CBS, pH= 6.8. Solid lines correspond to linear regression fits, and yielded the following regression parameters: $k_{obs(Cu)} = 1.6 \times 10^{-2} [H_2O_2] - 0.022$; $k_{obs(Fe)} = 5.6 \times 10^{-3} [H_2O_2] + 0.005$	26
2.3	Effect of (a) Cu(II) and (b) Fe(III) concentration on MS2 inactivation in the presence of 50 μM H ₂ O ₂ . Initial MS2 concentration= 10 ⁷ PFU mL ⁻¹ in CBS, pH= 6.8.	28
2.4	Solubility of (a) Cu(II) and (b) Fe (III) in bicarbonate-buffered saline solution at pH 6.8 modelled by PHREEQC-2.	29
2.5	Separation of MS2-adsorbed Cu from free Cu by FFF-ICP-MS. MS2 phage was detected by UV absorbance at 280 nm and coincided with the ICP-MS peaks shown in the graph. Changes in the Cu content were recorded by ICP-MS in counts per second (CPS). MS2= 2×10 ¹¹ PFU mL ⁻¹ in CBS, pH= 6.8. The small peak in the virus-free control with 10 μM Cu is indicative of the presence of Cu colloids.	30
2.6	ESR-measured formation of hydroxyl radicals (HO•) in the presence of 50 μM H ₂ O ₂ and different concentrations of (a) Cu(II) and (b) Fe(III) in CBS.	31

2.7	MS2 inactivation in the presence and absence of the hydroxyl radical and ferryl scavenger ethanol. (a) Cu/H ₂ O ₂ system without (hollow blue circle) and with (solid blue circle) ethanol; (b) Fe/H ₂ O ₂ without (hollow red square) and with (solid red square) ethanol. MS2= 10 ⁷ PFU mL ⁻¹ in CBS, metal concentrations= 2.0 μM, H ₂ O ₂ = 50 μM, ethanol= 10 mM, pH= 6.8.	34
2.8	Effect of the sunlight on (a) MS2 inactivation and (b) ESR-measured formation of hydroxyl radicals (HO•) in the presence of 50 μM H ₂ O ₂ and different concentrations of Fe(III). MS2= 10 ⁷ PFU mL ⁻¹ in CBS, pH= 6.8, I= 300 W m ⁻² for MS2 inactivation, I= 10 mW cm ⁻² (UVA) for HO• production	36
2.9	First-order inactivation rate constants measured for 1 and 10 μM Fe alone (simple bars) and in the presence of H ₂ O ₂ (lined bars), in the dark (white) and under sunlight (grey). MS2= 10 ⁷ PFU mL ⁻¹ in CBS, H ₂ O ₂ = 50 μM, pH= 6.8.	37
2.10	Scheme illustrating the inactivation of MS2 by (a) Cu- and Fe-catalyzed Fenton system in the dark, and by (b) Fe-catalyzed Fenton system under sunlight. Inactivation involves virus interactions with Cu ions and Fe colloids. Oxidants are produced from metal in close vicinity to the virus. In the Fe/H ₂ O ₂ system, ferryl ions dominate inactivation in the dark, whereas sunlight enhances production and contribution of HO•.	37
3.1	Absorbance spectra of the different iron (hydr-)oxide particles suspended in CBS. Spectra were obtained by UV/VIS spectrophotometer with an integrating sphere kit. Iron (hydr-)oxides= 200 mg L ⁻¹ , CBS buffer= 0.1 mM NaHCO ₃ +15 mM NaCl, pH= 6.9 (α-Fe ₂ O ₃ , α-FeOOH) and 6.4 (Fe ₃ O ₄ , Fe(OH) ₃).	49
3.2	(a) Concentration of infective suspended MS2 and (b) adsorbed MS2 as a function of time. MS2= 10 ⁷ PFU mL ⁻¹ , iron (hydr-)oxide particles= 200 mg L ⁻¹ , CBS buffer= 0.1 mM NaHCO ₃ +15 mM NaCl, stirring= 430 rpm.	51
3.3	Comparison of total virus loss from solution, loss attributable to irreversible adsorption and loss attributable to inactivation. MS2= 10 ⁷ PFU mL ⁻¹ , CBS buffer= 0.1 mM NaHCO ₃ +15 mM NaCl, BEEF solution= 3% beef extract+0.5 M glycine, pH= 6.9 (α-Fe ₂ O ₃ , α-FeOOH) and 6.4 (Fe ₃ O ₄ , Fe(OH) ₃), stirring= 430 rpm.	54
3.4	Figure MS2 inactivation by iron (hydr-)oxide particles in the presence and absence of sunlight and H ₂ O ₂ . (a) hematite, (b) goethite, (c) amorphous Fe(III) hydroxide and (d) magnetite. MS2= 10 ⁷ PFU mL ⁻¹ , Fe-bearing particles= 200 mg L ⁻¹ , H ₂ O ₂ = 50 μM, BEEF solution= 3% beef extract+0.5 M glycine, CBS buffer= 0.1 mM NaHCO ₃ +15 mM NaCl, pH= 6.9, irradiance= 320 W m ⁻² , stirring= 430 rpm.	57

4.1	MS2 inactivation by Cu(II)/H ₂ O ₂ and Fe(III)/H ₂ O ₂ /sunlight systems. Initial infective MS2 concentration= 10 ¹⁰ PFU mL ⁻¹ , metals= 10 μM, H ₂ O ₂ = 50 μM, EDTA= 2 μM, stirring= 400 rpm, I= 320 W m ⁻²	72
4.2	Damage to individual MS2 genome segments at different levels of inactivation for (a) Cu/H ₂ O ₂ system and (b) Fe/H ₂ O ₂ /sunlight system. Error bars represent the standard deviation of the triplicate samples	74
4.3	Comparison of the fractions of undamaged genome (N/N _o) and infectivity (C/C _o) for (a) Cu/H ₂ O ₂ and (b) Fe/H ₂ O ₂ /sunlight systems.	76
4.4	(a) Mass spectrum of native MS2 and labeled MS2 of capsid protein (1:1; t=0) by positive linear mode MALDI-TOF-MS analysis. (b) Sodium adduct peak.	77
4.5	Analysis of MS2 capsid protein damage in the full protein (FP) and peptides for (a) the Cu/H ₂ O ₂ system and (b) the Fe/H ₂ O ₂ /sunlight system. Error bars represent the standard deviation of triplicate samples.	80

List of Tables

1.1	List of waterborne viruses and their main physical and molecular properties	3
1.2	Physical and molecular characteristics of MS2 coliphage	5
3.1	Chemical formula, BET surface area and isoelectric point (IEP) of the particles investigated.	46
3.2	Fitted kinetic parameters of the MS2 adsorption onto iron particles evaluated from the pseudo-second order kinetic model expressed in mass and surface units.	52
3.3	Light screening corrected and surface area normalized pseudo-first order inactivation rate constants by particles-catalyzed photo-Fenton-like process.	58
4.1	Genome primer sets and segment sizes used upon the quantification of MS2 genome damage levels.	69
4.2	Amino acid sequence of the MS2 capsid protein.	70
4.3	Peptides generated by the protease enzymes of MS2 capsid protein.	71

Chapter 1

Introduction

1.1 Rationale

The spread of human enteric viruses in the different aquatic environments poses a threat to public health in both industrialized and developing countries [1–4]. They cause various types of diseases including gastroenteritis, hepatitis, encephalitis, meningitis [5, 6]. For example, rotaviruses cause more than 140 million cases of gastroenteritis in children, of which 600,000 to 800,000 die every year. This represents approximately 5% of deaths in children worldwide [7]. In addition, viruses are often more resistant to conventional disinfection methods in comparison with other pathogens [8, 9]. Effective and appropriate treatment practices are therefore needed. A promising alternative to ensure microbial water quality and public health safety is the application of advanced oxidation processes (AOP), such as the Fenton process. *In this thesis, the feasibility of Fenton and Fenton-like processes to inactivate viruses was assessed.*

The presence of viruses in water sources is due to contamination by raw or insufficiently treated sewage [10–12]. In industrialized countries, waterborne viruses are frequently detected in source water for drinking water production [13, 14], as well as in recreational waters [11]. However, this problem is even more significant in developing countries, due to the lack of access to sanitation in rural and peri-urban regions as well as the inefficient disinfection treatments often applied in urban regions [1, 2, 15]. In addition, current water disinfection methods, such as chlorination and ozonation, can generate disinfection by-products (DBPs) with carcinogenic and mutagenic potential [16, 17]. The proper treatment of water contaminated by enteric viruses therefore remains a remarkable challenge.

Advanced oxidation processes (AOPs) have emerged as an alternative method for water disinfection. They have recently been shown to efficiently inactivate pathogens [18–20].

One of the most promising AOP is the homogeneous Fenton process. This process is based on the reaction of H_2O_2 and dissolved Fe(II) ions, which leads to the formation of highly oxidizing species capable of inactivating viruses. Besides, the Fenton process can also take place in natural systems, due to the presence of both dissolved iron ions and H_2O_2 . It is well known that oxidative processes lead to pathogen disinfection in natural water [21, 22]. The Fenton process may thus contribute to the disinfection of pathogens by naturally occurring oxidative processes. However, data pertaining to virus disinfection by the homogeneous Fenton reaction remain scarce.

A promising alternative to the homogeneous Fenton treatment is the heterogeneous Fenton-like process, which uses iron-bearing particles as the source of reactive iron. It is known that the viruses are frequently attached to solid surfaces in natural waters and wastewaters [4, 23, 24]. Several studies have reported the effectiveness of iron (hydr-)oxide particles to remove waterborne virus from the solution phase, with their consequent inactivation as assumption [25, 26]. A recent study has demonstrated that zerovalent Fe particle caused inactivation of MS2 coliphage [27]. However, very little is known about the inactivation of viruses adsorbed onto iron (hydr-)oxide particles. In addition to serving as an adsorbent, iron (hydr-)oxide particles can also catalyze the Fenton reaction. Several groups have found that hematite, goethite, magnetite and ferrihydrite catalyze the oxidation of chemical pollutants by H_2O_2 over a range of pH from 3 to 7 [28–33]. These iron (hydr-)oxide particles are of great interest due to their high relative abundance in different water sources, and their formation during the coagulation step in water treatment. To date, the role of iron(hydr-)oxide particles with respect to the control of waterborne viruses by adsorption, Fenton process, or both, is not well understood.

Sunlight has been demonstrated markedly accelerate the Fenton reaction due to the additional production of highly oxidizing species (of HO^\bullet). It may contribute to virus inactivation in different aquatic environment by both homogeneous and heterogeneous processes. However to date, the effect of sunlight on the virus inactivation via Fenton and Fenton-like processes has not been addressed.

The focus of this thesis was to study the fate of virus in the homogeneous and heterogeneous Fenton processes, in the dark and under sunlight at neutral pH, and to characterize the molecular mechanisms that lead the inactivation.

1.2 Background

1.2.1 Enteric waterborne viruses and coliphages as their surrogates

Enteric viruses are small microorganisms, often of pathogenic nature, that reproduce within the cells of a host organism. Each virus contains a single type of nucleic acid (single- or double-stranded DNA or RNA) which is enclosed by a protein shell called capsid. Viruses may be present in human or animal waste, and they spread through the contaminated water. They are very small; their size ranges from 20 to 85 nm in diameter. The enteric viruses most commonly detected in drinking and recreational waters include rotaviruses, adenoviruses, hepatitis viruses and enteroviruses (such as Coxsackieviruses, Echoviruses, Polioviruses, among others). They can cause a variety of diseases, ranging from mild diarrhoea and respiratory infections to more severe illness such as hepatitis and polio. The characteristics of the most important waterborne viruses and diseases that they can cause, as well as its main physical and molecular properties are shown in Table 1.1. Images of coat protein of enteric viruses were obtained from VIPERdb website, which are shown in Figure 1.1.

Table 1.1: List of waterborne viruses and their main physical and molecular properties [34].

Enteric viruses	Diseases [2]	Size diameter (nm)	IEP	Genome type
Adenoviruses	Infection of respiratory and gastrointestinal illness	60 - 80	n.d. [8]	ds DNA
Rotaviruses	Gastroentiritis	70	3.9	dsRNA
Hepatitis A	Liver infection	27	2.8	ssRNA
Enteroviruses				
• Polio	Poliomyelitis	29	4.5 - 7.2	ssRNA
• Echo	Aseptic meningitis	29	5.0 - 6.4	ssRNA
• Coxsackie	Aseptic meningitis, diarrhoea infections respiratory	29	6.6 - 8.2	ssRNA

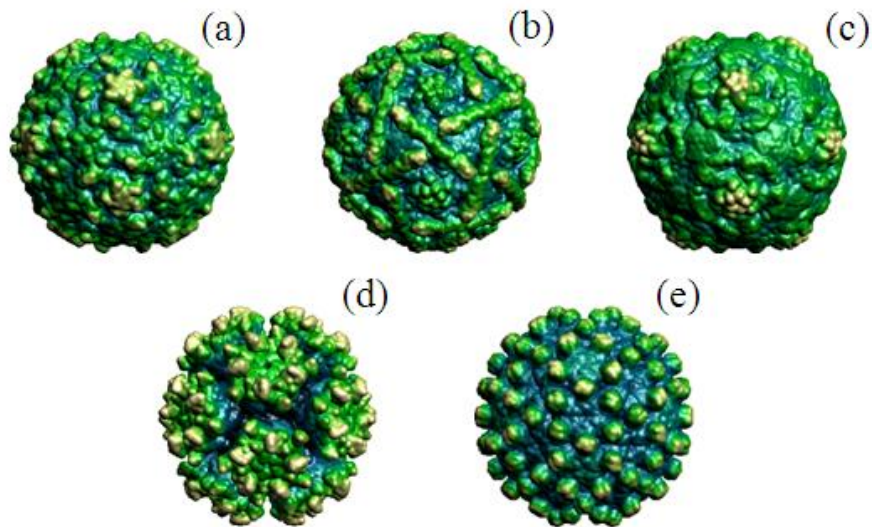


Figure 1.1: Images of capsid protein for the a) Poliovirus; b) Echovirus; c) Coxsackievirus; d) Adenovirus and e) Hepatitis B virus.

Pathogenic enteric viruses are often impossible or difficult and time-consuming to cultivate in the laboratory. Therefore coliphages are commonly used as indicators of microbiological water quality and as surrogates for human enteric viruses. Coliphages are group of viruses that infect a bacterial host. They often are found where enteric viruses occur, and their size and composition is similar to that of human enteric viruses. Coliphages are easily cultivated, and their handling is safe [35]. The infection of bacterial hosts by coliphages proceeds by four stages: 1) *adsorption* of phage to host cells, 2) *penetration* of phage nucleic acid, 3) *intracellular multiplication* using the host bacterium's metabolic machinery to produce viral structural components and viral enzymes until capsid assembles around viral genomes and, 4) *release* of phages by host cells lysis.

In this study, coliphage MS2 was used as surrogate of human enteric viruses. Its main physical and molecular properties are described in Table 1.2

Table 1.2: Physical and molecular characteristics of MS2 coliphage [8].

Coliphage surrogate	MS2
Bacterial host	<i>Escherichia coli</i> (DSMZ 5695)
Surrogate for	Polio, Echo, Hepatitis
Infection	Male-specific
Nucleic acid	ssRNA
Genome Topology	3569 nt
Genome length	Linear
Size (diameter)	24 - 27 nm
Isoelectric point (IEP)	3.5 - 3.9

1.2.2 Advanced oxidation processes

Advanced oxidation processes (AOPs) are widely studied treatment methods which have emerged as a promising alternative to conventional water treatment systems, which are not able to completely inactivate pathogens or degrade recalcitrant chemicals [18–20]. AOPs are based on the generation of reactive oxygen species (ROS), one of which are hydroxyl radicals, HO^\bullet . These radicals can be generated by a variety of processes as shown Figure 1.2. One of the most popular and widely applied AOP is the Fenton process, shown in red in Figure 1.2.

1.2.3 Fenton process

The Fenton chemistry has been known for more than a century. It was discovered in 1894, when H.J.H. Fenton found that tartaric acid was oxidized by hydrogen peroxide (H_2O_2) in the presence of Fe(II) salts [36]. In recent years, its application for oxidation of organic pollutants in wastewater treatment was demonstrated [37, 38].

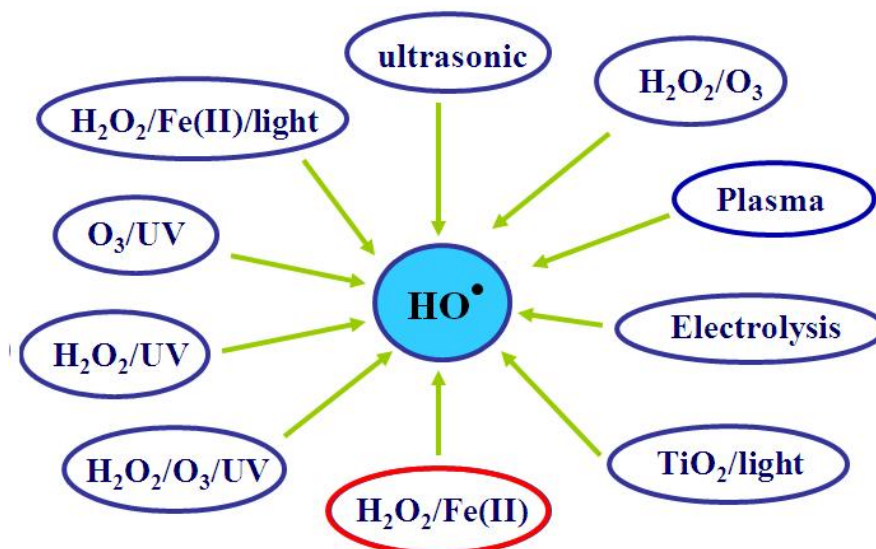


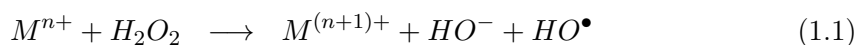
Figure 1.2: Generation of HO^\bullet radicals by different advanced oxidation processes (AOPs).

In this study, the Fenton process was divided into two types: 1) homogeneous Fenton using dissolved metal ions as source of metals; and 2) heterogeneous Fenton using particles as source of metals.

1.2.3.1. Homogeneous Fenton

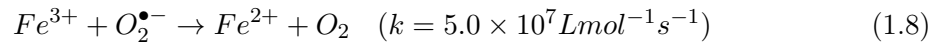
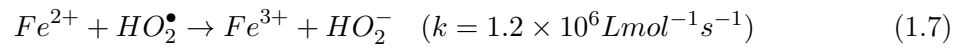
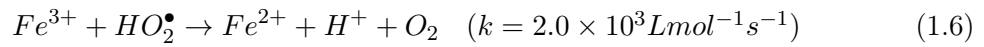
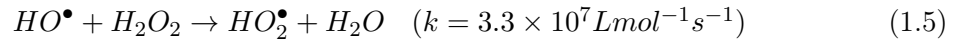
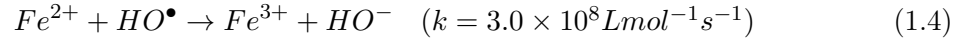
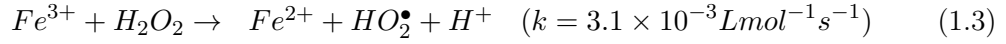
The homogeneous Fenton system consists in the decomposition of H_2O_2 by dissolved metal ions, which generates highly oxidizing species. Two types of reaction pathways have been postulated to be involved: formation of a radical (production of HO^\bullet) and a non-radical (mainly ferryl ion production, FeO^{2+}). The nature of these species has been questioned and widely investigated by several studies, but to date the exact nature of the oxidants created in the Fenton process is still under discussion in the scientific community.

In general, the Fenton reaction can be outlined as described in the Equation 1.1.



Where, M is a transition metal such as Fe (II) or Cu(I).

In homogeneous acidic solution, the most accepted mechanism of H_2O_2 decomposition involves the formation of superoxide radical and its conjugate acid ($\text{HO}_2^\bullet/\text{O}_2^{\bullet-}$) and hydroxyl radicals (HO^\bullet), according to the mechanisms outlined below [39].

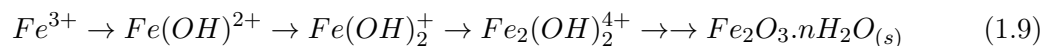


Equation 1.2 is known as the traditional Fenton reaction.

The regeneration of the reduced metal ions can follow different pathways. The most accepted mechanism is described in Equation 1.3 and 1.8.

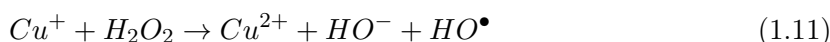
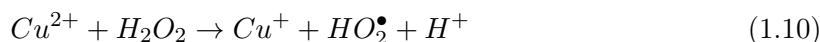
In addition, it has also been postulated that the reaction between H_2O_2 and Fe(II) undergo a non-radical reaction involving a ferryl species (FeO^{2+}) [40–43]. Its mechanism is not still clearly defined. However, both hydroxyl radicals and ferryl ions can coexist in the Fenton reaction and the prevalence of each depends of the environmental conditions.

At $pH < 2$, the predominant dissolved iron species is the iron hexaquo complex $[Fe(H_2O)_6]^{3+}$. At $pH > 2$, the hexaquo complex undergoes extensive hydrolysis to produce Fe(III)-hydroxy complexes, until the reactions are ended in precipitation of amorphous ferric (oxy)hydroxides (Equation 1.9). The production of this species depends on pH, counterion, ionic strength and total iron concentration [37].



At neutral pH, Fe(III)-hydroxy complexes are not stable and they rapidly hydrolyze and precipitate. These precipitates do not re-dissolve readily, making the Fenton reaction less efficient. The Fenton reaction thus is most efficient in acidic pH ($pH < 3$) where Fe(III) species remain soluble and the regeneration of reduced metal ions is possible.

If transition metals other than iron are used to catalyze the decomposition of H_2O_2 to HO_2^\bullet , the process is known as a Fenton-like reaction. For example, dissolved Cu exhibits a reaction mechanism similar to the Fenton chemistry. This consists in the reduction from Cu(II) to Cu(I), and subsequent formation of hydroxyl radicals, as shown in the Equation 1.10 and 1.11.



This reaction is considerably faster than the reaction with iron as a catalyst, in particular around neutral pH [44].

1.2.3.2. Heterogeneous Fenton

As under typical water treatment conditions, the Fenton reaction is less efficient due to the low stability and solubility of Fe(II) and Fe(III) at neutral pH. An alternative is to use iron-bearing particles as the source of reactive iron, which may catalyze the decomposition of H_2O_2 . The most common particles involved in heterogeneous Fenton reactions are iron (hydr-)oxides because they are abundant in both natural and engineered systems. In addition, iron (hydr-)oxide particles play an important role during coagulation process in water treatment.

Many investigations have demonstrated the effectiveness of this process for water treatment purposes. These studies have shown that iron-bearing minerals, namely goethite, hematite, magnetite and ferrihydrite can catalyze the oxidation of organic pollutants by H_2O_2 over a pH range from 3 to 7 [29, 31, 45]. The mechanism of reaction has not been elucidated to date. However, it is supposed that this process can be described by similar reactions as the homogeneous Fenton process, as described in section 1.2.3.1., with the unique difference that the decomposition of H_2O_2 takes place on the iron-bearing particle surface [46, 47]. Several investigations have suggested that the oxidation of organic pollutants take place via HO^\bullet radicals generated on the particle surface [29, 33, 45].

1.2.3.3. Photo-Fenton

Sunlight irradiation has been demonstrated to accelerate the homogeneous Fenton process at acidic pH (pH <3). This is due to the efficient photo-reduction of the main dissolved Fe(III) species ($Fe(OH)^{2+}$) to Fe(II), which leads to additional HO^\bullet genera-

tion [37]. This type of photo-assisted reaction is called photo-Fenton reaction.

The most accepted mechanism scheme is described in Equation 1.12.



At neutral pH, the homogeneous Fenton reaction is very slow due to the limitations of solubility of iron ions in solution. Sunlight may thus enhance this process. However, the acceleration at neutral pH is only minor, as the main photo-active $Fe(OH)^{2+}$ species is mainly present at acidic pH. The heterogeneous Fenton processes, however, can be enhanced by sunlight at neutral pH, following similar mechanism as described above, by promoting of photo-reduction of Fe(III), which reacts with H_2O_2 (Equation 1.2) and via the generation of additional HO^{\bullet} on the particle surface analogous to Equation 1.12.

1.2.4 Effect of the Fenton reaction on biological systems

The effect of Fenton chemistry on biological systems has been investigated by several authors. It was found that the Cu/amino acid system (CuL ; L= glycine, alanine or lysine) enhanced hydrogen peroxide decomposition. They found that the dominant species were CuL_2 (Cu^{2+}) in neutral and alkaline solutions. However, at $pH < 6.0$ the dominant species was CuL (Cu^+) [48, 49]. In addition, the oxidation rate was enhanced in Cu/amino acid/ H_2O_2 system when pH increased from 6 to 9. The same trend occurred in the production of hydroxyl radicals (HO^{\bullet}), which was favored in alkaline solutions. Finally, a possible mechanism was proposed for the hydrogen peroxide activation by Cu(II) [48], as shown in Figure 1.3. It has also been suggested that photoreactions of Cu(II)/amino acid complexes may contribute to biological damage in polluted water [49, 50]. Furthermore, various other studies have proposed that Fe(III) or Cu(II) species oxidize proteins via metal catalyzed oxidation (MCO) [51, 52].

The Fenton reaction has thus a high relevance on biological systems. In addition, sunlight may also play an important role on the virus inactivation in polluted water. The inactivation may be via the complexation of metal ions on the proteins of the viral capsid, and consequently photo-oxidative processes described above (section 1.2.3) may take place on the metal-binding sites.

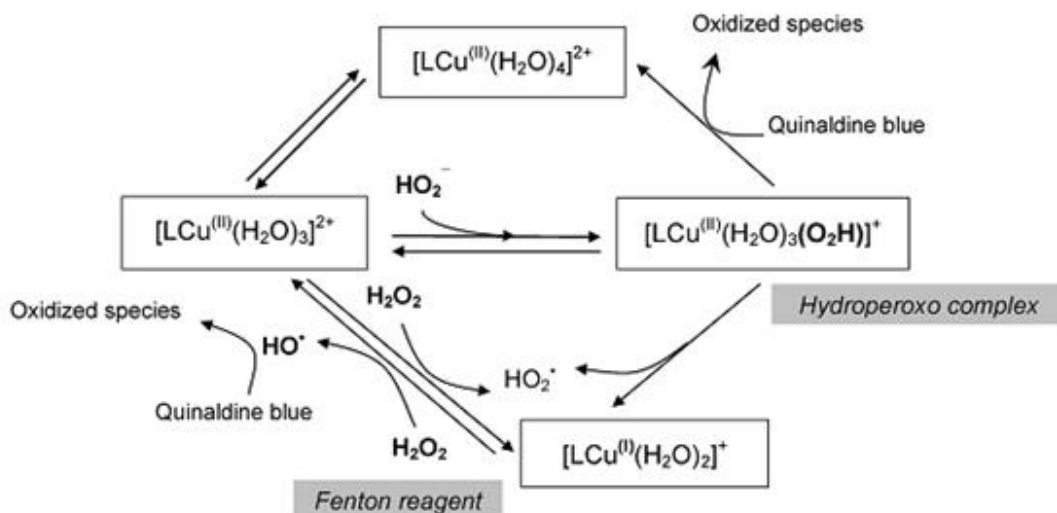


Figure 1.3: Proposed mechanism for the hydrogen peroxide activation by Cu(II) [48]. L=glycine, alanine or lysine.

1.3 Knowledge gaps

Despite the great promise of homogeneous and heterogeneous Fenton-like processes as disinfection methods in natural and engineered systems, to date very little is known about the molecular mechanisms that lead to virus inactivation. Only few investigations have been carried out which further our understanding of virus inactivation by homogeneous Fenton-like processes. In addition, the role of heterogeneous Fenton-like process, which may combine adsorption of viruses and their consequent inactivation, has not yet been investigated. Finally, the effect of sunlight upon virus inactivation has not been studied to date in either the homogeneous or the heterogeneous Fenton-like processes.

1.4 Objectives and hypotheses

The overall objective of this research was to acquire an in-depth understanding of virus inactivation by homogeneous and heterogeneous Fenton(-like) processes in the dark and under sunlight, as well as to elucidate the virus damage mechanisms that cause the inactivation by these processes at neutral pH.

This research was divided into three main objectives: the first objective was to study the factors that govern MS2 inactivation by homogeneous Fe- and Cu-catalyzed Fenton-like systems, and to assess the importance of this process for both AOP and natural systems, as described in chapter 2. The second objective was to investigate the fate of MS2 during adsorption onto iron (hydr-)oxide particles and inactivation by the hetero-

geneous Fenton-like processes, as described in chapter 3. Finally, the third objective was to elucidate the roles of genome and capsid protein damage during inactivation of MS2 bacteriophage by (photo-) Fenton-like systems, to better understand the biological consequences of these processes, as described in chapter 4.

The research objectives were designed to test three hypotheses, as described below.

Hypotheses I: The homogeneous Fenton-like process catalyzed by Cu or Fe causes virus inactivation.

Objectives I: Determine the factors that lead to the virus inactivation by homogeneous Fenton-like process.

To fill this knowledge gap, the following questions were addressed:

- Does the homogeneous Fenton-like system inactivate the viruses?
- Which are the main factors that cause the inactivation?
- Does sunlight enhance the inactivation?

Hypotheses II: Iron (hydr-)oxide particles cause virus inactivation by Fenton-like systems. Adsorption of viruses onto iron particles contributes to inactivation.

Objectives II: Characterize the adsorption of virus onto iron(hydr-)oxide particles and evaluate the effectiveness of the heterogeneous Fenton-like process to cause virus inactivation.

In this study the following questions were addressed:

- Does virus adsorption onto particles cause inactivation?
- Does heterogeneous Fenton system inactivate the viruses?
- Does sunlight enhance the inactivation in the heterogeneous Fenton system?

Hypotheses III: Virus inactivation by (photo-) Fenton-like processes causes damage to the genome and protein capsid.

Objectives III: Study the genome and capsid protein damage of MS2 bacteriophage upon inactivation by Fenton-like process.

To complete this objective the following questions were addressed:

- Does viral genome damage contribute to the inactivation?
- Which genome segments are most sensitive to degradation?
- Does viral capsid protein damage contribute to the inactivation?
- Which peptides segments are more susceptible to degradation?
- Do different Fenton-like systems differ in the mechanism by which MS2 is inactivated?

The final chapter (Chapter 5) of this thesis then offers general conclusions and an outlook over future work.

Bibliography

- [1] J. T. Dongdem, I. Soyiri, and A. Ocloo. Public health significance of viral contamination of drinking water. *African Journal of Microbiology Research*, 3(12):856–861, 2009.
- [2] N. J. Ashbolt. Microbial contamination of drinking water and disease outcomes in developing regions. *Toxicology*, 198(1-3):229–238, 2004.
- [3] D. Werber, D. Lausevic, B. Mugosa, Z. Vratnica, L. Ivanovic-Nikolic, L. Zizic, A. Alexandre-Bird, L. Fiore, F. M. Ruggeri, I. Di Bartolo, A. Battistone, B. Gassilloud, S. Perelle, D. N. Kaluski, M. Kivi, R. Andraghetti, and K. G. J. Pollock. Massive outbreak of viral gastroenteritis associated with consumption of municipal drinking water in a European capital city. *Epidemiology and Infection*, 137(12):1713–1720, 2009.
- [4] A. P. Wyn-Jones and J. Sellwood. Enteric viruses in the aquatic environment. *Journal of Applied Microbiology*, 91(6):945–962, 2001.
- [5] N. Nwachuku and C. P. Gerba. Health risks of enteric viral infections in children. In G. W. Ware, editor, *Reviews of Environmental Contamination and Toxicology*, volume 186, pages 1–56. Springer, New York, 2006.
- [6] C. P. Gerba, J. B. Rose, C. N. Haas, and K. D. Crabtree. Waterborne rotavirus: A risk assessment. *Water Research*, 30(12):2929–2940, 1996.
- [7] U. D. Parashar, C. J. Gibson, J. S. Bresee, and R. I. Glass. Rotavirus and severe childhood diarrhea. *Emerging Infectious Diseases*, 12(2):304–306, 2006.
- [8] M. Abbaszadegan, P. Monteiro, N. Nwachuku, A. Alum, and H. Ryu. Removal of adenovirus, calicivirus, and bacteriophages by conventional drinking water treatment. *Journal of Environmental Science and Health Part a: Toxic/Hazardous Substances and Environmental Engineering*, 43(2):171–177, 2008.
- [9] Mark W. LeChevallier and Kwok-Keung Au. *Water Treatment and Pathogen Control: Process Efficiency in Achieving Safe Drinking Water*. WHO, IWA, London, UK., 2004.
- [10] I. Xagorarakis, D. H. W. Kuo, K. Wong, M. Wong, and J. B. Rose. Occurrence of human adenoviruses at two recreational beaches of the great lakes. *Applied and Environmental Microbiology*, 73(24):7874–7881, 2007.
- [11] R. G. Sinclair, E. L. Jones, and C. P. Gerba. Viruses in recreational water-borne disease outbreaks: A review. *Journal of Applied Microbiology*, 107(6):1769–1780, 2009.

-
- [12] S. H. Lee and S. J. Kim. Detection of infectious enteroviruses and adenoviruses in tap water in urban areas in Korea. *Water Research*, 36(1):248–256, 2002.
- [13] S. A. Rutjes, W. J. Lodder, A. Docters van Leeuwen, and A. M. de Roda Husman. Detection of infectious rotavirus in naturally contaminated source waters for drinking water production. *Journal of Applied Microbiology*, 107(1):97–105, 2009.
- [14] W. J. Lodder, H. H. J. L. van den Berg, S. A. Rutjes, and A. M. de Roda Husman. Presence of enteric viruses in source waters for drinking water production in the Netherlands. *Applied and Environmental Microbiology*, 76(17):5965–5971, 2010.
- [15] K. E. Gibson, M. C. Opryszko, J. T. Schissler, Y. Y. Guo, and K. J. Schwab. Evaluation of human enteric viruses in surface water and drinking water resources in Southern Ghana. *American Journal of Tropical Medicine and Hygiene*, 84(1):20–29, 2011.
- [16] S. W. Krasner, H. S. Weinberg, S. D. Richardson, S. J. Pastor, R. Chinn, M. J. Scilimenti, G. D. Onstad, and A. D. Thruston. Occurrence of a new generation of disinfection byproducts. *Environmental Science and Technology*, 40(23):7175–7185, 2006.
- [17] J. Y. Hu, Z. S. Wang, W. J. Ng, and S. L. Ong. Disinfection by-products in water produced by ozonation and chlorination. *Environmental Monitoring and Assessment*, 59(1):81–93, 1999.
- [18] Julian Blanco-Galvez, Pilar Fernandez-Ibanez, and Sixto Malato-Rodriguez. Solar photocatalytic detoxification and disinfection of water: Recent overview. *Journal of Solar Energy Engineering-Transactions of the Asme*, 129(1):4–15, 2007.
- [19] G. A. Shin and M. D. Sobsey. Reduction of Norwalk virus, Poliovirus 1, and bacteriophage MS2 by ozone disinfection of water. *Applied and Environmental Microbiology*, 69(7):3975–3978, 2003.
- [20] M. Cho, H. M. Chung, W. Y. Choi, and J. Y. Yoon. Different inactivation behaviors of MS2 phage and Escherichia coli in TiO₂ photocatalytic disinfection. *Applied and Environmental Microbiology*, 71(1):270–275, 2005.
- [21] R. J. Davies-Colley, A. M. Donnison, D. J. Speed, C. M. Ross, and J. W. Nagels. Inactivation of faecal indicator microorganisms in waste stabilisation ponds: Interactions of environmental factors with sunlight. *Water Research*, 33(5):1220–1230, 1999.
- [22] L. W. Sinton, C. H. Hall, P. A. Lynch, and R. J. Davies-Colley. Sunlight inactivation of fecal indicator bacteria and bacteriophages from waste stabilization pond effluent in fresh and saline waters. *Applied and Environmental Microbiology*, 68(3):1122–1131, 2002.

-
- [23] M. R. Templeton, R. C. Andrews, and R. Hofmann. Particle-associated viruses in water: Impacts on disinfection processes. *Critical Reviews in Environmental Science and Technology*, 38(3):137–164, 2008.
- [24] A. Sakoda, Y. Sakai, K. Hayakawa, and M. Suzuki. Adsorption of viruses in water environment onto solid surfaces. *Water Science and Technology*, 35(7):107–114, 1997.
- [25] Y. W. You, J. Han, P. C. Chiu, and Y. Jin. Removal and inactivation of waterborne viruses using zerovalent iron. *Environmental Science and Technology*, 39(23):9263–9269, 2005.
- [26] J. Zhuang and Y. Jin. Interactions between viruses and goethite during saturated flow: Effects of solution pH, carbonate, and phosphate. *Journal of Contaminant Hydrology*, 98(1-2):15–21, 2008.
- [27] J. Y. Kim, C. Lee, D. C. Love, D. L. Sedlak, J. Yoon, and K. L. Nelson. Inactivation of MS2 coliphage by ferrous ion and zero-valent iron nanoparticles. *Environmental Science and Technology*, 45(16):6978–6984, 2011.
- [28] W. P. Kwan and B. M. Voelker. Decomposition of hydrogen peroxide and organic compounds in the presence of dissolved iron and ferrihydrite. *Environmental Science and Technology*, 36(7):1467–1476, 2002.
- [29] W. P. Kwan and B. M. Voelker. Rates of hydroxyl radical generation and organic compound oxidation in mineral-catalyzed Fenton-like systems. *Environmental Science and Technology*, 37(6):1150–1158, 2003.
- [30] R. Matta, K. Hanna, and S. Chiron. Fenton-like oxidation of 2,4,6-trinitrotoluene using different iron minerals. *Science of the Total Environment*, 385(1-3):242–251, 2007.
- [31] R. Matta, K. Hanna, T. Kone, and S. Chiron. Oxidation of 2,4,6-trinitrotoluene in the presence of different iron-bearing minerals at neutral pH. *Chemical Engineering Journal*, 144(3):453–458, 2008.
- [32] J. C. Barreiro, M. D. Capelato, L. Martin-Neto, and H. C. B. Hansen. Oxidative decomposition of atrazine by a Fenton-like reaction in a H₂O₂/ferrihydrite system. *Water Research*, 41(1):55–62, 2007.
- [33] M. D. Gurol and S. S. Lin. Hydrogen peroxide/iron oxide-induced catalytic oxidation of organic compounds. *Journal of Advanced Oxidation Technologies*, 5(2):147–154, 2002.
- [34] C. Ferguson, A. M. D. Husman, N. Altavilla, D. Deere, and N. Ashbolt. Fate and transport of surface water pathogens in watersheds. *Critical Reviews in Environmental Science and Technology*, 33(3):299–361, 2003.

- [35] A. H. Havelaar, M. Butler, S. R. Farrah, J. Jofre, E. Marques, A. Ketratanakul, M. T. Martins, S. Ohgaki, M. D. Sobsey, and U. Zaiss. Bacteriophages as model viruses in water-quality control. *Water Research*, 25(5):529–545, 1991.
- [36] H.J.H. Fenton. Oxidation of tartaric acid in presence of iron. *Journal of the Chemical Society*, 65:899–910, 1894.
- [37] J. J. Pignatello, E. Oliveros, and A. MacKay. Advanced oxidation processes for organic contaminant destruction based on the Fenton reaction and related chemistry. *Critical Reviews in Environmental Science and Technology*, 36(1):1–84, 2006.
- [38] P. Bautista, A. F. Mohedano, J. A. Casas, J. A. Zazo, and J. J. Rodriguez. An overview of the application of Fenton oxidation to industrial wastewaters treatment. *Journal of Chemical Technology and Biotechnology*, 83(10):1323–1338, 2008.
- [39] J. De Laat and H. Gallard. Catalytic decomposition of hydrogen peroxide by fe(III) in homogeneous aqueous solution: mechanism and kinetic modeling. *Environmental Science and Technology*, 33(16):2726–2732, 1999.
- [40] W. C. Bray and M. H. Gorin. Ferryl ion, a compound of tetravalent iron. *Journal of the American Chemical Society*, 54:2124–2125, 1932.
- [41] M. L. Kremer. Mechanism of the Fenton reaction. Evidence for a new intermediate. *Physical Chemistry Chemical Physics*, 1(15):3595–3605, 1999.
- [42] J. T. Groves. High-valent iron in chemical and biological oxidations. *Journal of Inorganic Biochemistry*, 100(4):434–447, 2006.
- [43] O. Pestovsky and A. Bakac. Reactivity of aqueous fe(IV) in hydride and hydrogen atom transfer reactions. *Journal of the American Chemical Society*, 126(42):13757–13764, 2004.
- [44] M. Akagawa and K. Suyama. Oxidative deamination by hydrogen peroxide in the presence of metals. *Free Radical Research*, 36(1):13–21, 2002.
- [45] S. Lee, J. Oh, and Y. Park. Degradation of phenol with Fenton-like treatment by using heterogeneous catalyst (modified iron oxide) and hydrogen peroxide. *Bulletin of the Korean Chemical Society*, 27(4):489–494, 2006.
- [46] S. S. Lin and M. D. Gurol. Catalytic decomposition of hydrogen peroxide on iron oxide: Kinetics, mechanism, and implications. *Environmental Science and Technology*, 32(10):1417–1423, 1998.
- [47] M. C. Lu, J. N. Chen, and H. H. Huang. Role of goethite dissolution in the oxidation of 2-chlorophenol with hydrogen peroxide. *Chemosphere*, 46(1):131–136, 2002.

- [48] T. Y. Lin and C. H. Wu. Activation of hydrogen peroxide in copper(II)/amino acid/H₂O₂ systems: Effects of pH and copper speciation. *Journal of Catalysis*, 232(1):117–126, 2005.
- [49] K. Hayase and R. G. Zepp. Photolysis of copper(II)-amino acid complexes in water. *Environmental Science and Technology*, 25(7):1273–1279, 1991.
- [50] M. H. Robbins and R. S. Drago. Activation of hydrogen peroxide for oxidation by copper(II) complexes. *Journal of Catalysis*, 170(2):295–303, 1997.
- [51] E. R. Stadtman and B. S. Berlett. Fenton chemistry - amino acid oxidation. *Journal of Biological Chemistry*, 266(26):17201–17211, 1991.
- [52] E. R. Stadtman. Oxidation of free amino acids and amino acid residues in proteins by radiolysis and by metal-catalyzed reactions. *Annual Review of Biochemistry*, 62:797–821, 1993.

Chapter 2

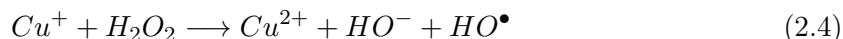
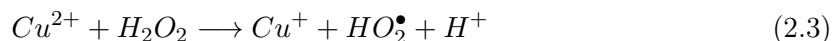
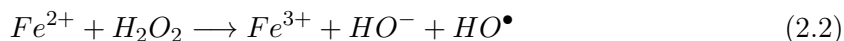
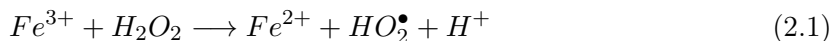
Inactivation of MS2 coliphage in Fenton and Fenton-like systems: influence of transition metals, hydrogen peroxide and sunlight

2.1 Introduction

Human enteric viruses are present in wastewater as well as in natural waters impacted by raw or insufficiently treated sewage [1]. These viruses can cause various waterborne diseases, hence their presence in waters used for drinking or recreational purposes presents a risk to public health. Conventional disinfection practices are not always sufficient to completely disinfect viruses [2, 3]. Therefore, more efficient practices are needed to ensure microbial water safety.

Advanced oxidation processes (AOPs) such as TiO₂-mediated heterogeneous catalysis [4, 5], disinfection treatment with UV alone [6] or UV in conjunction with oxidizing chemicals [7, 8] have emerged as alternatives to inactivate pathogens. One of the most promising AOPs involves the Fenton reaction. This process is based on the formation of oxidants, such as hydroxyl radicals (HO•), generated via the decomposition of H₂O₂ and catalyzed by transition metal ions including Fe or Cu. Besides AOPs, oxidant production via the Fenton reaction can also occur in natural waters. It has been estimated that the Fenton process contributes up to 50% of HO• in sunlit surface waters [9].

The first and rate-limiting step in the decomposition of H_2O_2 by Fe or Cu is the reduction of the transition metal by H_2O_2 (summarized by Eqs. 2.1 and 2.3). Subsequently, the metal is re-oxidized by H_2O_2 while forming the highly reactive HO^\bullet (Eqs. 2.2 and 2.4). Equation 2.2 is known as the Fenton reaction, whereas Equation 2.4 is referred to as a Fenton-like reaction.



The predominant Fe(III) species involved in the Fenton process are the iron hexaquo complexes, $[Fe(H_2O)_6]^{3+}$, and their first hydrolysis species, $[FeOH(H_2O)_5]^{2+}$ [10]. At neutral pH, however, Fe(III) is only sparingly soluble and precipitates as amorphous iron (oxy)hydroxide. Iron (oxy)hydroxides can still participate in the Fenton reaction, albeit at slower rates than dissolved iron [11–14]. It has furthermore been proposed that the main oxidant formed in the Fenton process at neutral pH is not HO^\bullet , but a less reactive, high-valent iron-oxo species, such as the ferryl ion, FeO^{2+} [15–17].

Compared to iron, Cu(II) aqua species are more soluble at neutral pH. While the hexaquo complex ($[Cu(H_2O)_6]^{2+}$) is the predominant Cu species at neutral pH, the $Cu(OH)_2$ hydrolyzed species has been implicated as the most Fenton-reactive species [18]. Cu oxides, such as CuO, can also decompose H_2O_2 to generate HO^\bullet at neutral pH [19].

The effect of a Fenton-like system on the inactivation of viruses was first investigated by Yamamoto et al. [20], who studied the inactivation of MS2 coliphage at low concentrations of H_2O_2 (0.00015%) and $CuSO_4$ (0.1–100 μM). It was found that MS2 inactivation increased with increasing Cu concentration, from 2.8 log units die-off within 4 hours at 0.1 μM Cu to > 5.9 log units at 100 μM Cu. In a second study involving several RNA and DNA phages [21], these authors reported that 10 μM of Cu and 0.00015% of H_2O_2 inactivated RNA phages (MS2, f2) very rapidly. However, higher concentrations of Cu (100 μM) were necessary to achieve moderate inactivation of single-stranded DNA phages (phi-X174, S13) and slow inactivation of double-stranded DNA phages (T2, T5, Salmonella phage P22). Sagripanti et al. [22] investigated the inactivation of different phages and viruses by both 1 mg/L Cu(II) or 30 mg/L Fe(III) alone and in the presence

of H_2O_2 . They showed that the addition of H_2O_2 (100 mg/L) produced an increase in inactivation of all viruses by Cu, and in a subset of viruses by Fe. On a mass basis, the Fenton-like system was more efficient at inactivating viruses than the Fenton system.

Despite the demonstrated efficiency of virus and phage inactivation by Cu/ H_2O_2 and Fe/ H_2O_2 , a systematic investigation of the inactivation kinetics remains elusive. Furthermore, even though light in the near UV and visible ranges is known to enhance the Fenton reaction [13] and references therein), the effect of sunlight on virus inactivation by Fenton/Fenton-like processes has never been addressed. The overall goal of this work was therefore to investigate the factors that control virus inactivation in Fe- and Cu-catalyzed Fenton-type systems, in order to assess the importance of this process for both AOPs and natural systems. MS2 coliphage, a commonly used surrogate for human enteric viruses [23], was used as the model organism. The effects of low Cu, Fe, and H_2O_2 concentrations on inactivation were studied, and the effect of sunlight was considered. Based on our results, a scheme of the inactivating mechanisms was proposed.

2.2 Experimental section

Experiments were carried out in batch reactors containing MS2 in carbonate buffered-saline (CBS) at neutral pH. Inactivation rate constants as well as hydroxyl radical production rates were obtained for different concentrations of Cu(II), Fe(III), and H_2O_2 , in the presence and absence of simulated sunlight.

2.2.1 Reagents and Organisms

2.2.1.1. Reagents

Copper sulphate ($\text{CuSO}_4 \cdot 5\text{H}_2\text{O}$) and hydrogen peroxide (H_2O_2 , 30%), catalase (2000-5000 units/mg protein), 5,5,-dimethylpyrroline N-oxide (DMPO, $\geq 97\%$) and streptomycin sulphate were obtained from Sigma, Aldrich, St. Louis, Missouri. Ferric chloride ($\text{FeCl}_3 \cdot 6\text{H}_2\text{O}$), sodium bicarbonate (NaHCO_3), calcium chloride (CaCl_2), sodium chloride (NaCl) and D-glucose, all reagents 99+ $\%$ extra pure, were obtained from Acros organics. Ethanol ($\text{C}_2\text{H}_5\text{OH}$, 99.98%) was obtained from Fluka. Bactotryptone and yeast extract were purchased from Becton Dickinson, Sparks, MD and Fisher, Wohlen, Switzerland, respectively.

2.2.1.2. Organisms

MS2 Phage (DSMZ 13767) and its bacterial host *E. coli* (DSMZ 5695) were purchased from German collection of microorganisms and cell cultures, Braunschweig, Germany. The propagation of MS2 bacteriophage was performed in 1 liter of LB medium (10 g of Bactotryptone, 1 g of yeast extract, 8 g NaCl, 1 g D-glucose, 0.3 g CaCl₂ and 2 mg of streptomycin sulphate) containing *E. coli*. When the optical density of this culture reached 0.04 measured at 600 nm, the midlog phase *E. coli* was inoculated with MS2 at a multiplicity of infection (MOI; ratio between phage and bacteria) of 0.1. After five hours of incubation at 37 °C, the bacterial cells were lysed with chloroform (5 mL) and immediately purified as described elsewhere [24].

The MS2 stock solution obtained had a concentration of 10¹⁴ PFU mL⁻¹ and was stored in dilution buffer (DB; 5 mM NaH₂PO₄, 10 mM NaCl, pH 7.4) at 4 °C.

2.2.2 Phage quantification

The infective MS2 phage was quantified by double-layer agar technique as described previously [24]. The infective MS2 phage concentrations were measured in plaque forming units per mL (PFU mL⁻¹).

2.2.3 Experimental setup

Experiments were performed in glass reactors (100 mL) containing 50 mL CBS (0.1 mM NaHCO₃, 15 mM NaCl) at pH 6.8, with an initial effective MS2 concentration of 10⁷ PFU mL⁻¹. The solution was continuously stirred with a magnetic stir bar at 250 rpm, and the temperature was kept at 20 ± 2 °C. For dark Fenton experiments, the reactors were covered with aluminium foil, to protect the samples from light. Experiments with sunlight were carried out using solar simulator (ABET Technologies, Sun 2000) with 1000 W Xe lamp, an AM1.5 filter and UVB cut-off filter, to avoid confounding influence from inactivation via direct damage by UVB light. The irradiance was 300 W m⁻². During the simulated sunlight experiments, the sample temperature was controlled by placing the reactors in a cooled water bath.

2.2.4 Inactivation experiments

Reactors containing CBS and MS2 were spiked with Cu(II) or Fe(III) from freshly prepared CuSO₄ or FeCl₃ stock solutions (1 mM) to obtain final metal concentrations from 1 to 10 μM. H₂O₂, which was added as the last component, was spiked into the re-

actors from a stock solution (25 mM) to obtain final concentrations between 3 and 50 μM . Corresponding control samples containing MS2 and metals or H_2O_2 alone, were also conducted. In the metal-free control experiments, 0.1 μM EDTA was added to the buffer to complex any trace metals that may lead to Fenton/Fenton-like reactions. This concentration of EDTA did not cause virus inactivation. During the inactivation, 100 μL sample aliquots were periodically collected and immediately diluted in 100 μL of buffer amended with catalase (500 units mL^{-1}), to scavenge the remaining H_2O_2 . All inactivation experiments were conducted in duplicates with good reproducibility.

2.2.5 Electron spin resonance (ESR) measurements

ESR-measured formation of HO^\bullet was determined for a subset of the solution conditions used for the inactivation experiments, in the absence of viruses. For performing ESR reactive scavenging (spin-trapping) of HO^\bullet , a standard commercial cyclic nitron spin trap, 5,5-dimethyl-1-pyrroline N-oxide (DMPO) was used. Before application, DMPO was purified by filtration on charcoal. Subsequently, the obtained stock solution of 1 M of DMPO was stored at -20°C . 1-mL volumes of prepared solutions containing DMPO (50 mM), H_2O_2 (50 μM) and metals (varying from 1 to 10 μM) were transferred into a Pyrex beaker (5 mL). Aliquots of 10 μL of prepared solutions were immediately transferred into 0.7 mm ID and 0.87 mm OD quartz capillary tubes (VitroCom, NJ, USA; sample height of 25 mm) and sealed on both ends with Cha-SealTM tube sealing compound (Medex International, Inc. USA). To maximize the sample volume in the active zone of the ESR cavity, assemblies consisting of seven tightly packed capillaries were used and positioned in a wider quartz capillary (standard ESR tube, 2.9 mm ID and 4 mm OD, Wilmad LabGlass, Vineland, NJ, USA). Such a setup resulted in a ca. 65 μL sample volume in the active zone of the ESR cavity. The division of the sample into seven subsamples markedly improved the overall sensitivity of measurements, as described elsewhere [25].

For HO^\bullet measurements in photo-Fenton reactions, solutions were exposed to UV light outside the ESR cavity. Light from a spot source (LightingcureTM, model LC-8, Hamamatsu Photonics, France) was delivered via a flexible quartz light guide to a small Pyrex beaker (5 mL) containing the solutions. The light source was equipped with a 200 W Mercury-Xenon lamp (model L7212-01) emitting in the 300-450 nm range. The light guide termination was positioned at a distance of 0.5 cm above the open face of the beaker, yielding an illumination power density of 10 mW cm^{-2} (for the lamp power setting at 20%). To exclude UVB/C portions, the same AM 1.5 and UB/C cut-off filters were used as for the solar simulator.

ESR measurements were carried out at room temperature using X-band spectrometer, Model ESP300E (Bruker BioSpin, Karlsruhe, Germany), which was equipped with a standard rectangular mode (TE_{102}) cavity. Routinely, for each experimental point, five-

scan field-swept ESR spectra were recorded. The typical instrumental settings were: microwave frequency 9.38 GHz microwave power 2.0 mW, sweep width 120 G, modulation frequency 100 kHz, modulation amplitude 0.5 G, receiver gain 4×10^4 , time constant 20.48 ms, conversion time 40.96 ms, and time per single scan 41.9 sec.

2.2.6 Asymmetrical Flow Field-Flow Fractionation connected to inductively coupled plasma/mass spectrometry (aFIFFF-ICP-MS) analyses

aFIFFF-ICP-MS analyses were performed to monitor Cu adsorption onto the viral capsid. In this technique, colloidal particles are separated according to size by way of exposing them to a flow velocity gradient. This leads to the separation of viruses from other components, including dissolved or colloidal metals, in the solution. Direct coupling to an ICP-MS enabled the online determination of the Cu content associated with the viruses. Experiments were performed using the solution conditions described above, but with a higher virus concentration (2×10^{11} PFU mL⁻¹), to meet instrumental detection limits.

aFIFFF measurements were performed using a aFIFFF2000 system (Postnova Analytics) equipped with UV, seven angles laser light scattering and differential refractive index detectors. A regenerated cellulose membrane and spacer nominal thickness of 10 kDa and 350 μ M respectively was used. The carrier solution was the same bicarbonate-buffered saline used in the experiments. Samples containing 2×10^{11} PFU mL⁻¹ of MS2 as well as virus- and metal-free controls, were injected through a fixed loop of 1 mL. This high virus concentration was necessary to meet instrumental detection limits. The channel flow rate, cross-flow rate and relaxation time were 1 mL min⁻¹, 0.25 mL min⁻¹ and 1 min respectively. The aFIFFF was connected to an ICP-MS system (Sciex/Elan 200, Perkin Elmer Instruments) for metal analysis. The presence of Cu was monitored using the ⁶⁵Cu isotope.

2.2.7 Metal solubility calculations

Solubility calculations of metals in bicarbonate-buffered saline were carried out using the program PHREEQC-2 and the minteq.v4 database.

2.2.8 Data analysis

First-order inactivation rate constants were determined from the slope of a linear regression of $\ln([\text{virus}]/[\text{virus}]_o)$ vs. time, and are reported as k_{obs} (min⁻¹). Hydroxyl radical production rates HO[•] (M s⁻¹) were determined from the time evolution of the doubly

integrated ESR signal of the paramagnetic spin adduct, DMPO-OH. To enhance the accuracy of calculations, prior to double-integration, the experimental ESR traces were fitted to the theoretical pattern of the ESR signal of DMPO-OH using the Mathcad software. Uncertainties were reported as the 95% confidence intervals of the fits to k_{obs} or r_{OH} .

2.3 Results and Discussion

To establish if Cu- and Fe-catalyzed Fenton systems cause virus inactivation, we compared MS2 inactivation in the presence of Cu, Fe or H_2O_2 alone with that in Fenton systems containing both H_2O_2 and Fe or Cu.

As can be seen in Figure 2.1, efficient inactivation occurred in both Cu/ H_2O_2 and Fe/ H_2O_2 systems, and inactivation followed first-order kinetics. Negligible inactivation was observed in the presence of H_2O_2 alone. However, a 50% decrease in plaques over 30 min was observed in the samples containing 1 μ M of Fe only. This may be due to virus inactivation by the metal ions alone, or to virus aggregation, which would also be manifested in a decrease of plaques. The possibility of aggregation by metal ions is supported by a study by Abad et al. [26], who reported the formation of small aggregates of enteric virus in the presence of low concentrations of metal ions (700 μ g L^{-1} Cu or 70 μ g L^{-1} Ag) and free chlorine, but no inactivating effect of metal ions was observed. We therefore consider it likely that the loss of plaques in the absence of H_2O_2 is a result of virus aggregation, not inactivation. Furthermore, the decrease in plaques in the presence of Fe or Cu alone accounted for only 10% of k_{obs} in the Fe/ H_2O_2 system, and was negligible in the Cu/ H_2O_2 system. These findings confirm that only the simultaneous presence of H_2O_2 and Fe or Cu, hence exposure to a Fenton/Fenton-like system, leads to efficient virus inactivation.

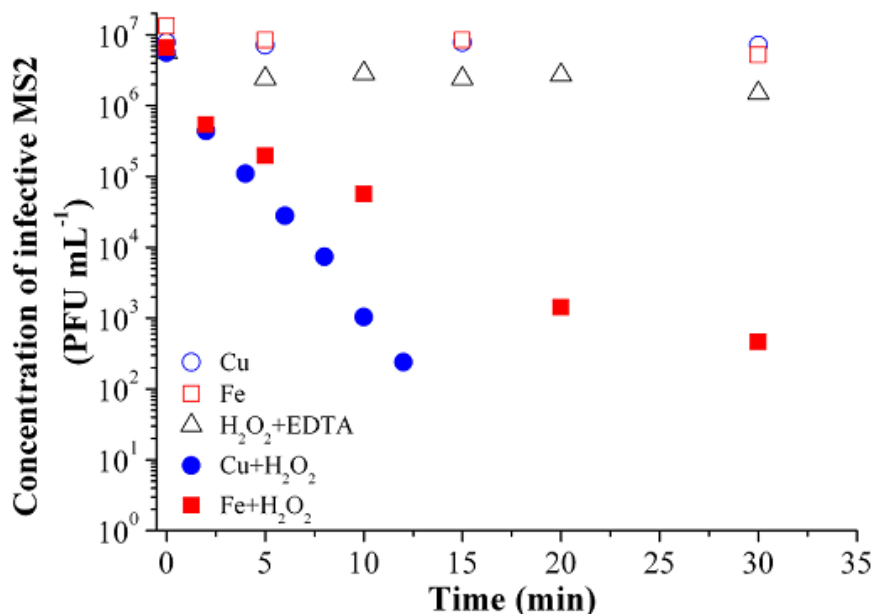


Figure 2.1: MS2 inactivation by Cu- and Fe- catalyzed Fenton process in CBS (0.1 mM NaHCO₃, 15 mM NaCl, pH= 6.8). Initial MS2= 10⁷ PFU mL⁻¹, metal concentrations= 1.0 μM, H₂O₂= 50 μM. The plots correspond to: Cu (hollow blue circle), Fe (hollow red square), H₂O₂ + 0.1 μM EDTA (hollow black triangle), Cu + H₂O₂ (solid blue circle), Fe+H₂O₂ (solid red square).

2.3.1 Effect of H₂O₂

To investigate if more environmentally relevant H₂O₂ concentrations can cause virus inactivation in Fenton/Fenton-like systems, we tested the influence of different low H₂O₂ concentration on MS2 survival. k_{obs} in both Cu and Fe systems exhibited a linear dependence on the H₂O₂ concentration between 0 and 50 μM (Figure 2.2), indicating that inactivation was first order with respect to H₂O₂. We can thus propose an inactivation rate expression that is first order with respect to both virus and H₂O₂, where k_{metal} is the respective rate constant for reactions involving a constant concentration of Cu or Fe:

$$\frac{d[virus]}{dt} = -k_{metal}[H_2O_2][virus] \quad (2.5)$$

For each metal, k_{metal} can be determined from the slopes of the linear regression of k_{obs} vs. H₂O₂ (Figure 2.2). For a metal concentration of 1 μM, k_{Fe} correspond to $5.6 \times 10^{-3} \mu\text{M}^{-1} \text{min}^{-1}$ and k_{Cu} to $1.65 \times 10^{-2} \mu\text{M}^{-1} \text{min}^{-1}$. Under these experimental conditions, the Cu system was thus about three times more efficient at inactivating MS2 than the Fe system.

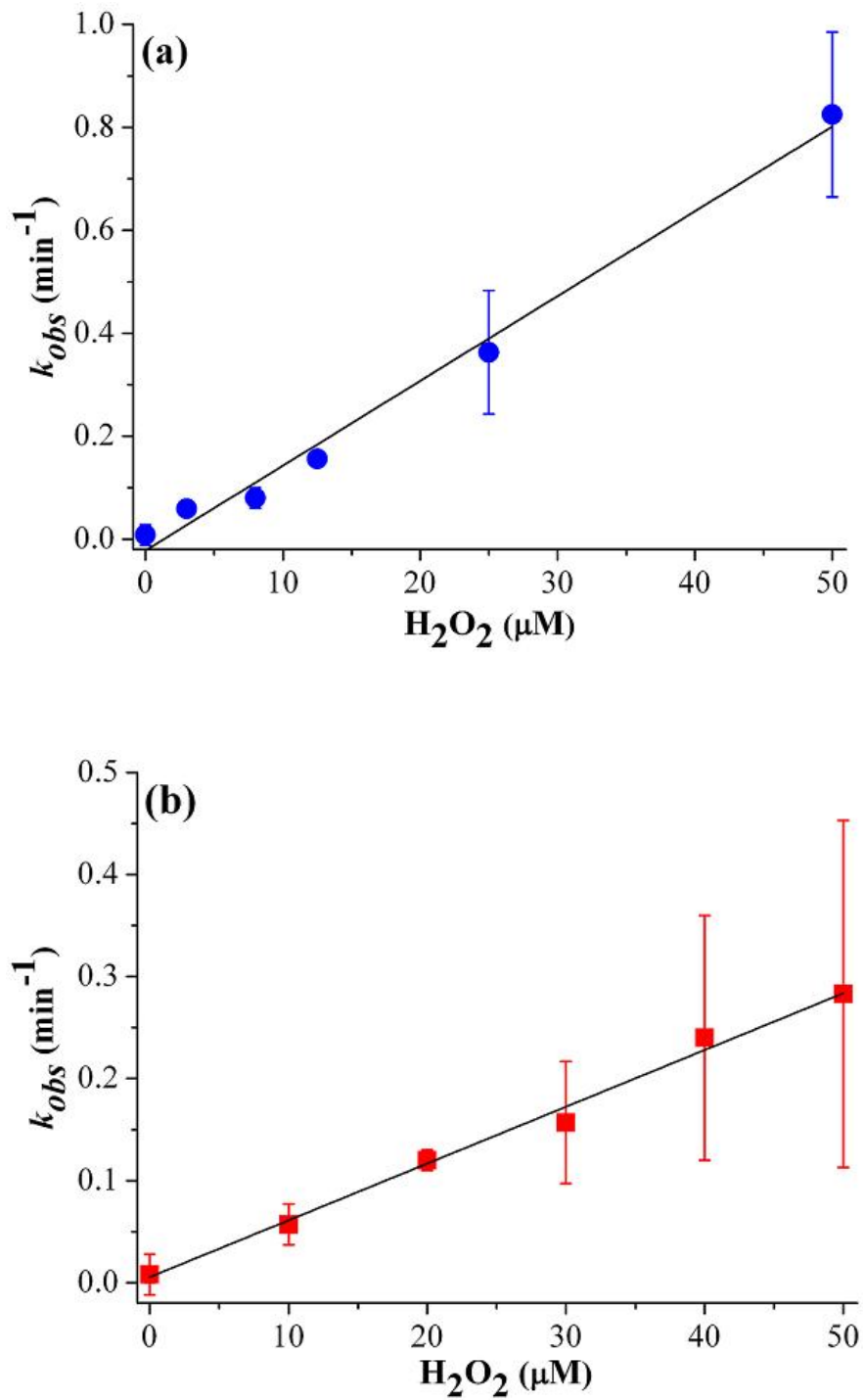


Figure 2.2: Effect of H_2O_2 concentration activated by (a) $1 \mu M$ Cu(II) and (b) $1 \mu M$ Fe(III) on MS2 inactivation in bicarbonate-buffered saline. MS2 = 10^7 PFU mL^{-1} in CBS, pH = 6.8. Solid lines correspond to linear regression fits, and yielded the following regression parameters: $k_{obs(Cu)} = 1.6 \times 10^{-2}[H_2O_2] - 0.022$; $k_{obs(Fe)} = 5.6 \times 10^{-3}[H_2O_2] + 0.005$.

2.3.2 Effect of metal concentrations

The effect of increasing concentrations of Cu(II) and Fe(III) on MS2 inactivation by Fenton/Fenton-like systems is shown in Figure 2.3. In the Cu/H₂O₂ system, k_{obs} first increased with increasing Cu concentrations, but leveled off above 2.5 μ M of added Cu(II) (Fig. 2.3a). This plateau effect could be a result of two processes: first, inactivation may be governed by Cu adsorption onto the MS2 capsid, which reached saturation above 2.5 μ M Cu. However, further experiments using initial MS2 concentrations varying over four orders magnitude (10^5 - 10^9 PFU mL⁻¹) exhibited equal inactivation rate constants (data not shown), indicating that inactivation was not limited by Cu saturation of the virus capsid. Alternatively, the plateau effect could be explained by Cu solubility considerations. Solubility calculations using tenorite (CuO) as the main precipitate indicated that under our experimental conditions, the concentration of dissolved Cu increased up to 2.5 μ M of added Cu(II) (Figure 2.4a). At higher concentrations, however, the solution was saturated in Cu and precipitates started to form. The dissolved Cu concentrations therefore remained constant beyond 2.5 μ M added Cu. The presence of colloidal Cu precipitates in our samples was verified by aFIFFF analysis for a solution containing 10 μ M Cu(II) (Figure 2.5). Assuming that Cu solubility accounted for the observed plateau effect, this indicates that the MS2 inactivation was mediated by dissolved Cu, whereas precipitates did not contribute significantly to inactivation.

Rate constants obtained for added Fe(III) between 1 and 10 μ M were not statistically different from each other (Fig. 2.3b). Nevertheless, k_{obs} in the Fe/H₂O₂ system continually increased with increasing concentration of added Fe(III) over the range investigated, and approximately doubled between 1 and 10 μ M added Fe(III). The slightly increasing trend of k_{obs} , albeit not statistically significant, was observed in replicate experiments. This trend could not be attributed to more extensive aggregation at higher Fe concentrations (determined in control experiments without H₂O₂), because the relative contribution of the Fenton reaction to the overall k_{obs} also increased with increasing Fe concentrations. Solubility calculations using ferrihydrite as the main precipitate showed that under our experimental conditions the solution was already saturated in Fe(III) at the lowest added Fe concentration of 1 μ M. The dissolved Fe concentration thus remained constant throughout the entire experiment, and all added Fe(III) was precipitated to iron colloids (Figure 2.4b). Based on these observations, we proposed that MS2 inactivation was mediated by iron colloids, rather than dissolved iron. However, as a result of the large error associate with k_{obs} in this system, we cannot conclusively rule out an involvement of dissolved iron.

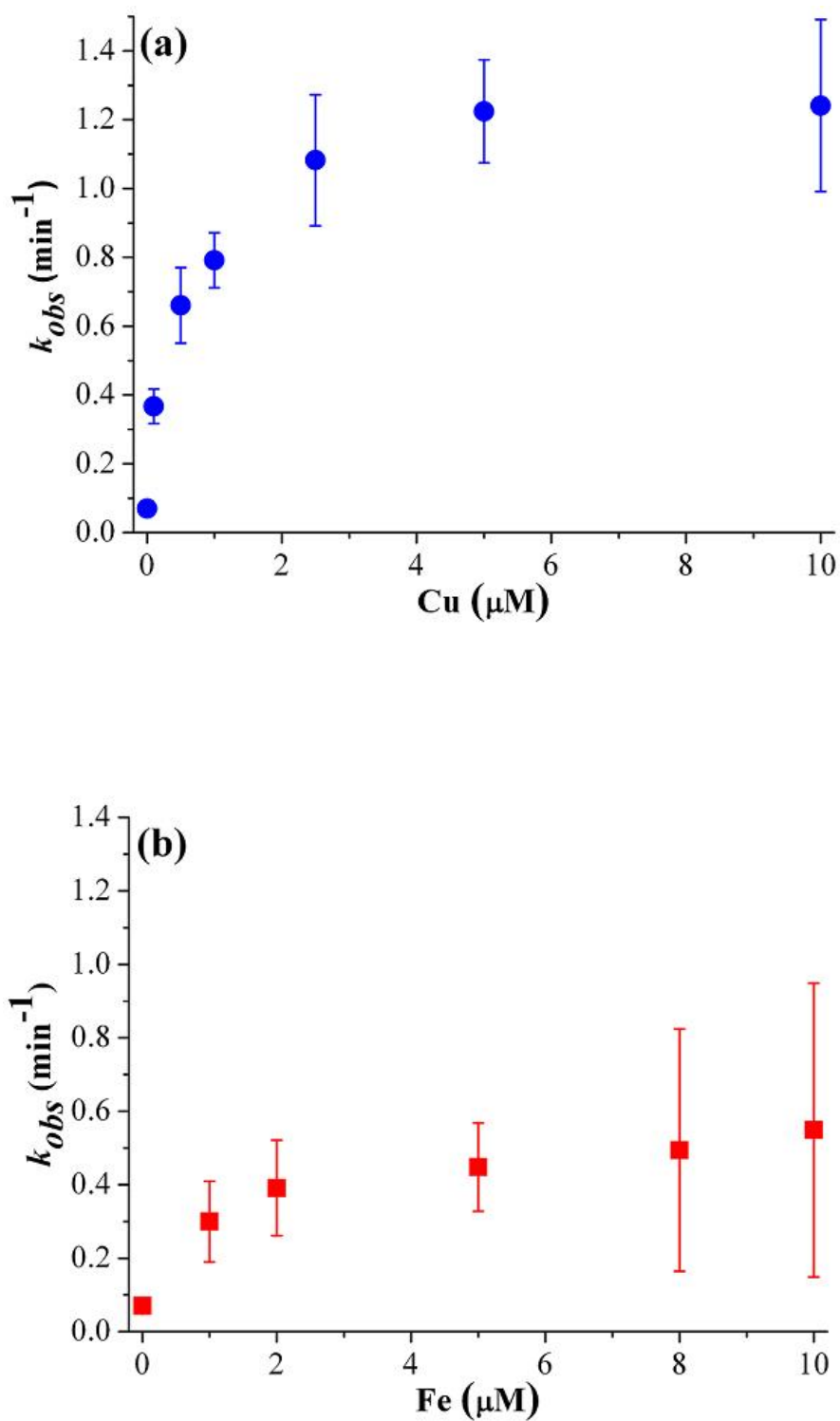


Figure 2.3: Effect of (a) Cu(II) and (b) Fe(III) concentration on MS2 inactivation in the presence of 50 μM H₂O₂. Initial MS2 concentration = 10⁷ PFU mL⁻¹ in CBS, pH = 6.8.

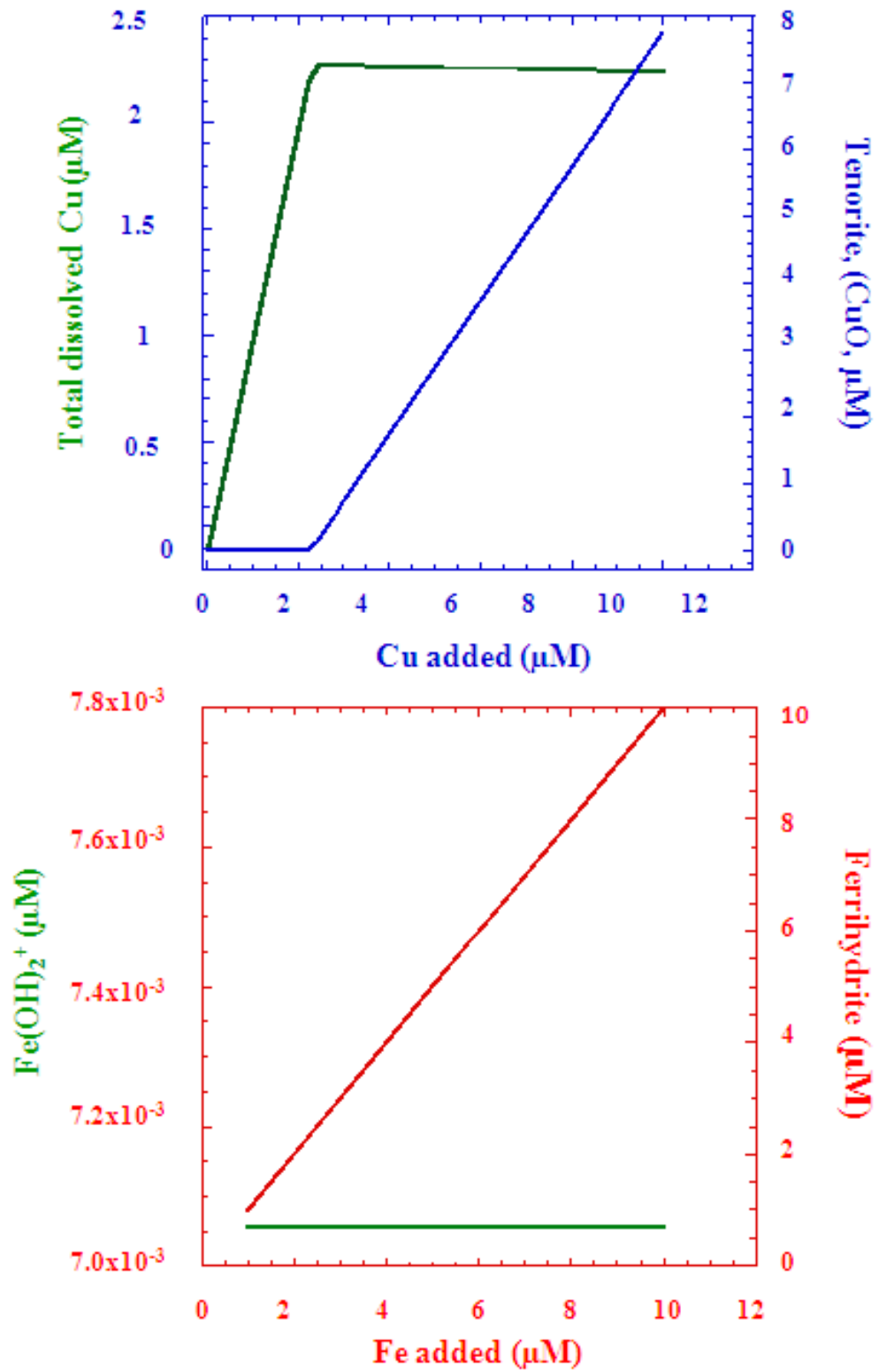


Figure 2.4: Solubility of (a) Cu(II) and (b) Fe (III) in bicarbonate-buffered saline solution at pH 6.8 modelled by PHREEQC-2.

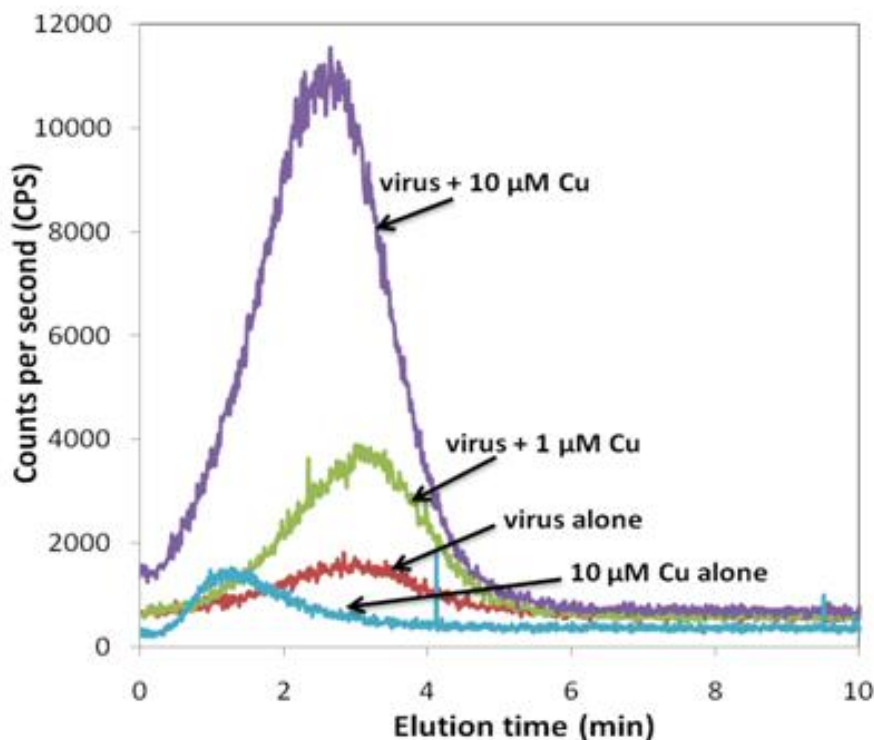


Figure 2.5: Separation of MS2-adsorbed Cu from free Cu by FFF-ICP-MS. MS2 phage was detected by UV absorbance at 280 nm and coincided with the ICP-MS peaks shown in the graph. Changes in the Cu content were recorded by ICP-MS in counts per second (CPS). MS2 = 2×10^{11} PFU mL⁻¹ in CBS, pH = 6.8. The small peak in the virus-free control with 10 μ M Cu is indicative of the presence of Cu colloids.

2.3.3 Dependence of inactivation on HO[•] production

The main role of transition metals in Fenton/Fenton-like processes is to act as the catalyst for the production of oxidants, such as HO[•], which subsequently inactivate the viruses. A more direct measure for the effect of different metal concentrations on inactivation is thus the corresponding hydroxyl radical production rate (HO[•]). HO[•] for different metal concentrations in the absence of virus were determined by ESR using the spin-trapping method (Figure 2.6).

Similar to what was observed for MS2 inactivation (Figure 2.3a), the Cu/H₂O₂ system exhibited an HO[•] production trend that levelled off around 4 μ M of added Cu (Figure 2.6a). This trend in r_{OH} gives further evidence that the system was limited by Cu solubility, implying that only soluble Cu contributed to oxidant formation. Alternatively, the observed trend in HO[•] production by Cu/H₂O₂ may also result from increasing scavenging of HO[•] by Cu(I) at higher concentrations of added Cu [27].

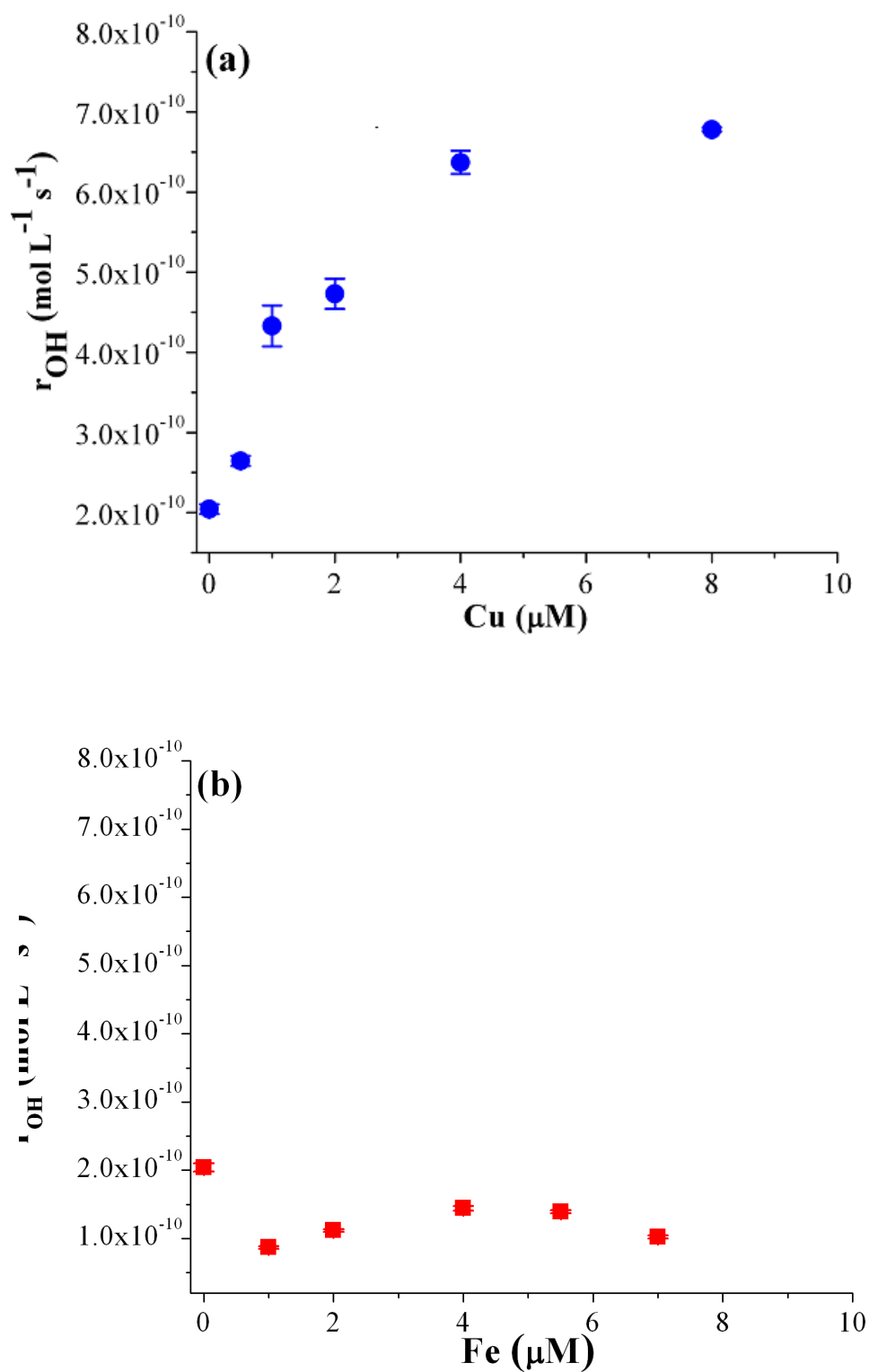


Figure 2.6: ESR-measured formation of hydroxyl radicals (HO^\bullet) in the presence of $50 \mu\text{M}$ H_2O_2 and different concentrations of (a) Cu(II) and (b) Fe(III) in CBS.

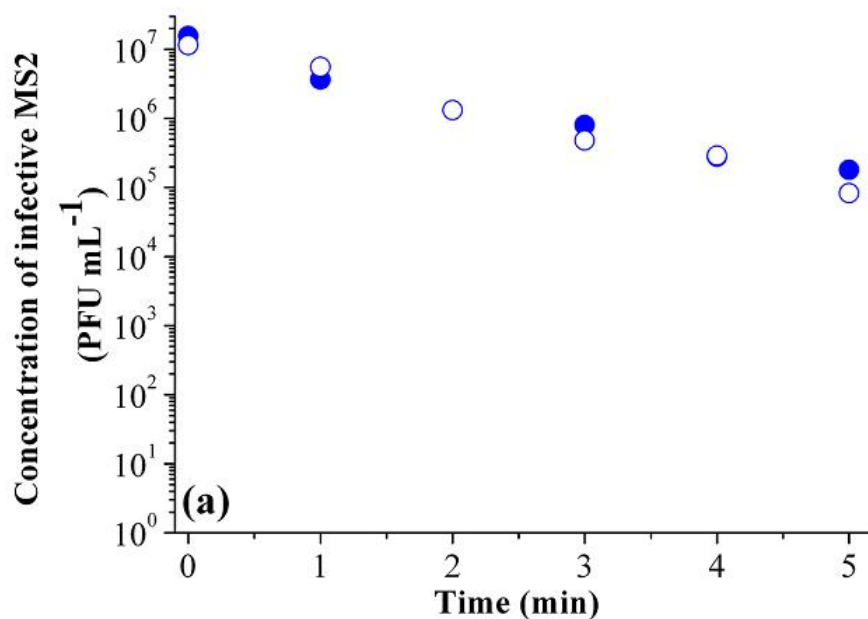
For the Fe/H₂O₂ system, the addition of 1 μ M Fe led to a decrease in r_{OH} compared to the r_{OH} in the Fe-free sample. The latter signal arises from traces amounts of oxidized DMPO present in the DMPO stock solution. This decrease in r_{OH} indicates that Fe acted as quencher for the background levels of oxidized DMPO [28]. A further increase in added Fe resulted in a slight increase in r_{OH} up to 4 μ M Fe. At higher added Fe concentrations, however, r_{OH} decreased (Fig. 2.6b). It should be noted that the DMPO-OH spin trapping product implicated in HO \bullet production can also arise from the spontaneous transformation of the spin trapping product of DMPO with superoxide [29]. Superoxide produced via Equation 2.1 and 2.3 may thus lead to an overestimation of HO \bullet . However, as the reaction rate constant of HO \bullet with DMPO at neutral pH is substantially higher than that of superoxide ($4.3 \times 10^9 \text{ M}^{-1} \text{ s}^{-1}$ and $30 \text{ M}^{-1} \text{ s}^{-1}$, respectively [30]), we believe that the contribution of superoxide to r_{OH} was insignificant in our experiments.

While HO \bullet production trend as a function of Cu concentration agreed well with the corresponding inactivation data, the dependence of r_{OH} and k_{obs} on the added Fe concentration differed considerably. Furthermore, k_{obs} for a given metal concentration varied by about a factor of 2-3 between the Cu- and the Fe- catalyzed systems (Fig. 2.3), but the corresponding HO \bullet varied by at least a factor of 4 (Fig. 2.6). These two findings illustrate that the production of HO \bullet in the bulk solution alone cannot account for the observed inactivation in both systems. This conclusion can be rationalized by assuming that HO \bullet was only the main oxidant in the Cu/H₂O₂ system, whereas inactivation in the Fe/ H₂O₂ system was dominated by an additional oxidant, presumably a ferryl species. The DMPO spin-trapping method does not yield information regarding the presence of ferryl species [31, 32], therefore its presence was not apparent from the ESR data. A contribution to inactivation from carbonate radicals, formed via the reaction of HO \bullet with the buffer, could be excluded, because the DMPO-adduct signal characteristic for carbonate radicals was not detected.

The inability of the bulk HO \bullet to account for inactivation could furthermore imply that only oxidants produced in close vicinity to the virus contributed to inactivation. A caged mechanism for protein oxidation mediated by protein-metal interactions has been proposed by various authors [33–35]. The observed differences in the Cu- and Fe- catalyzed Fenton systems may thus arise from different affinities of the two metals for the viral capsid. For example, Cu/H₂O₂ and Fe/H₂O₂ induced oxidation of albumin has been reported to occur by different mechanisms, with Cu ions binding to the protein and inducing site-specific damage, whereas Fe caused nonspecific oxidation [34]. The hypothesis of a caged inactivation mechanism in our systems was supported by the results obtained by aFIFFF-ICP-MS for the Cu-catalyzed system. This analysis revealed that Cu is adsorbed onto the viral capsid, and that the virus-associated Cu content increased with increasing Cu concentrations (Figure 2.5).

To test the involvement of a caged mechanism, inactivation experiments were conducted

in the presence of a scavenger. A negative effect of scavengers on k_{obs} is only apparent if bulk oxidants are involved in the inactivation process. Oxidants produced by a caged mechanism, however, are not susceptible to the presence of scavengers. Due to their close vicinity to the virus they cannot be scavenged before reaction with the virus capsid [34]. To ensure that both bulk ferryl and HO^\bullet were captured, the scavenger of choice was ethanol, which has been found to react with both oxidants [16]. Control experiments were conducted to verify that ethanol alone did not cause virus inactivation. The presence of ethanol did not decrease inactivation in either the $\text{Cu}/\text{H}_2\text{O}_2$ or the $\text{Fe}/\text{H}_2\text{O}_2$ system (Figure 2.7). This supports the proposition that only oxidants produced via a metal catalyst adsorbed onto or located in close vicinity to the virus contribute to inactivation. This result corresponds to previous findings by Kohn et al. [36], who showed that MS2 inactivation mediated by another oxidant, singlet oxygen, was governed by interactions of the oxidant source with the virus, whereas the contribution of the bulk singlet oxygen was secondary. Similarly, MS2 inactivation by heterogeneous photocatalysis using TiO_2 was found to correlate with virus adsorption onto the photocatalyst particles [37].



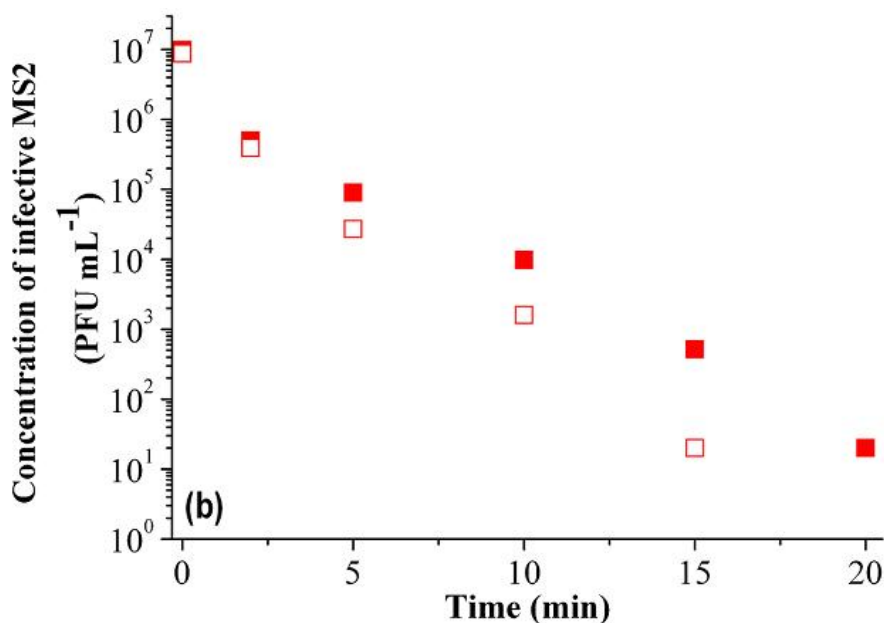


Figure 2.7: MS2 inactivation in the presence and absence of the hydroxyl radical and ferryl scavenger ethanol. (a) Cu/H₂O₂ system without (hollow blue circle) and with (solid blue circle) ethanol; (b) Fe/H₂O₂ without (hollow red square) and with (solid red square) ethanol. MS2= 10⁷ PFU mL⁻¹ in CBS, metal concentrations= 2.0 μM, H₂O₂= 50 μM, ethanol= 10 mM, pH= 6.8.

2.3.4 Influence of sunlight

At neutral pH, the Fe(III) surface hydroxyl species of amorphous iron(oxy)hydroxides can undergo photo-reduction to Fe(II) [38]. Light can furthermore exert an iron-reducing effect on Fe(III) complexed by organic ligands, such as natural organic matter [39, 40]. These ligands, which facilitate light absorption in the near UV and visible region, can cause a ligand-to-metal-charge transfer (LMCT), leading to the production of reduced Fe and oxidized ligands. Hence, light accelerates the rate-limiting production of Fe(II) and thus enhances the overall mechanism of oxidant production in the Fenton system.

Contrary to iron, the photoreduction of Cu(II) aqua species has not been reported. When complexed by organic ligands, however, Cu(II) has been found to undergo photoreduction induced by light in the UV/visible spectrum [41]. The relevance of this process in the production of oxidants via Fenton-like processes, however, has not been investigated.

Irradiation of our samples by simulated sunlight did not alter the MS2 inactivation kinetics in the Cu/H₂O₂ system compared to the corresponding system in the dark (data not shown). Even though we found that Cu adsorbed onto the viral capsid (Figure 2.5),

and such Cu-amino acid complexes readily photo-reduce Cu(II) [42], this process did not accelerate virus inactivation. Furthermore, the lack of virus inactivation by Cu and light in the absence of H₂O₂ indicates that direct oxidation of viral protein residues via LMCT either did not occur, or did not affect virus infectivity.

Irradiation of the Fe/H₂O₂ system, in contrast, had a drastic effect on inactivation. When experiments were conducted in the presence of Fe and 50 μM of H₂O₂, k_{obs} reached values of up to 3.1 min⁻¹ (Fig. 2.8a). This constitutes a 5.5-fold increase compared to the corresponding Fe/H₂O₂ system in the dark (Fig. 2.3b). Control experiments conducted in the absence of H₂O₂ exhibited a 3-fold increase in k_{obs} compared to the corresponding experiments in the dark, up to 0.38 min⁻¹ for 10 μM of Fe (III) (Figure 2.9). This indicates that viral protein oxidation by LMCT contributed to virus inactivation under simulated sunlight, but accounted for only a small fraction of the overall k_{obs} in the photo-Fenton system.

The rapid inactivation of MS2 in the photo-Fenton system coincided with a greatly enhanced production of HO• (Figure 2.8b) compared to the dark Fenton system (Figure 2.6b). The increase in r_{OH} upon irradiation, however, was significantly more pronounced than the corresponding effect of light on k_{obs} . The bulk production of HO• thus again cannot be responsible for the observed inactivation trend. As in the dark Fenton system, both ferryl and HO• can be produced in the photo-Fenton system [13]. However, the contribution of HO•, the stronger of the two oxidants, to inactivation is likely more significant in the photo-Fenton system than in the dark Fenton system, where HO• production was only minimal. This explains why in the photo-Fenton system k_{obs} and r_{OH} exhibit similar dependencies on the added Fe concentration (Figure 2.8), whereas this was not the case in the dark Fenton system, where inactivation was governed by ferryl (Figure 2.3b and 2.6b).

Based on our data, we can propose a mechanistic scheme for the inactivation of MS2 in Fenton/Fenton-like systems (Figure 2.10) that involves 1) the adsorption of Cu ions or Fe colloids onto the virus; 2) the production of HO• from virus-associated Cu, or of ferryl and minor amounts of HO• from virus-associated iron colloids. These oxidants react with the virus constituents and cause inactivation. In the photo-Fenton system, step 2) is shifted to a larger contribution of HO•-mediated inactivation compared to ferryl, as a result of increased HO• production upon irradiation by light.

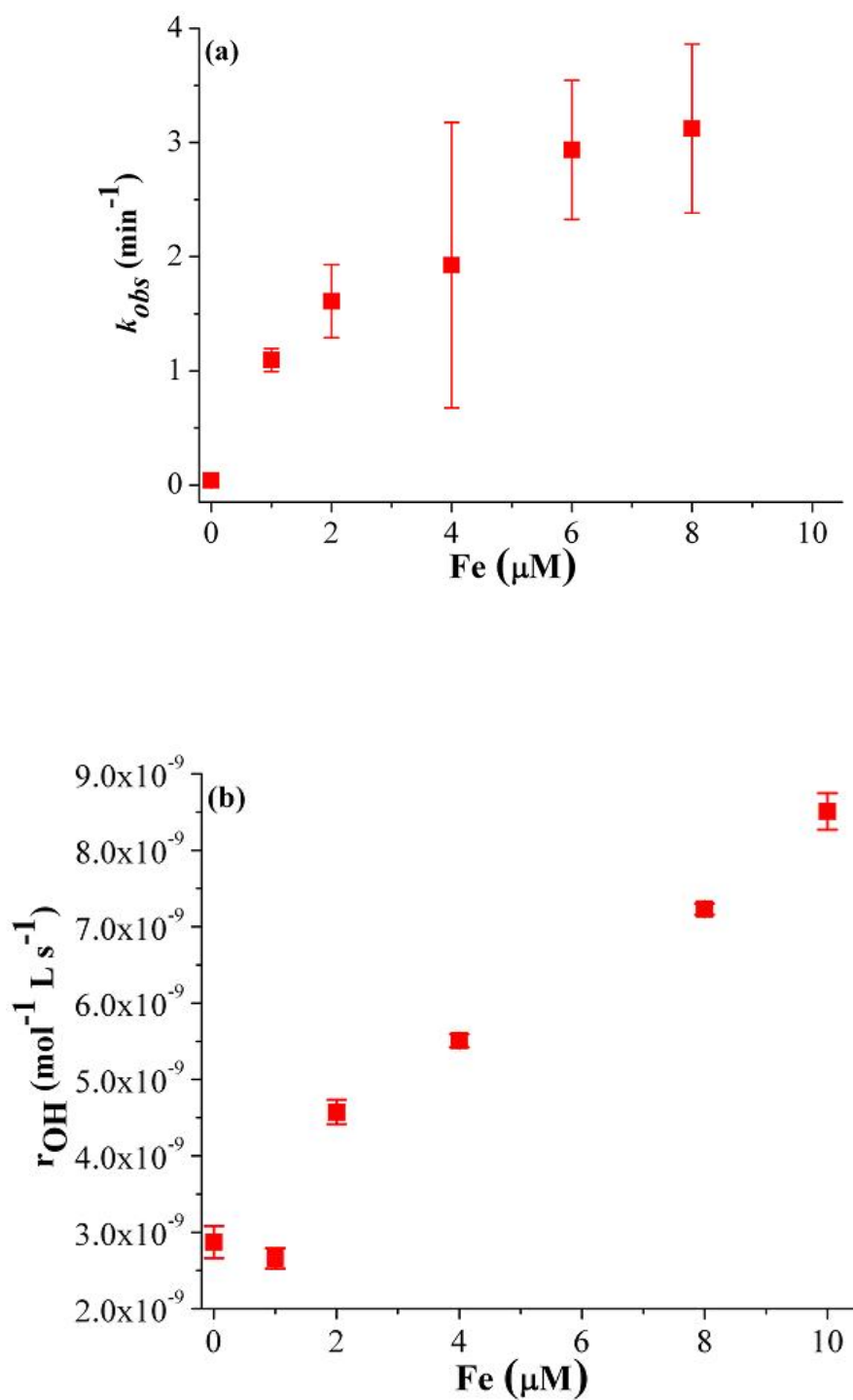


Figure 2.8: Effect of the sunlight on (a) MS2 inactivation and (b) ESR-measured formation of hydroxyl radicals (HO^\bullet) in the presence of $50 \mu\text{M H}_2\text{O}_2$ and different concentrations of Fe(III). MS2 = 10^7 PFU mL⁻¹ in CBS, pH = 6.8, $I = 300 \text{ W m}^{-2}$ for MS2 inactivation, $I = 10 \text{ mW cm}^{-2}$ (UVA) for HO^\bullet production

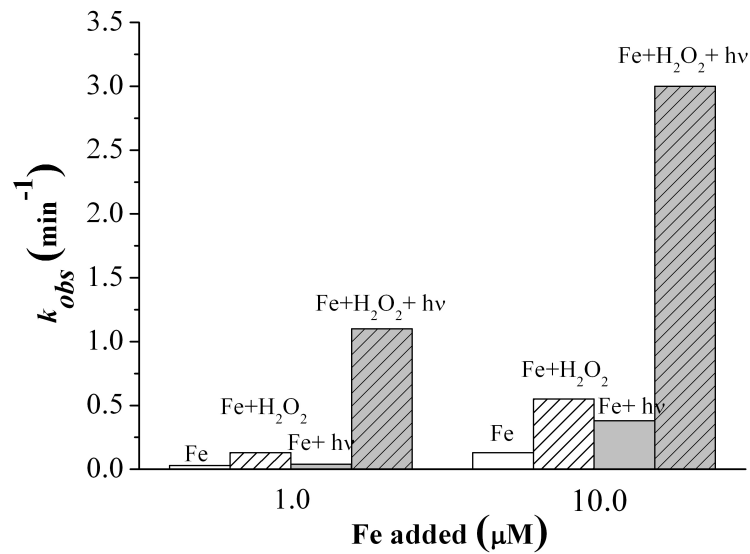


Figure 2.9: First-order inactivation rate constants measured for 1 and 10 μM Fe alone (simple bars) and in the presence of H_2O_2 (lined bars), in the dark (white) and under sunlight (grey). $\text{MS2} = 10^7$ PFU mL^{-1} in CBS, $\text{H}_2\text{O}_2 = 50$ μM , $\text{pH} = 6.8$.

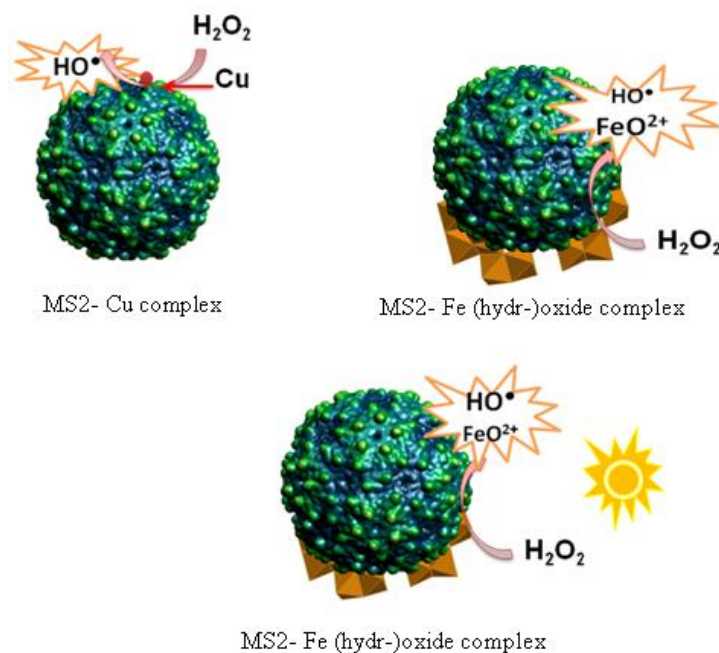


Figure 2.10: Scheme illustrating the inactivation of MS2 by (a) Cu- and Fe-catalyzed Fenton system in the dark, and by (b) Fe-catalyzed Fenton system under sunlight. Inactivation involves virus interactions with Cu ions and Fe colloids. Oxidants are produced from metal in close vicinity to the virus. In the Fe/ H_2O_2 system, ferryl ions dominate inactivation in the dark, whereas sunlight enhances production and contribution of HO^\bullet .

2.4 Conclusions

In AOPs, Fe and H₂O₂ concentrations significantly higher than the ones studied herein can be applied [13]. In conjunction with exposure to sunlight, photo-Fenton-based AOPs can therefore be expected to very rapidly inactivate viruses with morphological structures similar to that of MS2. Because inactivation proceeds efficiently even at low Fe concentrations and at neutral pH, it may be possible to avoid the two most common limitations of Fenton-based AOPs, namely sludge generation and pH control [13]. Compared to other light-based AOPs including UV/H₂O₂ or TiO₂/UV, the photo-Fenton process furthermore has the benefit of not requiring an energy-intensive light source. While heterogeneous photocatalysis using TiO₂ may also be modified to function with sunlight, Gerrity et al. [5] found that virus inactivation can be inhibited by insufficient interaction between the catalyst and the virus at the pH values encountered in water treatment applications. In contrast to TiO₂ used in that study (isoelectric point from 5.2 to 5.7), many iron (hydr-)oxides carry a positive charge at neutral pH [43], which facilitates interactions of iron colloids with the typically negatively charged viruses. We therefore believe that photo-Fenton-based AOPs have the potential to serve as efficient disinfection processes for waterborne viruses. Their applicability to other pathogens, however, remains to be fully tested. While viruses can be inactivated by direct reaction of disinfectants with the viral capsid [44], other organisms may require the diffusion of the disinfectant through an outer membrane to achieve an activating effect. For the inactivation of those pathogens, disinfectants with a short lifetime as the oxidants produced in the photo-Fenton process may not be suited.

In natural waters, the concentrations of H₂O₂ and metals are typically lower than those used in this study. Furthermore, in natural waters the complexation of the trace metals by organic matter may lead to a reduced Fenton activity. We therefore compared the virucidal activity of a sample containing 1 μ M Fe or Cu and 50 μ M H₂O₂ in carbonate-buffered saline to the same experimental conditions in a sample of Lake Geneva water. The constituents present in Lake Geneva water did not influence virus inactivation in the Cu/H₂O₂ system, whereas k_{obs} of the Fe/H₂O₂ system decreased to a third of the value obtained in buffer (data not shown). Taking into account this loss of reactivity in the Fe/H₂O₂ system, and assuming a linear dependence of k_{obs} down to environmentally relevant concentrations (500 nM H₂O₂, 1 μ M Fe), we can estimate k_{obs} arising from the photo-Fenton process to be $3 \times 10^{-3} \text{ min}^{-1}$. This implies that over the course of a day with 12 hours of sunlight, the virus concentration would decrease by approximately one order of magnitude due to inactivation by the photo-Fenton process. This estimate, however, is very rough, and further investigations are needed to more realistically evaluate the importance of the photo-Fenton reaction to virus inactivation in surface waters.

Bibliography

- [1] A. Bosch. Human enteric viruses in the water environment: A minireview. *International Microbiology*, 1:191–196, 1998.
- [2] B. H. Keswick, T. K. Satterwhite, P. C. Johnson, H. L. Dupont, S. L. Secor, J. A. Bitsura, G. W. Gary, and J. C. Hoff. Inactivation of Norwalk virus in drinking-water by chlorine. *Applied and Environmental Microbiology*, 50(2):261–264, 1985.
- [3] J. A. Thurston-Enriquez, C. N. Haas, J. Jacangelo, K. Riley, and C. P. Gerba. Inactivation of feline calicivirus and adenovirus type 40 by UV radiation. *Applied and Environmental Microbiology*, 69(1):577–582, 2003.
- [4] M. Cho, H. M. Chung, W. Y. Choi, and J. Y. Yoon. Different inactivation behaviors of MS2 phage and escherichia coli in TiO₂ photocatalytic disinfection. *Applied and Environmental Microbiology*, 71(1):270–275, 2005.
- [5] D. Gerrity, H. Ryu, J. Crittenden, and M. Abbaszadegan. Photocatalytic inactivation of viruses using titanium dioxide nanoparticles and low-pressure UV light. *Journal of Environmental Science and Health Part a: Toxic/Hazardous Substances and Environmental Engineering*, 43(11):1261–1270, 2008.
- [6] J. Simonet and C. Gantzer. Inactivation of poliovirus 1 and F-specific RNA phages and degradation of their genomes by UV irradiation at 254 nanometers. *Applied and Environmental Microbiology*, 72(12):7671–7677, 2006.
- [7] H. Mamane, H. Shemer, and K. G. Linden. Inactivation of E-coli, B-subtilis spores, and MS2, T4, and T7 phage using UV/H₂O₂ advanced oxidation. *Journal of Hazardous Materials*, 146(3):479–486, 2007.
- [8] J. Koivunen and H. Heinonen-Tanski. Inactivation of enteric microorganisms with chemical disinfectants, UV irradiation and combined chemical/UV treatments. *Water Research*, 39(8):1519–1526, 2005.
- [9] P. P. Vaughan and N. V. Blough. Photochemical formation of hydroxyl radical by constituents of natural waters. *Environmental Science and Technology*, 32(19):2947–2953, 1998.
- [10] H. Gallard, J. De Laat, and B. Legube. Spectrophotometric study of the formation of iron(III)-hydroperoxy complexes in homogeneous aqueous solutions. *Water Research*, 33(13):2929–2936, 1999.
- [11] S. Lee, J. Oh, and Y. Park. Degradation of phenol with Fenton-like treatment by using heterogeneous catalyst (modified iron oxide) and hydrogen peroxide. *Bulletin of the Korean Chemical Society*, 27(4):489–494, 2006.

-
- [12] S. S. Lin and M. D. Gurol. Catalytic decomposition of hydrogen peroxide on iron oxide: Kinetics, mechanism, and implications. *Environmental Science and Technology*, 32(10):1417–1423, 1998.
- [13] J. J. Pignatello, E. Oliveros, and A. MacKay. Advanced oxidation processes for organic contaminant destruction based on the Fenton reaction and related chemistry. *Critical Reviews in Environmental Science and Technology*, 36(1):1–84, 2006.
- [14] A. L. Teel, C. R. Warberg, D. A. Atkinson, and R. J. Watts. Comparison of mineral and soluble iron Fenton’s catalysts for the treatment of trichloroethylene. *Water Research*, 35(4):977–984, 2001.
- [15] S. J. Hug and O. Leupin. Iron-catalyzed oxidation of arsenic(iii) by oxygen and by hydrogen peroxide: pH-dependent formation of oxidants in the Fenton reaction. *Environmental Science and Technology*, 37(12):2734–2742, 2003.
- [16] C. R. Keenan and D. L. Sedlak. Factors affecting the yield of oxidants from the reaction of manoparticulate zero-valent iron and oxygen. *Environmental Science and Technology*, 42(4):1262–1267, 2008.
- [17] L. A. Reinke, J. M. Rau, and P. B. McCay. Characteristics of an oxidant formed during iron(II) autoxidation. *Free Radical Biology and Medicine*, 16(4):485–492, 1994.
- [18] F. J. Millero, R. L. Johnson, C. A. Vega, V. K. Sharma, and S. Sotolongo. Effect of ionic interactions on the rates of reduction of cu(II) with H₂O₂ in aqueous-solutions. *Journal of Solution Chemistry*, 21(12):1271–1287, 1992.
- [19] J. K. Kim and I. S. Metcalfe. Investigation of the generation of hydroxyl radicals and their oxidative role in the presence of heterogeneous copper catalysts. *Chemosphere*, 69(5):689–696, 2007.
- [20] N. Yamamoto, W. Haller, and C. W. Hiatt. Mechanism of inactivation of bacteriophages by metals. *Biochimica Et Biophysica Acta*, 91(2):257–&, 1964.
- [21] N. Yamamoto. Damage, repair and recombination. 2. Effect of hydrogen peroxide on bacteriophage genome. *Virology*, 38(3):457–&, 1969.
- [22] J. L. Sagripanti, L. B. Routson, and C. D. Lytle. Virus inactivation by copper or iron ions alone and in the presence of peroxide. *Applied and Environmental Microbiology*, 59(12):4374–4376, 1993.
- [23] A. H. Havelaar, M. Vanolphen, and Y. C. Drost. F-specific RNA bacteriophages are adequate model organisms for enteric viruses in fresh-water. *Applied and Environmental Microbiology*, 9(9):2956–2962, 1993.

- [24] B. M. Pelson, L. V. Martin, and T. Kohn. Quantitative PCR for determining the infectivity of bacteriophage MS2 upon inactivation by heat, UV-B radiation, and singlet oxygen: Advantages and limitations of an enzymatic treatment to reduce false-positive results. *Applied and Environmental Microbiology*, 75(17):5544–5554, 2009.
- [25] Y. E. Nesmelov and D. D. Thomas. Multibore sample cell increases EPR sensitivity for aqueous samples. *Journal of Magnetic Resonance*, 178(2):318–324, 2006.
- [26] F. X. Abad, R. M. Pinto, J. M. Diez, and A. Bosch. Disinfection of human enteric viruses in water by copper and silver in combination with low-levels of chlorine. *Applied and Environmental Microbiology*, 60(7):2377–2383, 1994.
- [27] G. V. Buxton, C. L. Greenstock, W. P. Helman, and A. B. Ross. Critical-review of rate constants for reactions of hydrated electrons, hydrogen-atoms and hydroxyl radicals (HO/O) in aqueous-solution. *Journal of Physical and Chemical Reference Data*, 17(2):513–886, 1988.
- [28] L. X. Li, Y. Abe, K. Kanagawa, N. Usui, K. Imai, T. Mashino, M. Mochizuki, and N. Miyata. Distinguishing the 5,5-dimethyl-1-pyrroline n-oxide (DMPO)-OH radical quenching effect from the hydroxyl radical scavenging effect in the ESR spin-trapping method. *Analytica Chimica Acta*, 512(1):121–124, 2004.
- [29] G. Bacic, I. Spasojevic, B. Secerov, and M. Mojovic. Spin-trapping of oxygen free radicals in chemical and biological systems: New traps, radicals and possibilities. *Spectrochimica Acta Part a: Molecular and Biomolecular Spectroscopy*, 69(5):1354–1366, 2008.
- [30] R. P. Mason, P. M. Hanna, M. J. Burkitt, and M. B. Kadiiska. Detection of oxygen-derived radicals in biological-systems using electron-spin-resonance. *Environmental Health Perspectives*, 102:33–36, 1994.
- [31] M. J. Burkitt. ESR spin-trapping studies into the nature of the oxidizing species formed in the Fenton reaction-pitfalls associated with the use of 5,5-dimethyl-1-pyrroline-N-oxide in the detection of the hydroxyl radical. *Free Radical Research Communications*, 18(1):43–57, 1993.
- [32] I. Yamazaki and L. H. Piette. EPR spin-trapping study on the oxidizing species formed in the reaction of the ferrous ion with hydrogen-peroxide. *Journal of the American Chemical Society*, 113(20):7588–7593, 1991.
- [33] M. Chevion. A site-specific mechanism for free-radical induced biological damage - the essential role of redox-active transition-metals. *Free Radical Biology and Medicine*, 5(1):27–37, 1988.

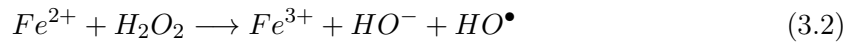
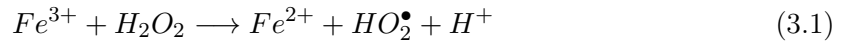
-
- [34] T. Kocha, M. Yamaguchi, H. Ohtaki, T. Fukuda, and T. Aoyagi. Hydrogen peroxide-mediated degradation of protein: Different oxidation modes of copper- and iron-dependent hydroxyl radicals on the degradation of albumin. *Biochimica Et Biophysica Acta-Protein Structure and Molecular Enzymology*, 1337(2):319–326, 1997.
- [35] E. R. Stadtman. Oxidation of free amino-acids and amino-acid-residues in proteins by radiolysis and by metal-catalyzed reactions. *Annual Review of Biochemistry*, 62:797–821, 1993.
- [36] T. Kohn, M. Grandbois, K. McNeill, and K. L. Nelson. Association with natural organic matter enhances the sunlight-mediated inactivation of MS2 coliphage by singlet oxygen. *Environmental Science and Technology*, 41(13):4626–4632, 2007.
- [37] Y. Koizumi and M. Taya. Kinetic evaluation of biocidal activity of titanium dioxide against phage MS2 considering interaction between the phage and photocatalyst particles. *Biochemical Engineering Journal*, 12(2):107–116, 2002.
- [38] T. D. Waite and F. M. M. Morel. Photoreductive dissolution of colloidal iron oxides in natural waters. *Environmental Science and Technology*, 18(11):860–868, 1984.
- [39] B. A. Southworth and B. M. Voelker. Hydroxyl radical production via the photo-Fenton reaction in the presence of fulvic acid. *Environmental Science and Technology*, 37(6):1130–1136, 2003.
- [40] R. G. Zepp, B. C. Faust, and J. Hoigne. Hydroxyl radical formation in aqueous reactions (pH 3-8) of iron(II) with hydrogen peroxide: the photo-Fenton reaction. *Environmental Science and Technology*, 26(2):313–319, 1992.
- [41] G. Ferraudi and S. Muralidharan. Photochemical properties of copper-complexes. *Coordination Chemistry Reviews*, 36(1):45–88, 1981.
- [42] K. Hayase and R. G. Zepp. Photolysis of copper(II)-amino acid complexes in water. *Environmental Science and Technology*, 25(7):1273–1279, 1991.
- [43] R.M. Cornell and U. Schwertmann. *The Iron oxides: Structure, Properties, Reactions, Occurrences and Uses*. Wiley-VCH, Weinheim, 2nd edition, 2003.
- [44] R. B. Thurman and C. P. Gerba. Molecular mechanisms of viral inactivation by water disinfectants. *Advances in Applied Microbiology*, 33:75–105, 1988.

Chapter 3

Virus removal and inactivation by heterogeneous Fenton-like processes under sunlight and in the dark

3.1 Introduction

The presence of human enteric viruses in aquatic environments used as drinking water sources poses a threat to public health. Conventional disinfection methods are often not able to completely inactivate viruses [1, 2]. Therefore new and more efficient treatment methods are needed to ensure microbial water quality. Advanced oxidation processes (AOPs) have emerged as a promising alternative to inactivate pathogenic microorganisms [3–5]. One of the most popular and widely applied AOPs is based on the Fenton process (Eqs. 3.1-3.2). In this process the strong oxidants, in particular hydroxyl radicals (HO^\bullet), are generated from H_2O_2 and dissolved Fe(II) ions.



Under typical water treatment conditions, however, the Fenton process is limited due to the low solubility and stability of Fe(II) and Fe(III) at neutral pH. A promising alternative is the heterogeneous Fenton-like process which uses iron (hydr-)oxide particles as the reactive iron source. Several studies have demonstrated the effective use of heterogeneous Fenton-like processes for water treatment purposes. These studies have shown

that iron-bearing minerals including goethite, hematite, magnetite and ferrihydrite can catalyze the oxidation of organic compounds by H_2O_2 over a pH range from 3 to 7 [6–11]. The exact reaction mechanism of this process has not been established to date. However, it is assumed that this process can be described by similar reactions as the homogeneous Fenton process, but with the difference that the decomposition of H_2O_2 takes place on the iron-bearing particle surface [12, 13].

Sunlight has been demonstrated to accelerate the homogeneous Fenton-like process at acidic pH. This is due to the efficient photo-reduction of the main dissolved Fe(III) species, $\text{Fe}(\text{OH})^{2+}$, to Fe(II), which leads to additional HO^\bullet generation (Eq. 3.3) [14].



A recent study by Nieto-Juarez et al. has demonstrated that sunlight also enhanced virus inactivation by a heterogeneous Fenton-like process catalyzed by colloidal iron at neutral pH [15]. Thus, sunlight may also enhance the heterogeneous Fenton-like process by iron-bearing particles, both by promoting the photo-reduction of Fe(III), which subsequently reacts with H_2O_2 (Eq. 3.2), and via the generation of HO^\bullet radicals at the particle surface in a reaction analogous to Eq. 3.3.

Alternatively, iron (hydr-)oxide particles may inactivate viruses via a photocatalytic process. In this scenario, the particles can act as semiconductors, which upon irradiation by sunlight generate various reactive oxygen species (ROS) such as hydroxyl radical (HO^\bullet), superoxide anion radical ($\text{O}_2^{\bullet-}$) and consequent production of hydrogen peroxide (H_2O_2) on the catalyst surface. These ROS may then react with the virus and cause inactivation [3, 16, 17].

Viruses are frequently found attached to solid surfaces and suspended particles in natural and wastewater [18–22]. If these viruses remain infectious upon adsorption, they may eventually desorb and contaminate the water source upon changes in solution conditions [23]. It is therefore critical to better understand the role of adsorption on inactivation, and to contrive methods which combine virus adsorption and their inactivation.

In this context, iron (hydr-)oxide particles are an obvious resource to investigate for their effect on microbial water quality. Such particles are of great interest for controlling virus fate in both natural and engineered systems, due to their high relative abundance in different aquatic environments, and due to the frequent use of iron-bearing particles for coagulation purposes in water treatment. Iron (hydr-)oxide particles may serve as both an effective sorbent for viruses, and as a basis for virus disinfection by AOPs.

The goal of this research was to investigate the fate of bacteriophage MS2, a commonly used surrogate for human viruses [24], in iron-bearing particle suspensions. In particular, the ability of four commercial iron (hydr-)oxide particles to adsorb and subsequently inactivate MS2 was investigated. The effect of the different particle types, H₂O₂ and sunlight on virus inactivation was studied. Quantitative polymerase chain reaction (qPCR) in combination with culturing assays was used to differentiate between true virus inactivation and irreversible adsorption onto iron-bearing particles.

3.2 Experimental Section

All experiments were performed in glass reactors (50 mL) containing 20 mL carbonate-buffered saline (CBS, 0.1 mM NaHCO₃ + 15 mM NaCl) at circumneutral pH, with an initial infective MS2 concentration of 10⁷ plaque-forming units (PFU) mL⁻¹ and 200 mg L⁻¹ of iron-bearing particles. Adsorption experiments were conducted by analyzing the suspended virus concentration as a function of exposure time of the virus to the iron-bearing particles. To promote inactivation, the viruses were pre-adsorbed onto the iron-bearing particles. Once adsorption equilibrium was attained, the samples were exposed to H₂O₂ and sunlight over the course of ten minutes to two hours. After treatment, the viruses were desorbed from the particles by addition of an eluant solution (BEEF solution) and enumerated by culturing assays. In addition, qPCR analyses were used to determine if the adsorption process by itself caused virus inactivation. After each experiment, the reactors were rinsed with hot hydrochloric acid followed by extensive water wash and finally autoclaved. All experiments were conducted in duplicate or triplicate, with good reproducibility.

3.2.1 Reagents and Organisms

3.2.1.1. Reagents

Sodium bicarbonate (NaHCO₃, 99+%) and sodium chloride (NaCl, 99+%) were obtained from Acrōs organics; hydrogen peroxide (H₂O₂, 30%), catalase (2950 units/mg solid) and EDTA were obtained from Sigma, Aldrich (St. Louis, Missouri).

3.2.1.2. Organisms

MS2 coliphage (DSMZ 13767) and its bacterial host *E. coli* (DSMZ 5695) was purchased from the German collection of microorganisms and cell cultures (DSMZ, Braunschweig, Germany). The propagation and purification of MS2 was performed as described previ-

ously in chapter 2. Infective MS2 phage was enumerated by culturing using the double-layer agar method [25]. Infective MS2 phage concentrations were measured in plaque-forming units per mL (PFU mL⁻¹).

3.2.1.3. Iron-bearing particles

Commercial iron (hydr-)oxide particles, namely hematite (α -Fe₂O₃), goethite (α -FeOOH), magnetite (Fe₃O₄) and an iron(III) hydroxide (Fe(OH)₃) slurry were purchased from NAOH Technologies Corporation, USA. All particles were of similar size (< 325 mesh, < 3 μ m). The main properties of the particles are shown in Table 3.1. The specific surface area of the particles was determined by the Brunauer-Emmett-Teller (BET) adsorption method (Nova 9000, Quantachrome instruments) using N₂ as the adsorbate. Isoelectric point measurements (IEPs) were conducted by AcoustoSizer (Colloidal Dynamics, USA), and IEPs were calculated assuming that all particles are spherical.

Table 3.1: Chemical formula, BET surface area and isoelectric point (IEP) of the particles investigated.

Name	Formula	BET surface area (m ² g ⁻¹)	IEP
Hematite	α -Fe ₂ O _{3(s)}	8.9	9.1
Goethite	α -FeOOH _(s)	13.7	6.34
Magnetite	Fe ₃ O _{4(s)}	1.6	6.0-6.8 [26] ¹
Fe(III) hydroxide	Fe(OH) _{3(slurry)}	— ¹	— ¹

¹not measurable by BET and Acoustosizer

3.2.2 Virus adsorption experiments

Reactors containing MS2 in CBS and 200 mg L⁻¹ of iron-bearing particles were stirred with a magnetic stir bar at 430 rpm in the dark on a multi-position stir plate. In the case of magnetite, virus adsorption was performed in plastic reactors (20 mL) and mixed on a rotator shaker (Labnet, LabRoller Rotators) at 30 rpm, to avoid particle

adhesion to the magnetic stir bar. Over the course of six hours, sample aliquots were periodically collected from the reactors, and the suspension was immediately filtered through a polyethersulfone membrane (0.2 μm pore size) to separate the adsorbed from the suspended viruses. The infective viruses in the filtrate were quantified by culturing.

3.2.3 Adsorption-mediated inactivation experiments

To determine if adsorption alone causes virus inactivation, MS2 phage was exposed to 200 mg L^{-1} of iron-bearing particles until adsorption was equilibrium attained (four hours). Then, the viruses were desorbed from the particles by adding an eluant solution (3% beef extract and 50 mM Glycine in CBS at pH 9.0; BEEF) [27]. 20 mL of a two-fold concentrated BEEF solution was added to the reactors containing 20 mL of sample. This suspension was stirred for 20 minutes to obtain an effective desorption of the viruses from the particles. The solution was subsequently filtered through a polyethersulfone membrane (0.2 μm pore size) to separate the particles from the suspended viruses. The concentration of infective viruses in solution was quantified by culturing. In addition, the total (both infective and inactivated) virus concentration was determined by qPCR. For this purpose, the viral RNA was extracted from 200 μL aliquots of the desorbed virus solution, and enumerated by qPCR as described previously [25].

3.2.4 (Photo-) Fenton-mediated inactivation experiments

Iron-bearing particles were added to a solution of MS2 in CBS to a concentration of 200 mg L^{-1} , and the virus was left to pre-adsorb until adsorption equilibrium was reached. Then, virus inactivation was studied for each particle type in the dark and under sunlight in a buffer only, as well as in the presence of H_2O_2 . H_2O_2 was added to the reactor as the last component, at a concentration of 50 μM . In addition, 2 μM of EDTA were added to complex any trace metals such as Cu, which has previously been found to cause inactivation at trace concentrations in the presence of H_2O_2 at neutral pH [15]. This concentration of EDTA did not cause virus inactivation (data not shown). In experiments involving sunlight, the H_2O_2 concentration was maintained approximately constant by continuously replenishing the decomposed H_2O_2 by means of a syringe pump filled with a 0.4 mM H_2O_2 solution and operating at rate of 9.5 $\mu\text{L min}^{-1}$ over 2 hours. This measure was necessary for experiments involving goethite and hematite particles only.

Sunlight experiments were carried out using a solar simulator (ABET Technologies, Sun 2000) equipped with a 1000 W Xe lamp, an AM1.5 filter and UVB cut-off filter. The last filter was used to avoid confounding effects arising from direct genome damage induced by UVB light. The irradiance was 320 W m^{-2} . The sample temperature was controlled by placing the reactors in a cooled water bath at 20 ± 2 $^\circ\text{C}$. For the experiments in the

dark, the reactors were covered with aluminium foil to protect the samples from light.

Virus inactivation was monitored over the course of 10 minutes to 2 hours. Aliquots (500 μL) were periodically collected from sacrificial reactors and filtered through a 0.2 μm membrane. This sample served to confirm that the virus had remained adsorbed during the experiment. In addition, 20 mL of BEEF was added to the remaining suspension in the reactor, to desorb and quantify the remaining infective virus concentration. All samples containing H_2O_2 , were immediately diluted with CBS amended with catalase (500 units mL^{-1}), to scavenge the remaining H_2O_2 .

3.2.5 Light screening correction and surface area normalization

The observed first-order inactivation rate constants (k_{obs} ; min^{-1}) were calculated from the slope of a linear regression between $\ln([\text{virus}]_t/[\text{virus}]_o)$ versus time. Due to the absorption and scattering of light in the particle-containing solution, k_{obs} was corrected by a light screening factor (SF), to obtain an inactivation rate constant for optically dilute solutions (k_{obs}^o). This correction enabled a direct comparison of the inactivation rate constants obtained for the different particles and allowed the extrapolation to other experimental configurations. The screening factor was calculated as described by Schwarzenbach et al. [28]. It takes into account the whole wavelength range of interest, where (cm^{-1}) is the absorbance of the suspension at each wavelength (λ).

$$SF = \frac{\sum_{\lambda}(1 - 10^{-\alpha(\lambda) \cdot z})}{\sum_{\lambda} 2.3 \cdot \alpha(\lambda) \cdot z} \quad (3.4)$$

α_{λ} was determined by spectrophotometer (Shimadzu, model UV 2450-2550) equipped with an integrating sphere attachment, to account for light scattering (Figure 3.1). z is the total depth of irradiated solution (cm). Light screening factors calculated by Eq. 3.4 were 0.66, 0.65, 0.95, 0.46 for $\alpha\text{-Fe}_2\text{O}_3$, $\alpha\text{-FeOOH}$, Fe_3O_4 and $\text{Fe}(\text{OH})_3$ respectively. The light screening-corrected inactivation rate constants (k_{obs}^o , min^{-1}) were calculated as:

$$k_{obs}^o = k_{obs}(SF)^{-1} \quad (3.5)$$

The inactivation rate constant was either expressed on a per mass basis (k_{obs}^o) or on a surface area-normalized basis (k_{obs}^1) as shown in Eq. 3.6.

$$k_{obs}^1 = k_{obs}^o(\rho_a)^{-1} \quad (3.6)$$

k_{obs}^1 ($L\ m^{-2}\ min^{-1}$) was expressed as a function of the surface concentration, ρ_a ($m^2\ L^{-1}$), which is the product of the particle concentration ($g\ L^{-1}$) and the surface area ($m^2\ g^{-1}$) [29].

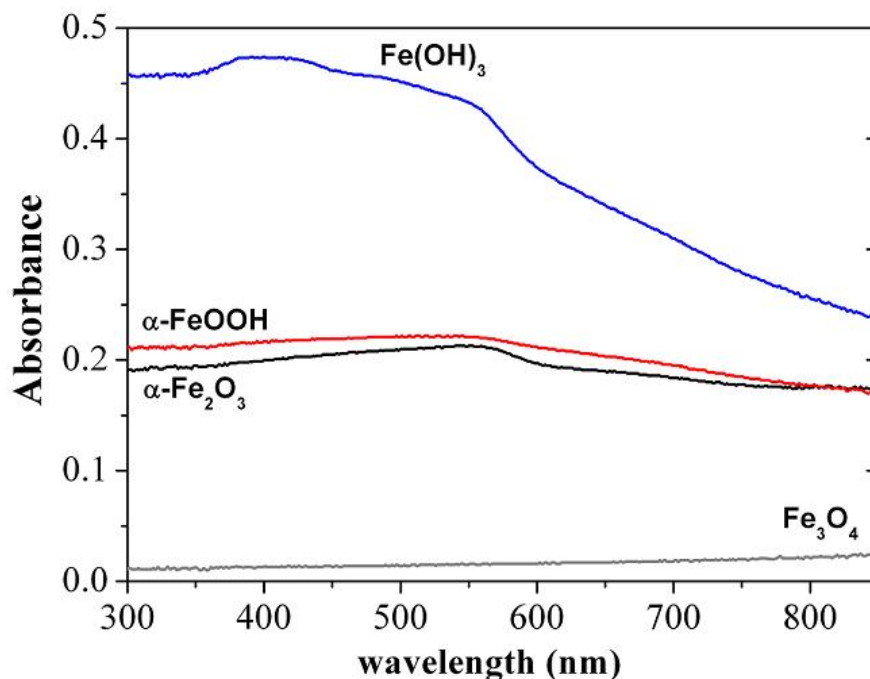


Figure 3.1: Absorbance spectra of the different iron (hydr-)oxide particles suspended in CBS. Spectra were obtained by UV/VIS spectrophotometer with an integrating sphere kit. Iron (hydr-)oxides= 200 mg L^{-1} , CBS buffer= 0.1 mM $NaHCO_3$ +15 mM $NaCl$, pH= 6.9 (α - Fe_2O_3 , α - $FeOOH$) and 6.4 (Fe_3O_4 , $Fe(OH)_3$).

3.3 Results and Discussion

3.3.1 Virus adsorption onto iron particles

Virus adsorption onto iron (hydr-)oxide particles was studied to establish the time to attain the superficial adsorption equilibrium, and the particle type with the highest adsorption capacity (Figure 3.2). Because adsorption around pH 7 was poor for Fe_3O_4 and $Fe(OH)_3$, the sample pH was adjusted at 6.4 to increase the adsorption of MS2 onto these two particles. Adsorption equilibrium was established within four hours for all particles investigated (Figure 3.2a). Adsorption kinetics were analyzed according to the model described by Ho and McKay [30, 31] which assumes a pseudo-second order adsorption rate, described by Eqs. 3.7 and 3.8.

$$\frac{t}{q_t} = \frac{1}{h} + \frac{1}{q_e}t \quad (3.7)$$

$$h = k_e q_e^2 \quad (3.8)$$

In this model, q_t is the virus adsorption capacity at any time t (PFU g^{-1}), q_e is the maximum adsorption capacity (PFU g^{-1}) and k_e is the pseudo-second order rate constant of adsorption (PFU $^{-1}$ g min^{-1}). When considering all values of q_t and t until adsorption equilibrium was reached, a linear relation between t/q_t versus t was obtained for all experiments ($R^2 \geq 0.99$). MS2 adsorption onto iron particles thus followed pseudo-second order kinetics, and the corresponding fitted parameters can be seen in Table 3.2. Notably, on a mass basis, all particles showed a similar maximum adsorption capacity of $5.2\text{-}6.1 \times 10^4$ PFU g^{-1} , resulting in $4 \log_{10}$ (99.99%) removal of virus from solution (Figure 3.2b). If normalized by surface area, the adsorption capacity of Fe_3O_4 particles was approximately one order of magnitude greater (3.30×10^4 PFU m^{-2}) than for the other particles (Table 3.2). In contrast, the pseudo-second order adsorption rate constants on a mass basis as well as normalized by surface area differed by two orders of magnitude, with α -FeOOH absorbing at the fastest and $Fe(OH)_3$ at the slowest rate.

The observed adsorption behaviour cannot be explained by electrostatic interactions alone. Based on the measured IEP (Table 3.1), only hematite carries a net positive charge under our experimental conditions, and would therefore exert an electrostatic attraction on the negatively charged MS2 (IEP of 3.9; [32]). However, similar adsorption capacities and faster adsorption rates were observed for those particles which had IEPs well below the solution pH. Therefore others factors must contribute to the observed adsorption, such as hydrophobic interactions or van der Waals forces [33]. In addition, it should be noted that measured IEP values were in poor agreement with values published in the literature and in the case of Fe_3O_4 , the surface charge was too low to obtain a measurement. This is indicative of impurities and organic coatings present on the particle surfaces which may further influence virus-particle interactions.

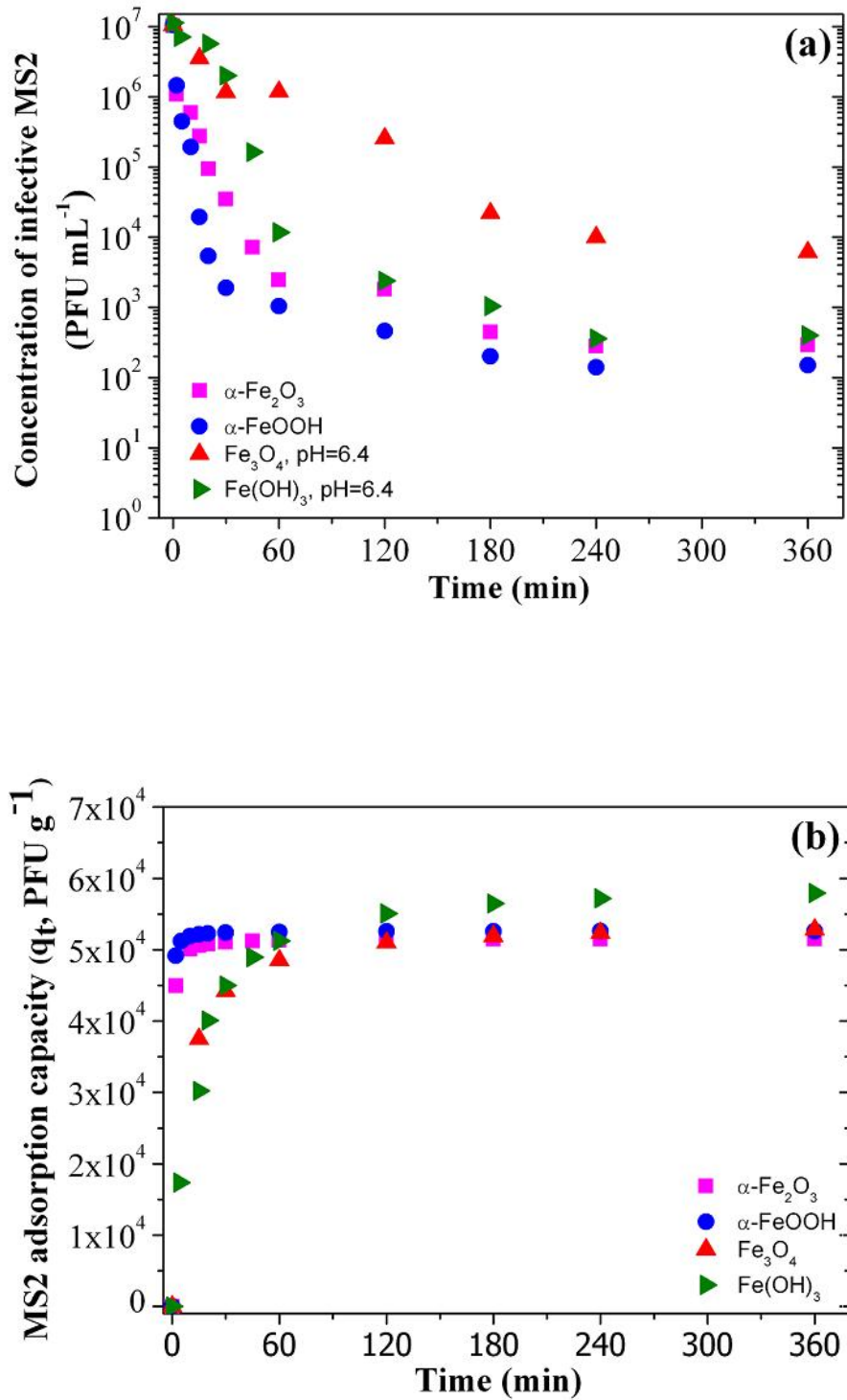


Figure 3.2: (a) Concentration of infective suspended MS2 and (b) adsorbed MS2 as a function of time. MS2= 10⁷ PFU mL⁻¹, iron (hydr-)oxide particles= 200 mg L⁻¹, CBS buffer= 0.1 mM NaHCO₃+15 mM NaCl, stirring= 430 rpm.

Table 3.2: Fitted kinetic parameters of the MS2 adsorption onto iron particles evaluated from the pseudo-second order kinetic model expressed in mass and surface units.

Iron (hydr-)oxide particles	Maximum adsorption capacity per mass q_e , (PFU g ⁻¹)	Rate constant of pseudo-second order adsorption k_e , (g PFU ⁻¹ min ⁻¹)
α -Fe ₂ O ₃	5.16×10^4	6.56×10^{-5}
α -FeOOH	5.26×10^4	1.35×10^{-4}
Fe ₃ O ₄	5.42×10^4	2.49×10^{-6}
Fe(OH) ₃	6.10×10^4	1.50×10^{-6}
Iron (hydr-)oxide particles	Maximum adsorption capacity per surface area q_e , (PFU m ⁻²)	Rate constant of pseudo-second order adsorption k_e , (m ² PFU ⁻¹ min ⁻¹)
α -Fe ₂ O ₃	5.82×10^3	5.82×10^{-4}
α -FeOOH	3.83×10^3	1.86×10^{-3}
Fe ₃ O ₄	3.30×10^4	4.09×10^{-6}
Fe(OH) ₃	—	—

3.3.2 Contribution of virus adsorption to inactivation

The loss of infectious virus from solution by adsorption onto various iron-bearing particles has received considerable scrutiny. However, only few investigations stringently differentiated between virus loss due to adsorption as opposed to true inactivation. Furthermore, the mechanisms leading to particle-mediated inactivation have not been clarified to date. Murray and Laband reported virus disintegration arising from adsorption to certain metal oxide particles [34]. In particular, they studied the adsorption of polioviruses consisting of ^3H -labelled RNA and ^{14}C -labelled protein onto various inorganic surfaces, and then compared infectivity and radioactivity (^3H and ^{14}C) upon elution of the viruses from the surfaces. For CuO , Al_2O_3 and MnO_2 , virus adsorption caused a greater loss of infectivity in comparison to the recovered radioactivity, indicating virus inactivation. Furthermore, in the case of CuO , the RNA and protein desorbed from the surfaces to a different extent, indicating that the virus had disintegrated. Fe_2O_3 and SiO_2 , in contrast, did not cause inactivation. A similar approach developed by Ryan et al. suggested that the adsorption of bacteriophage PRD1 (^{35}S - protein capsid labeled) and MS2 (^{35}S protein-capsid and ^{32}P -RNA labeled) to iron oxide coated quartz sand caused inactivation by capsid disintegration [35].

To differentiate between virus inactivation and irreversible adsorption by iron (hydr-) oxide particles used in this study, we applied an approach based on the combination of culturing assays and qPCR analysis. qPCR was used to determine the total virus content (of both infective and inactivated virus) in solution after virus desorption, while the culturing assays measured the infective virus only. The difference between the initial infective virus concentration (determined by culturing in particle-free control samples) and the infective virus concentration after desorption from the particles yielded the total loss of virus by irreversible adsorption as well as inactivation. The difference between the initial, qPCR-measured virus concentration and that measured after desorption indicated the amount of virus lost by irreversible adsorption only. Finally, the difference between the concentration determined by qPCR and by culturing upon desorption specified the contribution from true virus inactivation only.

Culturing results (Fig. 3.3) showed that goethite ($\alpha\text{-FeOOH}$), magnetite (Fe_3O_4) and amorphous Fe(III) hydroxide ($\text{Fe}(\text{OH})_3$) caused a total loss of infectious virus of 97.8% ($1.66 \log_{10}$), 87.4% ($0.90 \log_{10}$), 99.3% ($2.18 \log_{10}$) respectively. The loss in qPCR signal, and hence the contribution of irreversible adsorption, in contrast, amounted to only 85.5% ($0.84 \log_{10}$), 46.3% ($0.27 \log_{10}$) and 77.6% ($0.65 \log_{10}$) respectively. This indicates that the loss in infective MS2 from solution was a result of both virus inactivation and irreversible adsorption. While the contribution of inactivation was significant, it was not sufficient to ensure microbiologically safe water in the case that viruses desorb from the particles upon changes in solution conditions. Such an occurrence could arise upon an increase in organic matter content or pH [23].

In the case of $\alpha\text{-Fe}_2\text{O}_3$ a loss of infective virus of 88.5% ($0.94 \log_{10}$) was observed upon desorption from the particle. This loss could be entirely attributed to irreversible adsorption, as both the qPCR and the culturing signal exhibited the same concentration decrease compared to the control sample.

Our results show that virus inactivation by particle adsorption is not correlated to the adsorption rate constant, nor the adsorption capacity nor the IEP. The material property determining virus survival thus remains to be clarified. The data did indicate that hydroxides are more efficient at inactivating MS2 than oxides (Figure 3.3). This observation, however, remains to be confirmed with a bigger set of materials.

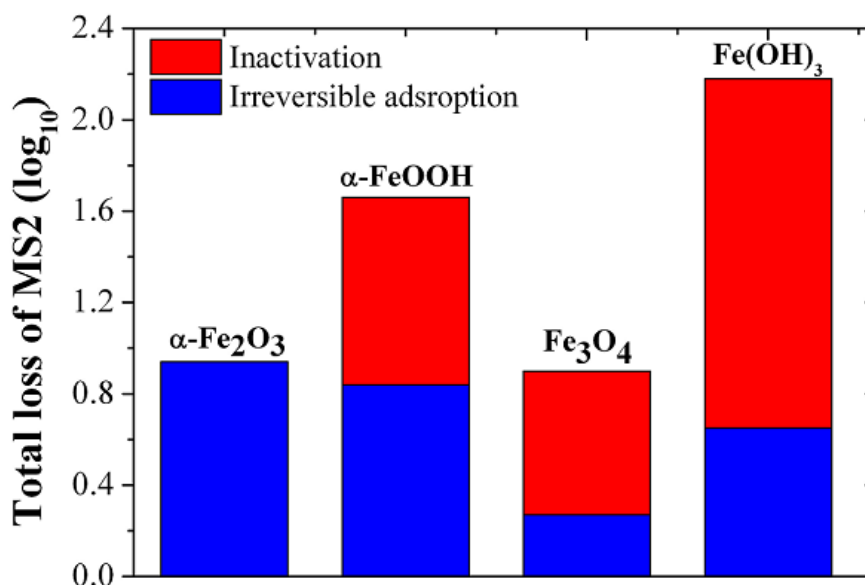


Figure 3.3: Comparison of total virus loss from solution, loss attributable to irreversible adsorption and loss attributable to inactivation. MS2= 10^7 PFU mL⁻¹, CBS buffer= 0.1 mM NaHCO₃+15 mM NaCl, BEEF solution= 3% beef extract+0.5 M glycine, pH= 6.9 ($\alpha\text{-Fe}_2\text{O}_3$, $\alpha\text{-FeOOH}$) and 6.4 (Fe_3O_4 , Fe(OH)_3), stirring= 430 rpm.

3.3.3 Contribution of the heterogeneous (photo-)Fenton-like process to virus inactivation

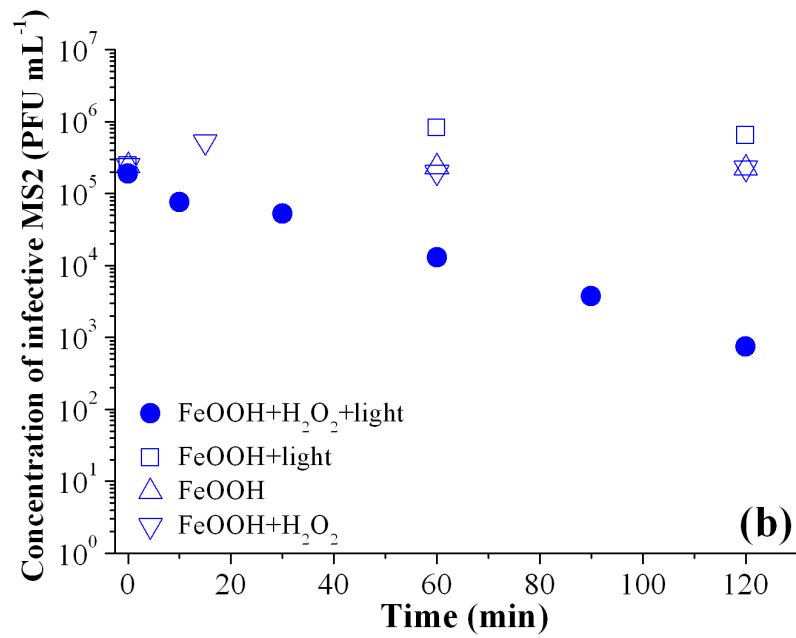
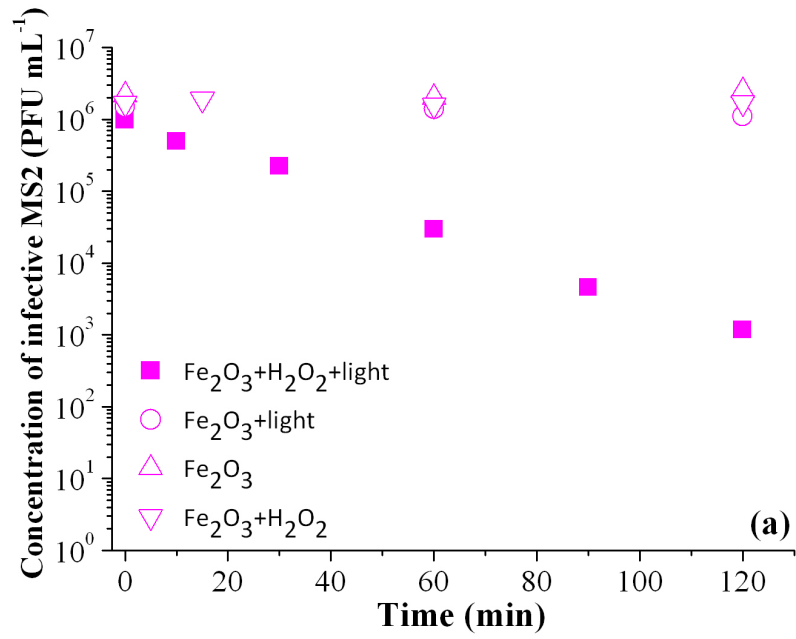
A controversy exists regarding the exact role of particles on virus survival during light-mediated disinfection. Some authors have demonstrated that particle association enhanced the survival of viruses during UV irradiation because particles exerted a light-shielding effect [36–38]. Others authors, however, have shown that virus adsorption onto a catalyst (TiO₂) surface was beneficial for photocatalytic inactivation, because it placed the virus in close vicinity to surface-produced oxidants such as HO• [39]. Similarly, in

our previous work, we have demonstrated that virus association with Fe colloids was beneficial for inactivation by a Fenton-like process, due to the virus proximity to the source of oxidants [15].

To determine if iron (hydr-)oxide particles cause virus inactivation by photocatalytic or Fenton-like reactions, we conducted MS2 inactivation studies in the presence of the different iron-bearing particles, as well as H_2O_2 and sunlight. The combination of particles and either H_2O_2 or sunlight alone did not yield inactivation for $\alpha\text{Fe}_2\text{O}_3$, $\alpha\text{-FeOOH}$, and amorphous $\text{Fe}(\text{OH})_3$ (Fig. 3.4a-c), indicating that neither dark Fenton-like processes, nor photocatalytic processes, contributed to virus inactivation under our experimental conditions. In the case of Fe_3O_4 , significant inactivation was observed in the dark in the presence of H_2O_2 (Fig. 3.4d), with a surface-normalized inactivation rate constant k_{obs}^l of $1.20 \text{ L m}^{-2} \text{ min}^{-1}$ (Table 3.3). The fact that only Fe_3O_4 was capable of inactivating viruses in the dark can be rationalized by the presence of structural Fe(II) and Fe(III), which could thus serve as a direct source of Fe (II) to catalyze the Fenton-like reaction. In contrast, the other particles which contain only Fe(III) have to rely on the reduction of Fe(III) by H_2O_2 (Eq. 3.1) to accumulate sufficient Fe(II) to induce a noticeable Fenton effect.

For all Fe(III)-containing particles, the simultaneous presence of sunlight and H_2O_2 caused considerable virus inactivation (Fig. 3.4). In the case of magnetite (Fe_3O_4), sunlight only slightly increased virus inactivation compared to the Fenton process in the dark. Light screening corrected rate constants on both a mass and a surface area-normalized basis followed the order k_{obs} (Fe(III) hydroxide) $\approx k_{obs}$ (magnetite) $> k_{obs}$ (hematite) $> k_{obs}$ (goethite) (Table 3.3).

Several authors have reported that particle-mediated Fenton-like processes generate reactive species on the particle surface, including hydroxyl radicals (HO^\bullet) [40, 41] and ferryl ions, Fe(IV) [42]. As all the particles investigated absorb light in the UVA and visible range used for irradiation in these experiments (Figure 3.1), we postulate that the simulated sunlight promoted photo-reduction of structural Fe(III) to Fe(II). The subsequent increase in oxidant formation compared to dark conditions may then be responsible for the observed virus inactivation under sunlight at neutral pH [41].



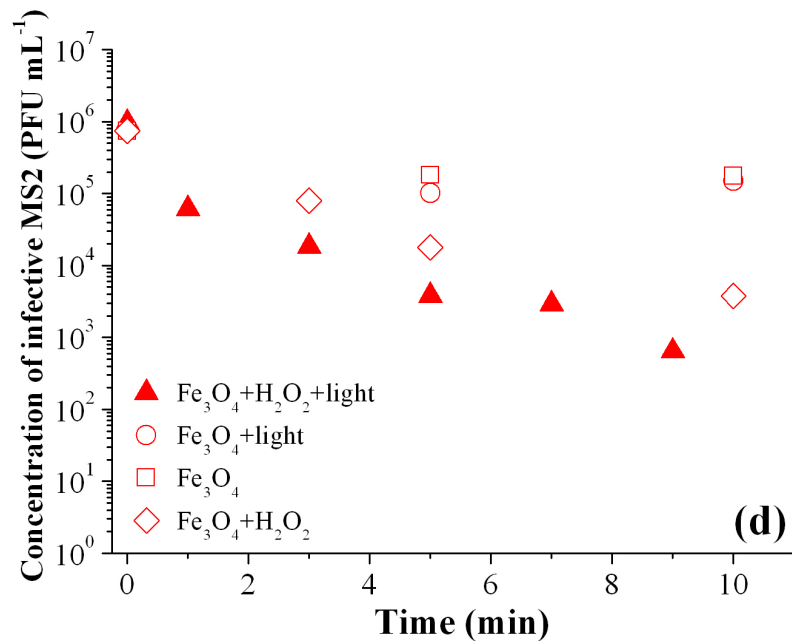
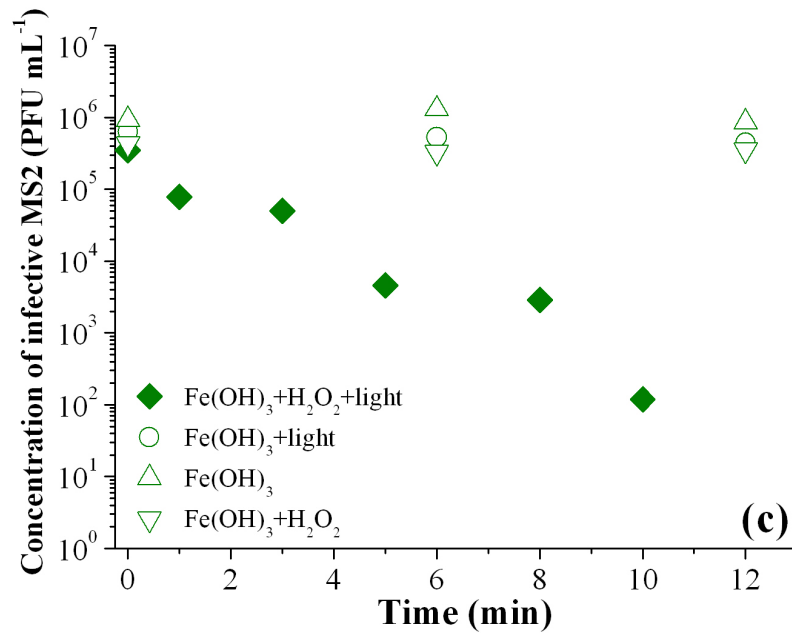


Figure 3.4: Figure MS2 inactivation by iron (hydr-)oxide particles in the presence and absence of sunlight and H₂O₂. (a) hematite, (b) goethite, (c) amorphous Fe(III) hydroxide and (d) magnetite. MS2= 10⁷ PFU mL⁻¹, Fe-bearing particles= 200 mg L⁻¹, H₂O₂= 50 μM, BEEF solution= 3% beef extract+0.5 M glycine, CBS buffer= 0.1 mM NaHCO₃+15 mM NaCl, pH= 6.9, irradiance= 320 W m⁻², stirring= 430 rpm.

Table 3.3: Light screening corrected and surface area normalized pseudo-first order inactivation rate constants by particles-catalyzed photo-Fenton-like process.

Iron (hydr-)oxide particles	Inactivation rate constants (corrected for light screening) k_{obs}^o (min^{-1})	R^2
$\alpha\text{-Fe}_2\text{O}_3$	1.44×10^{-3}	0.995
$\alpha\text{-FeOOH}$	1.09×10^{-3}	0.987
Fe_3O_4	0.58 (light) ² /0.39 (dark)	0.970/0.983
$\text{Fe}(\text{OH})_3$	1.48	0.912
Iron (hydr-)oxide particles	Inactivation rate constants (light screening corrected and surface area normalized) k_{obs}^1 ($\text{L m}^{-2} \text{min}^{-1}$)	R^2
$\alpha\text{-Fe}_2\text{O}_3$	8.14×10^{-4}	0.995
$\alpha\text{-FeOOH}$	3.99×10^{-4}	0.987
Fe_3O_4	1.76 (light) ² /1.20 (dark)	0.970/0.983
$\text{Fe}(\text{OH})_3$	—	—

²encompasses both dark and photo-Fenton

3.3.4 Importance of adsorption in the Fenton-mediated inactivation process

To demonstrate that adsorption was a necessary means to achieve inactivation, experiments using magnetite were conducted at pH 7.5, where the viruses were suspended, and at pH 6.4, where the viruses were adsorbed. This setup allowed us to compare the inactivation rates of suspended and adsorbed viruses in the presence of H_2O_2 and sunlight. Results showed that while the adsorbed virus was rapidly inactivated (Fig.

3.4d), the suspended virus remained infective (data not shown). Control experiments using hematite particles, which absorb viruses at both pH values, demonstrated that the difference in pH alone did not account for this difference in inactivation. This indicates that MS2 adsorption onto the particles is instrumental for promoting virus inactivation. The sole presence of particles in solution in the absence of virus-particle interaction, in contrast, has little or no effect on virus infectivity.

3.4 Conclusions

The main implication based on these results is that the heterogeneous photo-Fenton-like processes catalyzed by iron-bearing particles under sunlight may serve as a disinfection method for waterborne viruses. Due to their low cost, simple handling and safe use for water treatment, these materials may find applications in both developing and industrialized countries. This study thus has shown that iron (hydr-)oxide particles can combine physical virus removal from solution, with virus inactivation. All iron particles exhibited a virus removal of greater than 99.99% by partly irreversible adsorption. Adsorption furthermore caused slight inactivation, except in the case of hematite, for which particles desorbed in an infective state. In addition, all particles caused MS2 inactivation via a photo-Fenton-like process. In the dark and in the presence of H_2O_2 , only the magnetite particle caused significant virus inactivation.

An ideal particle for virus inactivation would fulfil several requirements: it would 1) adsorb viruses over a wide range of pH values; 2) achieve a high adsorption capacity; 3) inactivate viruses by adsorption alone or 4) inactivate viruses via a photo-Fenton-like process. None of the particles investigated fulfil all these requirements. Of the particles studied, amorphous $\text{Fe}(\text{OH})_3$ was found to be the most effective at inactivating MS2. This applies to both inactivation induced by adsorption alone, as well as to the photo-Fenton-like process. However, a limitation of this particle is that virus adsorption was slow compared to the other particles investigated. In addition, amorphous $\text{Fe}(\text{OH})_3$ required a pH below 7 to achieve significant virus adsorption, which was found to be a prerequisite for efficient inactivation. These limitations are overcome by goethite, which adsorbs particles at higher pH values, and at a faster rate. This, however, comes at the expense of less efficient adsorption-mediated-inactivation, as well as slower photo-Fenton-like inactivation. Further research should thus aim at identifying the most suited iron particles for this application, with respect to adsorption efficiency, inactivation efficiency, and stability over time. In addition, future studies should take into account the effect of co-solutes such as anions and natural organic matter present in natural and engineered systems, as they may compete with viruses for particle adsorption sites.

Bibliography

- [1] B. H. Keswick, T. K. Satterwhite, P. C. Johnson, H. L. Dupont, S. L. Secor, J. A. Bitsura, G. W. Gary, and J. C. Hoff. Inactivation of Norwalk virus in drinking-water by chlorine. *Applied and Environmental Microbiology*, 50(2):261–264, 1985.
- [2] J. A. Thurston-Enriquez, C. N. Haas, J. Jacangelo, K. Riley, and C. P. Gerba. Inactivation of feline calicivirus and adenovirus type 40 by UV radiation. *Applied and Environmental Microbiology*, 69(1):577–582, 2003.
- [3] M. Cho, H. M. Chung, W. Y. Choi, and J. Y. Yoon. Different inactivation behaviors of MS2 phage and escherichia coli in TiO₂ photocatalytic disinfection. *Applied and Environmental Microbiology*, 71(1):270–275, 2005.
- [4] J. Koivunen and H. Heinonen-Tanski. Inactivation of enteric microorganisms with chemical disinfectants, UV irradiation and combined chemical/UV treatments. *Water Research*, 39(8):1519–1526, 2005.
- [5] G. A. Shin and M. D. Sobsey. Reduction of Norwalk virus, Poliovirus 1, and bacteriophage MS2 by ozone disinfection of water. *Applied and Environmental Microbiology*, 69(7):3975–3978, 2003.
- [6] W. P. Kwan and B. M. Voelker. Decomposition of hydrogen peroxide and organic compounds in the presence of dissolved iron and ferrihydrite. *Environmental Science and Technology*, 36(7):1467–1476, 2002.
- [7] W. P. Kwan and B. M. Voelker. Rates of hydroxyl radical generation and organic compound oxidation in mineral-catalyzed Fenton-like systems. *Environmental Science and Technology*, 37(6):1150–1158, 2003.
- [8] M. D. Gurol and S. S. Lin. Hydrogen peroxide/iron oxide-induced catalytic oxidation of organic compounds. *Water Science and Technology: Water Supply*, 1(4):131–138, 2001.
- [9] E. Rodriguez, G. Fernandez, B. Ledesma, P. Alvarez, and F. J. Beltran. Photocatalytic degradation of organics in water in the presence of iron oxides: Influence of carboxylic acids. *Applied Catalysis B: Environmental*, 92(3-4):240–249, 2009.
- [10] R. Matta, K. Hanna, and S. Chiron. Fenton-like oxidation of 2,4,6-trinitrotoluene using different iron minerals. *Science of the Total Environment*, 385(1-3):242–251, 2007.
- [11] H. H. Huang, M. C. Lu, and J. N. Chen. Catalytic decomposition of hydrogen peroxide and 2-chlorophenol with iron oxides. *Water Research*, 35(9):2291–2299, 2001.

-
- [12] S. S. Lin and M. D. Gurol. Catalytic decomposition of hydrogen peroxide on iron oxide: Kinetics, mechanism, and implications. *Environmental Science and Technology*, 32(10):1417–1423, 1998.
- [13] M. C. Lu, J. N. Chen, and H. H. Huang. Role of goethite dissolution in the oxidation of 2-chlorophenol with hydrogen peroxide. *Chemosphere*, 46(1):131–136, 2002.
- [14] J. J. Pignatello, E. Oliveros, and A. MacKay. Advanced oxidation processes for organic contaminant destruction based on the Fenton reaction and related chemistry. *Critical Reviews in Environmental Science and Technology*, 36(1):1–84, 2006.
- [15] J. I. Nieto-Juarez, K. Pierzchała, A. Sienkiewicz, and T. Kohn. Inactivation of MS2 coliphage in Fenton and Fenton-like systems: role of transition metals, hydrogen peroxide and sunlight. *Environmental Science and Technology*, 44(9):3351–3356, 2010.
- [16] D. Gerrity, H. Ryu, J. Crittenden, and M. Abbaszadegan. Photocatalytic inactivation of viruses using titanium dioxide nanoparticles and low-pressure UV light. *Journal of Environmental Science and Health Part a: Toxic/Hazardous Substances and Environmental Engineering*, 43(11):1261–1270, 2008.
- [17] S. Lee, M. Nakamura, and S. Ohgaki. Inactivation of phage Q beta by 254nm UV light and titanium dioxide photocatalyst. *Journal of Environmental Science and Health Part a: Toxic/Hazardous Substances and Environmental Engineering*, 33(8):1643–1655, 1998.
- [18] P. Payment, E. Morin, and M. Trudel. Coliphages and enteric viruses in the particulate phase of river water. *Canadian Journal of Microbiology*, 34(7):907–910, 1988.
- [19] A. P. Wyn-Jones and J. Sellwood. Enteric viruses in the aquatic environment. *Journal of Applied Microbiology*, 91(6):945–962, 2001.
- [20] M. R. Templeton, R. C. Andrews, and R. Hofmann. Particle-associated viruses in water: Impacts on disinfection processes. *Critical Reviews in Environmental Science and Technology*, 38(3):137–164, 2008.
- [21] G. Bitton. Adsorption of viruses onto surfaces in soil and water. *Water Research*, 9(5-6):473–484, 1975.
- [22] A. Sakoda, Y. Sakai, K. Hayakawa, and M. Suzuki. Adsorption of viruses in water environment onto solid surfaces. *Water Science and Technology*, 35(7):107–114, 1997.
- [23] B. Pecson, L. Decrey, and T. Kohn. Photoinactivation of virus on iron-oxide coated sand: enhancing inactivation in sunlit waters. *Water Research*, 2012. In Press.

- [24] F. Lucena, F. Ribas, A. E. Duran, S. Skrabber, C. Gantzer, C. Campos, A. Moron, E. Calderon, and J. Jofre. Occurrence of bacterial indicators and bacteriophages infecting enteric bacteria in groundwater in different geographical areas. *Journal of Applied Microbiology*, 101(1):96–102, 2006.
- [25] B. M. Pecson, L. V. Martin, and T. Kohn. Quantitative PCR for determining the infectivity of bacteriophage MS2 upon inactivation by heat, UV-B radiation, and singlet oxygen: Advantages and limitations of an enzymatic treatment to reduce false-positive results. *Applied and Environmental Microbiology*, 75(17):5544–5554, 2009.
- [26] R.M. Cornell and U. Schwertmann. *The Iron oxides: Structure, Properties, Reactions, Occurrences and Uses*. WILEY-VCH, 2003.
- [27] L. Gutierrez, X. Li, J. W. Wang, G. Nangmenyi, J. Economy, T. B. Kuhlenschmidt, M. S. Kuhlenschmidt, and T. H. Nguyen. Adsorption of rotavirus and bacteriophage MS2 using glass fiber coated with hematite nanoparticles. *Water Research*, 43(20):5198–5208, 2009.
- [28] R.P. Schwarzenbach, P.M. Gschwend, and D.M. Imboden. *Environmental Organic Chemistry*. John Wiley & Sons, Inc., New Jersey, 2003.
- [29] D. M. Cwiertny and A. L. Roberts. On the nonlinear relationship between $k(\text{obs})$ and reductant mass loading in iron batch systems. *Environmental Science and Technology*, 39(22):8948–8957, 2005.
- [30] Y. S. Ho and G. McKay. Pseudo-second order model for sorption processes. *Process Biochemistry*, 34(5):451–465, 1999.
- [31] Y. S. Ho and G. McKay. A comparison of chemisorption kinetic models applied to pollutant removal on various sorbents. *Process Safety and Environmental Protection*, 76(B4):332–340, 1998.
- [32] B. Michen and T. Graule. Isoelectric points of viruses. *Journal of Applied Microbiology*, 109(2):388–397, 2010.
- [33] C. P. Gerba. Applied and theoretical aspects of virus adsorption to surfaces. *Advances in Applied Microbiology*, 30:133–168, 1984.
- [34] J. P. Murray and S. J. Laband. Degradation of Poliovirus by adsorption on inorganic surfaces. *Applied and Environmental Microbiology*, 37(3):480–486, 1979.
- [35] J. N. Ryan, R. W. Harvey, D. Metge, M. Elimelech, T. Navigato, and A. P. Pieper. Field and laboratory investigations of inactivation of viruses (PRD1 and MS2) attached to iron oxide-coated quartz sand. *Environmental Science and Technology*, 36(11):2403–2413, 2002.

- [36] M. R. Templeton, R. C. Andrews, and R. Hofmann. Inactivation of particle-associated viral surrogates by ultraviolet light. *Water Research*, 39(15):3487–3500, 2005.
- [37] H. Babich and G. Stotzky. Reductions in inactivation rates of bacteriophages by clay-minerals in lake water. *Water Research*, 14(2):185–187, 1980.
- [38] M. R. Templeton, R. C. Andrews, and R. Hofmann. Impact of iron particles in groundwater on the UV inactivation of bacteriophages MS2 and T4. *Journal of Applied Microbiology*, 101(3):732–741, 2006.
- [39] Y. Koizumi and M. Taya. Kinetic evaluation of biocidal activity of titanium dioxide against phage MS2 considering interaction between the phage and photocatalyst particles. *Biochemical Engineering Journal*, 12(2):107–116, 2002.
- [40] S. Lee, J. Oh, and Y. Park. Degradation of phenol with fenton-like treatment by using heterogeneous catalyst (modified iron oxide) and hydrogen peroxide. *Bulletin of the Korean Chemical Society*, 27(4):489–494, 2006.
- [41] J. He, W. H. Ma, J. J. He, J. C. Zhao, and J. C. Yu. Photooxidation of azo dye in aqueous dispersions of H₂O₂/α-FeOOH. *Applied Catalysis B: Environmental*, 39(3):211–220, 2002.
- [42] S. J. Hug and O. Leupin. Iron-catalyzed oxidation of arsenic(III) by oxygen and by hydrogen peroxide: pH-dependent formation of oxidants in the Fenton reaction. *Environmental Science and Technology*, 37(12):2734–2742, 2003.

Chapter 4

Protein and genome damage in MS2 coliphage upon inactivation by Fenton like-systems

4.1 Introduction

Advanced oxidation processes (AOPs) have emerged as efficient methods to inactivate pathogens in water [1–3]. A promising AOP is the Fenton process, due to its low-cost, simple handling and safe use for water treatment. Our previous study (chapter 2) has shown that virus inactivation can occur by (photo-) Fenton-like processes at neutral pH [4]. In particular, we have found that hydroxyl radicals (HO^\bullet), are generated from H_2O_2 and either dissolved $\text{Cu}(\text{II})$ in the dark or colloidal iron under sunlight. This radical was proposed to be responsible for inactivating MS2, a commonly used surrogate for human enteric viruses. However, very little is known about the nature of damage incurred in the virus and which virus constituents are the most susceptible to degradation by HO^\bullet .

Like human enteric viruses, MS2 is a non-enveloped virus which consist of a genome (single-stranded RNA, 3569 nucleotides) surrounded by a capsid composed of 180 copies of the capsid protein (13.7 kDa, 129 amino acids). In addition, the virus contains a single copy of an assembly protein (A protein, 43.9 kDa, 339 amino acids).

Oxidative damage to the virus capsid proteins, the A protein or the ssRNA may contribute to inactivation. Damage to the virus proteins may result in the inability of the virus to attach to its host, or to inject the genome into the host. Damage to the genome may inhibit replication of the virus by the host cell. Each of these occurrences would essentially constitute an inactivating event. However, oxidative damage to both proteins

and genome may also occur without disrupting any biological function.

Several authors have reported that reactive oxygen species (ROS), such as singlet oxygen ($^1\text{O}_2$) and hydroxyl radicals (HO^\bullet) cause protein modifications by oxidizing the amino acid residues in biological systems [5–7]. The amino acids cysteine, methionine, tryptophan, tyrosine and histidine are the most susceptible to oxidation by $^1\text{O}_2$ [8]. In contrast HO^\bullet radicals are more reactive and non-selective. They can therefore oxidize all amino acid residues in a protein. For example, Davies et al. showed that HO^\bullet radicals modified all the amino acids contained in bovine serum albumin; yet tryptophan, tyrosine, histidine and cysteine remained the most susceptible residues [9]. Despite the importance of protein oxidation by ROS, the oxidation products formed have not been completely characterized.

In addition, ROS induce not only oxidative modifications to the proteins. It is also known that in biological systems, the genome is damaged by ROS. All four bases (adenine, cytosine, guanine and either thymine for DNA or uracil for RNA), and its nucleic acids can be damaged by these oxidants (HO^\bullet , $^1\text{O}_2$) [10–12]. The four bases of RNA genome are affected by oxidants in the order: Guanine > Uracil > Adenine > Cytosine. [13].

Several studies exist which characterize the nature of virus damage upon disinfection by different oxidants. Sano et al. have reported Astrovirus capsid protein damage via the measurement of the capsid carbonyl content induced upon the disinfection by free chlorine [14]. Li et al. have shown RNA genome damage upon the inactivation of hepatitis A virus by chlorine [15]. Kim et al. proposed that bacteriophage f2's RNA degraded, but only after the coat protein modified during disinfection by ozone [16].

Only few studies, however have reported the cause of the virus inactivation by ROS. Previous studies used PCR and agarose gel electrophoresis to determine that HO^\bullet generated by the TiO_2 photocatalytic disinfection induced genome damage in coliphages (RNA and DNA phages) [17, 18]. A more recent study used protein mass spectrometry to show that MS2 coliphage inactivation via UV254 and singlet oxygen ($^1\text{O}_2$) caused damage to the virus capsid proteins [19] and quantitative PCR (qPCR) to demonstrate damage to the virus genome [20]. Hotze et al. used FTIR spectroscopy and SDS-PAGE gel electrophoresis to detect oxidative modifications of the capsid protein and genome damage upon bacteriophage inactivation (MS2, PR1, T7) by $^1\text{O}_2$ [21]. However to date, very little molecular level information exists regarding virus damage by hydroxyl radicals (HO^\bullet) generated in Fenton-like systems.

The goal of this work was to investigate the damage induced in the MS2 genome and capsid proteins during inactivation by (photo-) Fenton-like processes, and to link the observed damage to inactivation. A better knowledge of the damage incurred is instru-

mental for an understanding of the molecular-level mechanisms governing inactivation. The Cu-catalyzed Fenton-like system and the Fe-catalyzed photo-Fenton-like system were studied, and the patterns of damage compared. Between two and three levels of virus inactivation were investigated for each treatment. Damage to different segments of the viral genome was quantified by qPCR. Overall loss of viral capsid protein and identification of the peptide segments affected was determined by MALDI-TOF-MS.

4.2 Experimental Section

MS2 capsid protein and genome damage were characterized upon inactivation by Fe(III)-catalyzed photo-Fenton and Cu(II)-catalyzed Fenton-like processes as previously described by Nieto et al. [4].

4.2.1 Reagents and Organisms

4.2.1.1. Reagents

Copper sulfate ($\text{CuSO}_4 \cdot 5\text{H}_2\text{O}$), hydrogen peroxide (H_2O_2 , 30%), EDTA, catalase (2000-5000 units mg^{-1} protein); sinapic acid (SA) and α -cyano-4-hydroxycinnamic acid (αCN), as MALDI-MS matrix compounds, were purchased from Sigma-Aldrich (St. Louis, Missouri). Ferric chloride ($\text{FeCl}_3 \cdot 6\text{H}_2\text{O}$), sodium bicarbonate (NaHCO_3 , 99+%), NaCl (99+%), CaCl_2 (99+%), NaH_2PO_4 (99+%), trifluoroacetic acid (TFA), acetonitrile (ACN, HPLC grade) were obtained from Acrōs Organics. Trypsin and Chymotrypsin were purchased from Worthington Biochemical Corporation (Lakewood, NJ).

4.2.1.2. Organisms

MS2 coliphage (DSMZ 13767) and its bacterial host *E. coli* (DSMZ 5695) were purchased from the German collection of microorganisms and cell cultures (DSMZ, Braunschweig, Germany). The propagation and purification of MS2 was performed as previously described in Chapter 2. Infective MS2 phage concentrations were enumerated by the double-layer agar method and measured in plaque-forming units per ml (PFU mL^{-1}). The MS2 stock solution obtained had a concentration of 10^{14} PFU mL^{-1} and was stored in dilution buffer (DB; 5 mM NaH_2PO_4 , 10 mM NaCl, pH 7.4) at 4 °C.

Bacterial *E. coli* (ATTC 15597) was obtained from LGC Standards, Molsheim, France, as the bacterial host for the propagation of ^{15}N -labeled MS2 phage. The bacterial culture was performed three times in a minimal M9 media using $^{15}\text{NH}_4\text{Cl}$ (Sigma-Aldrich, St.

Louis, Missouri) until reaching an optical density between 0.2 and 0.4 measured at 600 nm. A MS2 stock solution aliquot was spiked in a midlog phase *E coli* (roughly 10^8 CFU mL^{-1}) at a multiplicity of infection (ratio of phage to bacteria) of 1. For the propagation of ^{15}N -labeled MS2, the infected *E coli* was incubated at 37 °C for 24 hours. Then the bacterial cells were lysed with chloroform (5 mL) and immediately purified as previously described by Pecson et al. [20]. The ^{15}N -labeled MS2 phage stock solution obtained had a concentration of 10^{13} PFU mL^{-1} and was stored in DB at 4 °C.

4.2.2 Inactivation experiments

Experiments were carried out in sacrificial glass reactors (50 mL), with an initial infective MS2 concentration of 10^{10} PFU mL^{-1} (detection limit for the protein mass measurements) in 20 mL of CBS (0.1 mM NaHCO_3 +15 mM NaCl) at pH 6.9. Cu(II) or Fe(III) were added to the reactors from freshly prepared stock solutions (1 mM) to obtain a final concentration of 10 μM . H_2O_2 was added from a 25 mM stock solution to a final concentration of 50 μM . EDTA (2 μM) was added to the buffer to complex any trace metals, which have shown to catalyze Fenton-like process [4]. This EDTA concentration did not cause virus inactivation. The solutions were stirred at 400 rpm on a multi-position stir plate. To obtain different levels of inactivation, 500 μL of catalase (500 units mL^{-1}) were added to sacrificial reactors at different times to scavenge the remaining H_2O_2 and halt the Fenton-like reactions. Two or three levels of inactivation, as well as H_2O_2 -free control samples were evaluated. After catalase addition, sample aliquots were withdrawn from reactors for virus quantification by culturing. The remainder of the solution was used for genome and protein analysis as described below. All experiments were performed in triplicate.

Sunlight experiments were carried out using a solar simulator (ABET Technologies, Sun 2000) with 1000 W Xe lamp, an AM1.5 filter and UVB cut-off filter. The last filter was used to avoid confounding effects arising from direct genome damage induced by UVB light. The irradiance was 320 W m^{-2} . The sample temperature was controlled by placing the reactors in a cooled water bath at 20 ± 2 °C. For the experiments in the dark, the reactors were covered with aluminium foil, to protect the samples from light.

4.2.3 Measurements of genome damage by qPCR

Quantitative polymerase chain reaction (qPCR) was used to evaluate the genome damage of MS2 upon inactivation. 200 μL of samples were withdrawn from the reactors for the immediate extraction of virus genomes using a PureLink Viral RNA/DNA extraction kit (Invitrogen, Carlsbad, CA) according the manufacturer's procedure. Genome extracts were stored at 4 °C for the later quantification by PCR (RotorGene 3000 quantitative

PCR platform; Corbett Life Science, Sydney, Australia). Damage to six different genome segments of approximately 300 nucleotides was quantified. Jointly, the six segments covered around 50% of the entire genome. The exact location of the segments within the genome, as well as the primers used is described in Table 4.1. Each segment was first reverse transcribed and then amplified using the one step SYBR PrimeScript RT-PCR kit according the manufacturer’s procedure (Takara Bio Inc., Shiga, Japan). SYBR green was used as the fluorescent probe for all segments.

Damage to the entire genome was extrapolated from the measured damage to the six segments as described by Pecson et al. [22]. Briefly, the Pecson approach assumes that quantifying damage to half the genome is sufficient to even out any variation in the level of damage in different parts of the genome. The proportion of entirely intact genomes (N/N_o) in the sample at any level of inactivation can then be calculated as:

$$Proportion_{(intactgenome)} = (Proportion_{(intactover6segments)})^{\frac{genomelength}{lengthof6genomesegments}} \quad (4.1)$$

Where the proportion (intact over 6 segments) corresponds to the product of the intact proportions of each of the individual genome segments considered. Genome length corresponds to the MS2 total genome size (3569 nucleotides) and length of 6 genomes segments is the sum of each genome segment size shown in the Table 4.1.

4.2.4 Measurements of protein damage by MALDI-TOF-MS

Protein mass spectrometry was used to analyze the overall loss of intact capsid protein, as well as to identify the regions of the protein that were most susceptible to damage. To do so, first the loss of the full capsid protein was quantified. Subsequently, the protein was denatured, alkylated and digested into small peptides, and their individual losses were monitored.

12 μ L of 15 N-labeled MS2 virus was added to each reactor, as an internal standard, for the quantification of protein damage. The ratio of initial native MS2 (at $t=0$) to labeled MS2 was 1:1. These samples were concentrated to a volume of approximately 20 μ L using a centricon tube (Millipore, Billerica, MA). Aliquots of 5 μ L were withdrawn of the concentrated samples for full protein analysis by MALDI-TOF-MS. The remaining samples were denatured at 95 °C for 10 minutes, alkylated with iodoacetamide solution (25 mM) and digested by Trypsin and Chymotrypsin in Tris buffer (50 mM Tris-HCl, 2 mM $CaCl_2$, pH 8). The digestions were incubated while shaking overnight at 37 °C. The digested samples were eluted in acetonitrile (ACN) for analysis by mass spectrometry.

Table 4.1: Genome primer sets and segment sizes used upon the quantification of MS2 genome damage levels.

Primers^a	Direction	Primer sequence (5' to 3')	MS2 target location (nucleotide position)	Genome size (nt)
2	Forward	AAGGTGCCTACAAGCGAAGT	344 to 678	335
	Reverse	TTCGTTTAGGGCAAGGTAGC		
3	Forward	CCGCTACCTTGCCCTAAAC	657 to 959	303
	Reverse	GACGACAACCATGCCAAAC		
6	Forward	CCTAAAGTGGCAACCCAGAC	1530 to 1818	289
	Reverse	AAAGATCGCGAGGAAGATCA		
7	Forward	CGCGATCTTTCTCTCGAAAT	1809 to 2125	317
	Reverse	GACGATCGGTAGCCAGAGAG		
10	Forward	ATAGTCAAAGCGACCCAAATC	2724 to 3033	310
	Reverse	GGCGTGGATCTGACATACCT		
12	Forward	GAAATCACCGACAGCATGAA	3285 to 3528	244
	Reverse	AATCCCGGGTCCTCTCTTTA		

Calibration curves were obtained for the quantification of protein damage by analyzing six different ratios of native to labeled MS2 (ratio range 0.2-1.2). The standards were denatured, alkylated and digested in the same way as the samples (procedure described above) for the full protein and peptide analyses. MS2 capsid protein sequences and peptides generated by the digestion of protease enzymes (trypsin and chymotrypsin) are shown in Tables 4.2 and 4.3. Jointly, peptides digested by protease enzymes achieved a 98% coverage of the capsid protein.

Full protein and peptides analyses in the samples and standards were carried out by positive ion linear mode MALDI-TOF-MS (ABI 4800; Applied Biosystems, Rotkreuz, Switzerland). For the full protein analysis, the MALDI matrix used was 14 mg mL⁻¹ of sinapic acid solution in 50% ACN and 50% TFA (0.1%) as the solvent; the matrix used for peptide analysis was 7 mg mL⁻¹ of α -cyano-4-hydroxy-cinnamic acid diluted in the same solvent. The ratio between matrix and sample was 10 to 1. These mixtures of each sample were placed on the MALDI plate by quadruped and air-dried for analysis. MALDI spectra were analyzed with Applied Biosystems Data Explorer Software.

Table 4.2: Amino acid sequence of the MS2 capsid protein.

Amino acid sequence

ASNFTQFVLV¹⁰DNGGTGDVTV²⁰APSNFANGVA³⁰EWISSNSRSQ⁴⁰
AYKVTCSVRQ⁵⁰SSAQNRKYTI⁶⁰KVEVPKVATQ⁷⁰TVGGVELPVA⁸⁰
AWRSYLN MEL⁹⁰TIPIFATNSD¹⁰⁰CELIVKAMQG¹¹⁰LLKDGNPIPS¹²⁰
AIAANS GIY¹²⁹

Table 4.3: Peptides generated by the protease enzymes of MS2 capsid protein.

M+1	Position	sequence
<i>Chymotrypsin</i>		
814.373	1-7	ASNFTQF
1761.865	8-25	VLVDNGGTGDVTVAPSNF
746.347	26-32	ANGVAEW
1112.533	33-42	ISSNSRSQAY
2492.412	59-82	TIKVEVPKVATQTVGGVELPVAAW
1687.865	113-129	DGNPIPSAIAANSGIY
<i>Trypsin</i>		
596.304	39-43	SQAYK
664.345	44-49	VTCSVR
790.380	50-56	QSSAQNR
1753.960	67-83	VATQTVGGVELPVAAWR
2614.314	84-106	SYLNMELTIPIFATNSDCELIVK
760.438	107-113	AMQGLLK

4.3 Results and Discussion

Inactivation experiments were conducted for Cu(II)/H₂O₂ and Fe(III)/H₂O₂/sunlight systems (Figure 4.1). As observed previously inactivation only occurred if a metal ion and H₂O₂ were present simultaneously. In the H₂O₂-free control samples, an apparent decrease of approximately 90% (1 log loss) in infective virus was observed for both systems (Figure 4.1). This decrease in the number of plaques may be due to either virus aggregation or inactivation [23, 24]. Analyses by qPCR and MALDI-TOF-MS showed that the virus capsid protein and genome remained intact under these concentrations of metal ions (data not shown). This finding is consistent with the loss of plaques being a result of virus aggregation due to the presence of 10 μ M Cu or Fe ions, rather than inactivation. Furthermore, our previous studies, showed that no inactivation was observed in the metal-free control samples i.e. in the presence of H₂O₂ alone [4].

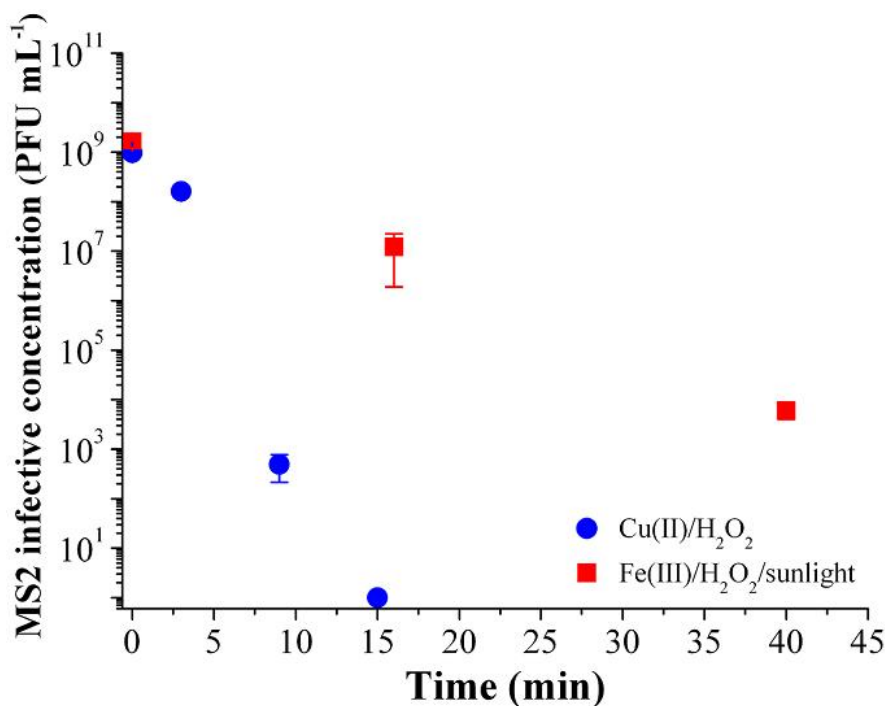


Figure 4.1: MS2 inactivation by Cu(II)/H₂O₂ and Fe(III)/H₂O₂/sunlight systems. Initial infective MS2 concentration= 10¹⁰ PFU mL⁻¹, metals= 10 μ M, H₂O₂= 50 μ M, EDTA= 2 μ M, stirring= 400 rpm, I= 320 W m⁻².

4.3.1 MS2 genome damage upon virus inactivation

Genome damage upon treatment by two Fenton-like systems was assessed by qPCR. By determining the intact portion of the genome at different levels of inactivation, several

aspects regarding the mechanism of virus inactivation upon treatment by Fenton-like processes could be addressed. Namely, we could assess 1) whether inactivation by these process lead to genome damage; 2) whether damage is homogeneous across the entire genome or whether selectivity for particular genome regions exists; 3) whether genome damage is sufficiently extensive to account for the entire observed inactivation, and 4) whether genome-based inactivation was by a single-hit or a multi-hit mechanism.

Genome damage was studied using six different amplicons distributed throughout the genome (Figure 4.2). Jointly, they covered the 50% of total genome. The extent of genome damage was assessed at two or three levels of inactivation. The inactivation levels studied were 2 log, 7.5 log and 10 log for Cu/H₂O₂ system and 3 log and 6.5 log for the Fe/H₂O₂/sunlight system.

A measurable decrease in qPCR signal indicative of genome damage was observed at each level of inactivation and in both treatment systems studied. At the lowest level of inactivation (2 log for Cu and 3 log for Fe), a heterogeneous pattern of damage was found in both systems. However, the pattern varied between the two treatments: for the Cu system, the extent of damage varied greatly between the different amplicons. The most affected genome segment was amplicon 2, which is located near the 5'-end of the genome. In the case of Fe, in contrast, damage was more evenly distributed, and amplicons 10 and 12, which are close to 3'-end, were most damaged. This indicates that the terminal segments of the genome were more susceptible to attack by oxidants than segments in the center of the genome.

The difference in the damage pattern between the two systems indicates that, even though inactivation is likely induced by the same oxidants (HO•; [4]), the source of oxidants, i.e., the metal, may influence the physical distribution of damaged sites. This may be due to the fact that under the experimental conditions used, Cu is mainly present in dissolved form, whereas Fe is present as colloids [4]. It can thus be expected that the interactions of the two metals with the genome differ with respect to the accessible genome sites.

At higher levels of inactivation, a more homogeneous pattern of genome damage was obtained in both systems. This may be due to enhanced accessibility of the genome for the metals and oxidants as a result of protein capsid degradation, genome release from the capsid during treatment, or genome denaturation during treatment. Alternatively, the homogeneous pattern may be an experimental artifact induced by the fact that qPCR cannot differentiate between one or multiple hits to the same genome segment. At high levels on inactivation, segments with equal loss in qPCR signal may thus be subject to differing amounts of oxidative lesions.

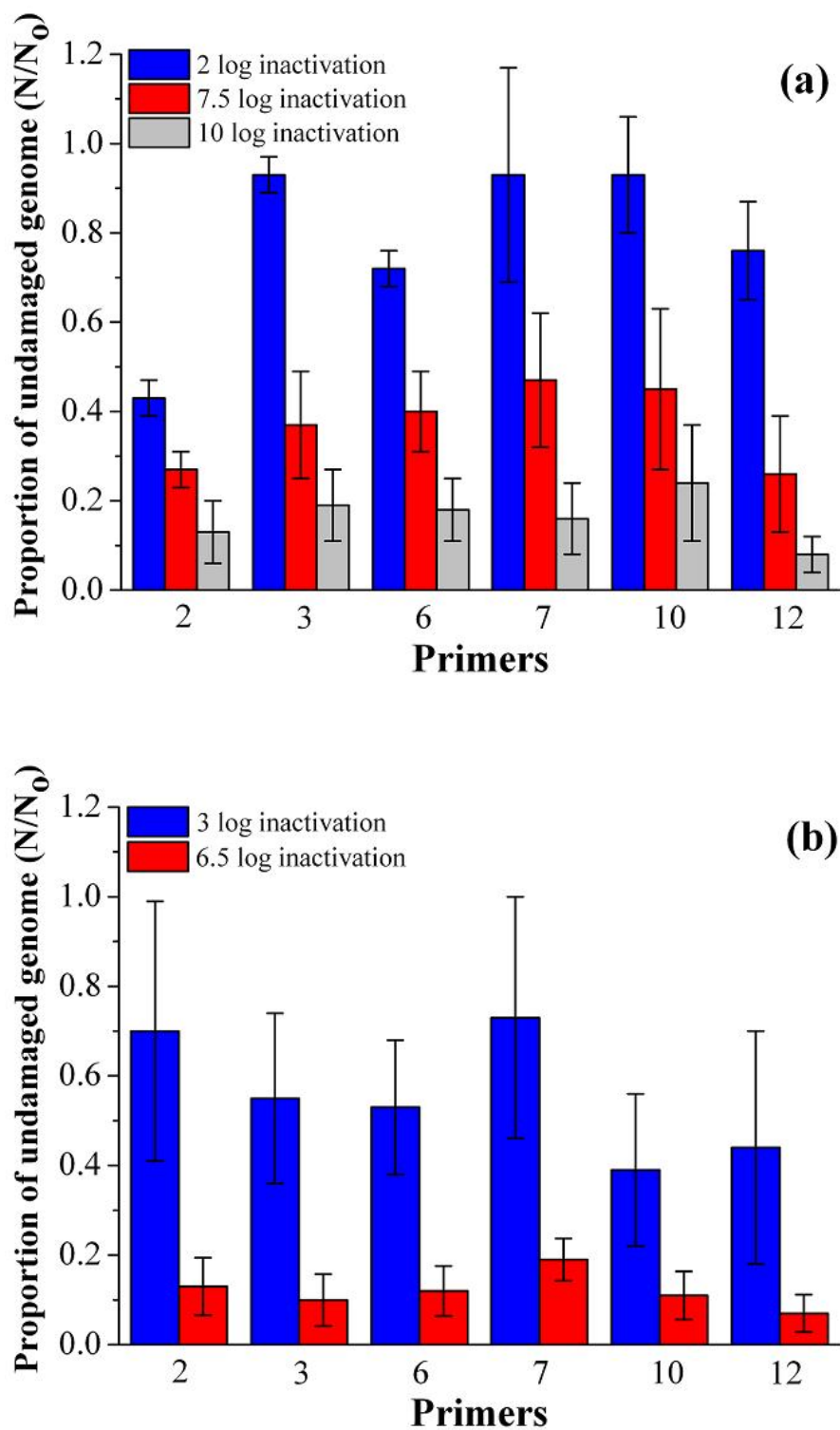
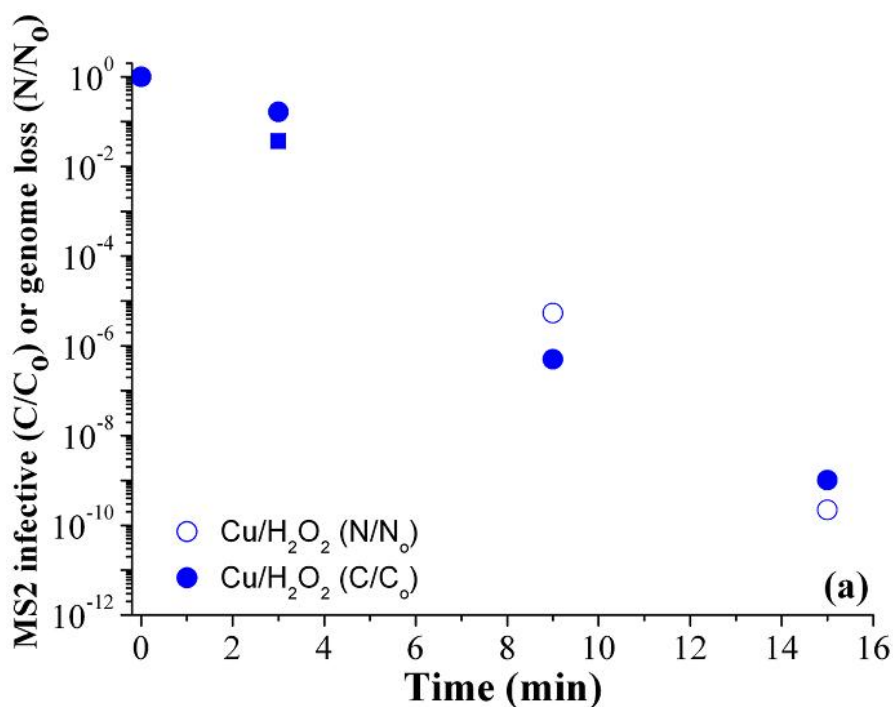


Figure 4.2: Damage to individual MS2 genome segments at different levels of inactivation for (a) Cu/H₂O₂ system and (b) Fe/H₂O₂/sunlight system. Error bars represent the standard deviation of the triplicate samples

To determine if genome damage was sufficient to account for inactivation, the proportions of undamaged genome (N/N_o) measured by qPCR and remaining infectivity (C/C_o) measured by culturing were compared. For the Cu-based system, the extent of genome integrity loss was approximately equal to that of infectivity loss (Figure 4.3a). This is consistent with a single genome lesion being sufficient to inactivate MS2. However, it is unlikely that each oxidative lesion detected by qPCR causes MS2 inactivation. It is conceivable that some oxidative lesions can be over-read by the host during replication, and therefore are of no biological relevance. In fact, several studies have demonstrated that oxidative damage of the genome via one initial radical hit is not sufficient to cause inactivation. Hence tandem and clustered lesions are responsible for genome modifications ([10]; and references therein). Thus, even though a 1:1 ratio between loss of genome integrity and inactivation was found in the Cu system, we can nevertheless assume that genome damage alone was not sufficient to account for the observed inactivation of MS2. Instead, protein damage must play a role.

In contrast, in the Fe-photo-Fenton system, the extent of genome damage was much greater than inactivation (Figure 4.3b). This indicates that if inactivation occurs via genome damage, that the mechanism must be via multi-hit lesions (Figure 4.3b). This is consistent with the statement made above that not all of oxidative damage measurable by qPCR leads to virus inactivation.



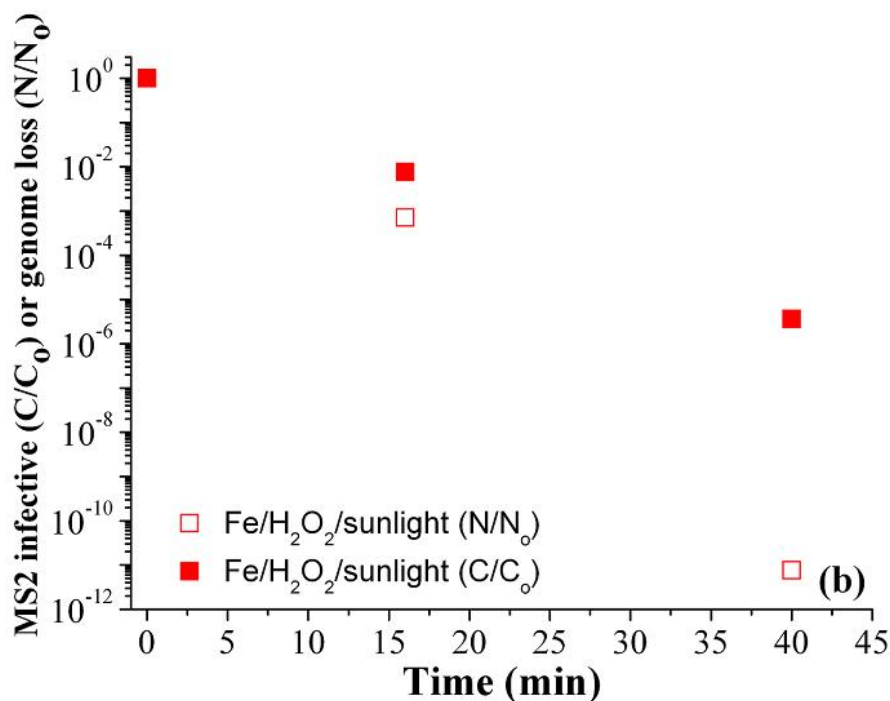


Figure 4.3: Comparison of the fractions of undamaged genome (N/N_0) and infectivity (C/C_0) for (a) Cu/H₂O₂ and (b) Fe/H₂O₂/sunlight systems.

4.3.2 MS2 protein damage upon virus inactivation

The damage of the full MS2 capsid protein and of its individual peptides was studied by protein mass spectrometry (MALDI-TOF-MS). As for genome damage, two and three different levels of inactivation were evaluated for Cu/H₂O₂ and Fe/H₂O₂/sunlight systems, respectively. To determine the extent of MS2 capsid protein damage during inactivation, we evaluated 1) whether the inactivation by these treatments leads to protein damage; 2) which peptide segments are susceptible to damage; 3) whether the location of the damaged peptide in the capsid (surface or inside) influence the extent of damage; and 4) whether the source of oxidants, i.e., Cu or Fe plays a role in the observed damage.

The quantification of damage to the full protein and its individual peptides was assessed by comparing the MS signal of the native MS2 to that of an internal standard. The internal standard was ¹⁵N-labeled MS2, which was added to the samples after the inactivating treatment, but before further processing for mass spectrometric analysis.

Excerpts of the mass spectra of the intact capsid protein of native MS2 and labeled MS2 are shown in Figure 4.4. The full protein $[M+H]^+$ and $[M+2H]^{2+}$ peaks obtained in H₂O₂-free control samples (t=0) were positioned at m/z 13729.8 and 6861.4 respectively for native MS2, and at m/z 13893.6 and 6942.8 respectively for labelled MS2

(Figure 4.4a). In addition, a sodium adduct peak $[M+H+23]^+$ was frequently observed in the mass spectra of the samples (Figure 4.4b).

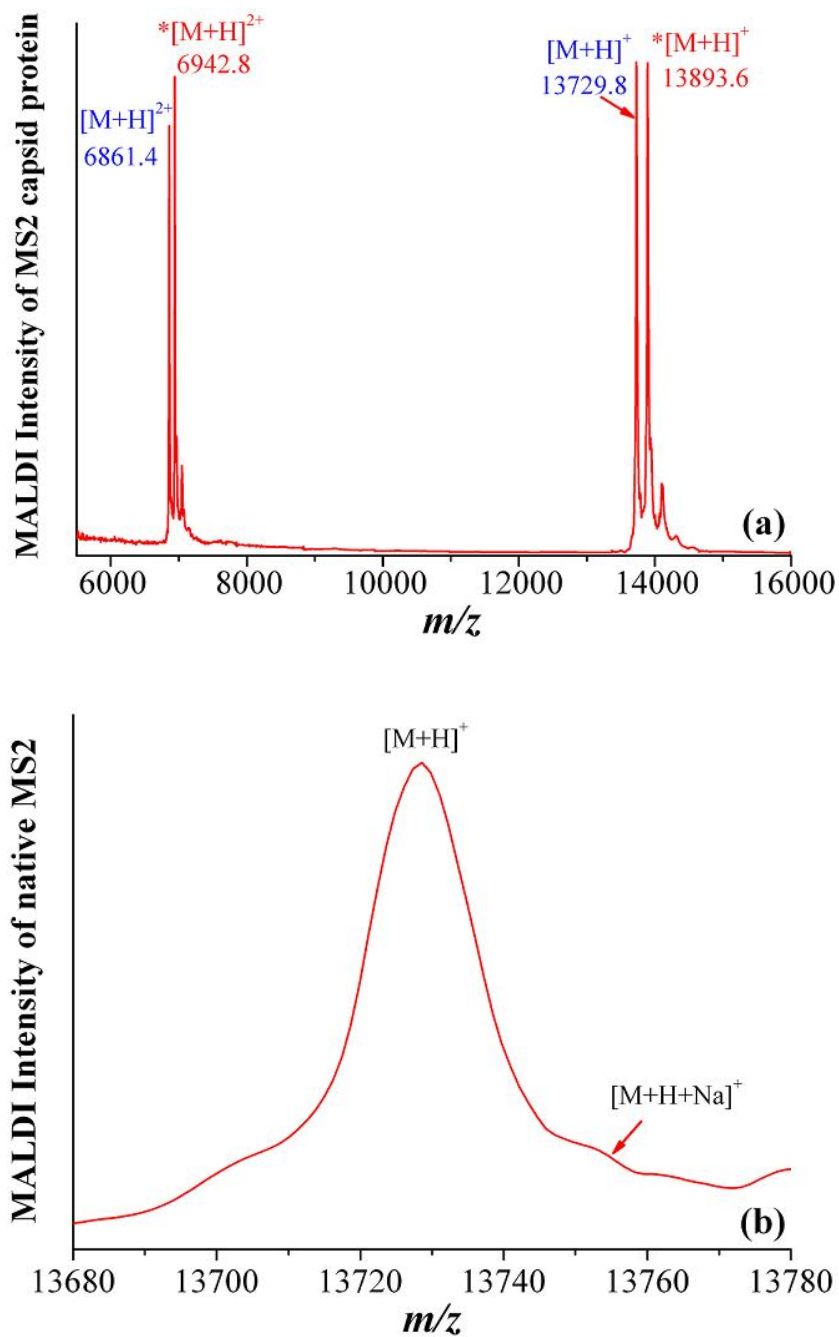


Figure 4.4: (a) Mass spectrum of native MS2 and labeled MS2 of capsid protein (1:1; $t=0$) by positive linear mode MALDI-TOF-MS analysis. (b) Sodium adduct peak.

For both inactivating treatments, some damage to the capsid protein was observed; however, the extent of damage differed slightly between the two inactivating treatments (Figure 4.5). At the lowest level of inactivation, no loss of viral capsid protein was observed for Cu/H₂O₂ system whereas a slight loss of capsid protein was noted for the Fe/H₂O₂/sunlight system. At the highest level of inactivation the overall loss of intact capsid protein was of roughly 10% for both Cu and Fe systems. In the case of Cu system, no further loss of capsid protein occurred when the inactivation increased beyond 7.5 log. This indicates that a large proportion of MS2 capsid protein remained unaffected by these treatments.

To identify the specific region where damage to the capsid protein occurred, individual peptide segments produced during trypsin and chymotrypsin digest were analyzed by MALDI-TOF-MS. As for the genome, the extent of damage differed between the two Fenton-like systems studied. For the Cu system, a prominent feature was that the peptide concentrations at 2 logs of inactivation (blue bars) were consistently higher than the control concentrations. This can be rationalized by considering that the inactivating treatment may loosen or rearrange the capsid structure, thereby allowing the proteolytic enzymes to more efficiently digest the sample than in the control. Furthermore, a slight loss in intact peptide concentration was observed for only a few peptides, whereas most did not exhibit significant decays (Figure 4.5a). The most extensively damaged peptide was found at m/z 2492.41 (84-106 position).

In contrast, for the Fe system, a relatively homogeneous loss of 20% was observed for most peptides. This homogeneity of damage is evidence that OH radicals attack all amino acids to a similar extent due to their non-selectivity [9], and that all regions of the protein were equally accessible to the oxidant. As found in the Cu system, the notable exception was the peptide at m/z 2492.41 (84-106 position), which was again damaged the most extensively (Figure 4.5b). Interestingly, for all other peptides the loss of concentration was very similar for the two levels of inactivation studied (3 log and 6.5 log). A possible explanation for this finding could be the following: as discussed in the previous chapter (chapter 3), a part of the MS2 population can be inactivated by interaction with some iron (hydr-)oxide particles alone [25], possibly due to disintegration of the viral capsid [26–28]. This could explain the greater and more homogeneous accessibility of the oxidant to the protein (as well as the genome, as discussed above) compared to the Cu system. While the Fe colloids did not seem to inactivate the viruses [4], they may nevertheless loosen the capsid of a virus sub-population in the sample, allowing the colloids to access the virus interior and to extensively damage both the protein and the genome. Inactivating treatment leading to 3 logs of inactivation was already sufficient to reach the maximal level of damage of the loosened viruses, and additional inactivating treatment did not cause further damage to the proteins. This hypothesis would, of course, also stipulate that the observed damage to all peptides exhibiting this behavior did not cause inactivation, but was only a concurrent phenomenon.

It should furthermore be noted that in the Fe system, the observed decay of the individual peptides was greater than that of the full protein. The reason for this finding is likely attributable to an experimental artifact, but it is not yet understood.

Besides the different physical properties of the oxidants, Fe and Cu, which are present as dissolved Cu and colloidal Fe [4], the difference in the extent of protein damage between the two treatment systems may be due to the greater production of HO• radicals and additional presence of ferryl species in the Fe system [4]. Furthermore, the more significant protein damage in the Fe system may be due to differences in the interaction of the metals with the amino acids. Several authors have reported protein oxidative degradation by metal-catalyzed oxidation (MCO). For example, Stadtman has studied the damage of amino acids residues catalyzed by metals. They found that Fe(III) or Cu(II) bind to the amino acids, where they were reduced to Fe(II) or Cu(I) at the metal-binding sites. Then, they reacted with hydrogen peroxide to yield OH radicals and finally oxidized the amino acids of proteins [29–31].

The higher susceptibility of segments 84-106 in both treatment systems may be due to the location of this segment within the capsid, i.e., whether it is located on the solvent-accessible outside or a less accessible part of viral capsid protein. MS2 crystal structures of the capsid protein indicate that residues Tyr85, Met88, Ser99, Cys101 and Lys106 are located on the outer surface of the viral capsid [32, 33]. A large fraction of the susceptible segment is thus exposed to solvent. However, other portions of the capsid which are also solvent exposed (e.g., residues Ile60, Tyr71; ref. [27, 28]) were not degraded. This indicates that the composition of the segment also plays a role in its propensity to degrade. This is in agreement with previous work which has shown that both the location of a segment and its amino acids composition govern its susceptibility to oxidation [19]. In particular, the sulfur-containing residues methionine and cysteine have been demonstrated to be the most affected to the degradation by Fenton-like treatments [30, 34]; they are known to bind metal species well, and to form of oxidants [35]. Segment 84-106 contains both a methionine (Met88) and a cysteine (Cys101), which may account for its propensity to degrade.

As observed in previous work, the other sulfur-containing residues (e.g., Cys46 in segment 44-49), which are not exposed to the solvent, were less susceptible to degradation. Our findings thus confirm that easily oxidizable amino acids residues located on the outer surface of the capsid are most susceptible to oxidation. This indicated that residues on the capsid surface may play a more important role in inactivation than residues located on the inside.

The identity of the peptide segments and amino acid residues oxidized is likely to change with different disinfectants. Previous investigations studying viral protein damage reported that the most susceptible amino acids toward free chlorine and ozone were Lys,

Arg, Pro [14], and Trp, and Tyr [13], respectively. The findings from the Fenton-like systems may thus not be directly transferable to other disinfecting systems.

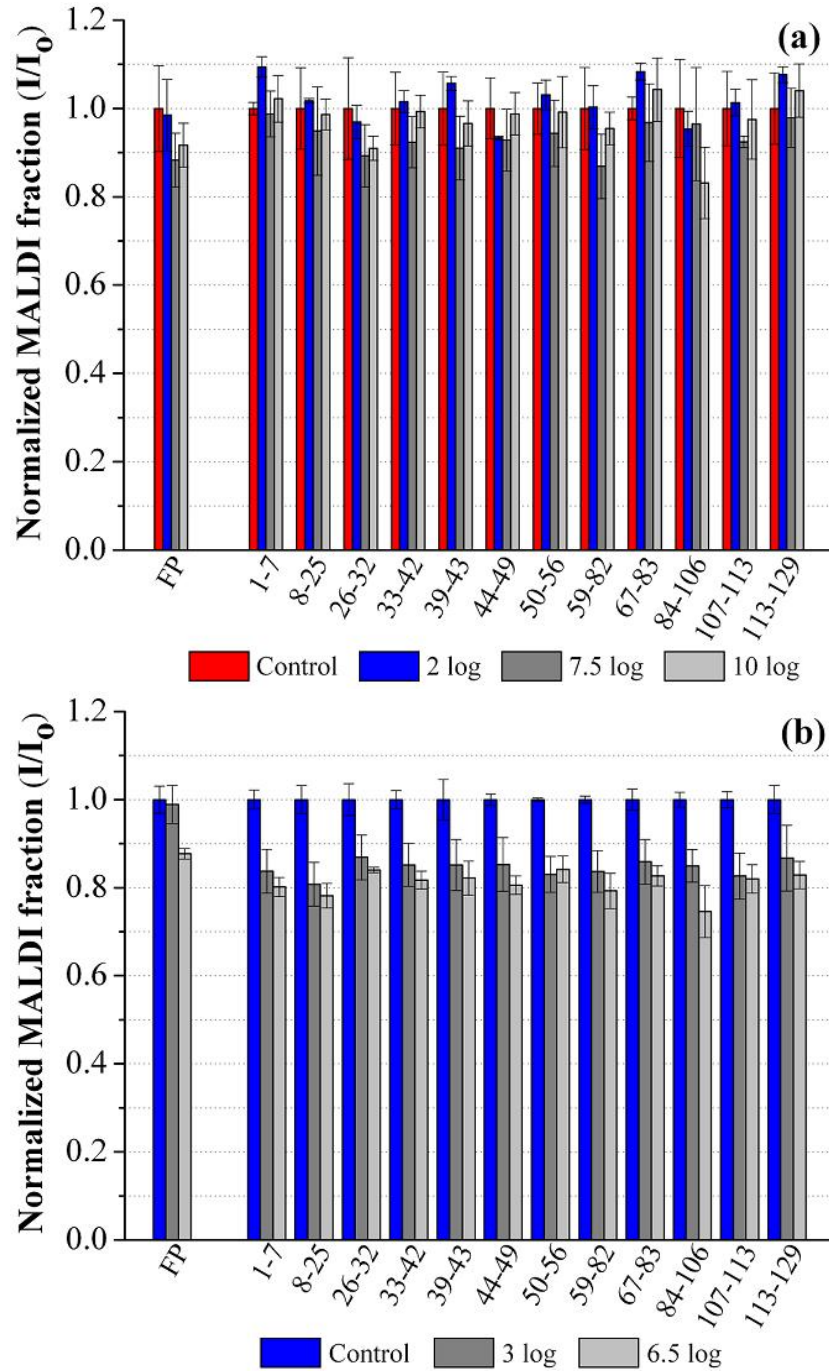


Figure 4.5: Analysis of MS2 capsid protein damage in the full protein (FP) and peptides for (a) the Cu/H₂O₂ system and (b) the Fe/H₂O₂/sunlight system. Error bars represent the standard deviation of triplicate samples.

4.4 Conclusions

In summary, the nature of virus damage upon MS2 inactivation by (photo-) Fenton-like processes, may involve both genome and protein damage. Differences between the Fe-based and the Cu-based systems were observed, even though the same oxidant ($\cdot\text{OH}$) was present in both processes, indicating the source of metal is important.

For the Cu system, the main inactivation mechanism involves genome damage only if each qPCR-measured lesion actually is sufficient to inactivate virus. If that is not the case, then protein damage must play a role. Our previous results (chapter 2) have shown that Cu ions were adsorbed on the viral capsid protein by aFIFFF-ICP-MS [4], indicating inactivation may occur via capsid damage. Mainly, segment 84-106 may be involved, as it was the most susceptible to degradation. Furthermore, denaturing or unfolding of the proteins without chemical reaction may contribute to inactivation in the Cu system.

For the Fe system, the damage of genome and of capsid protein was more homogeneous and intensive than in the Cu system. This indicates that the oxidants had better accessibility to the protein and the genome than in the Cu system. Furthermore, genome damage was very extensive in comparison to inactivation. This signifies that genome damage may cause inactivation by a multi-hit mechanism. In contrast, most peptides are unlikely to be involved in inactivation, as their decay did not show much difference between 3 log and 6.5 log of inactivation. As for Cu, the only exception is segment 84-106, which degraded proportionally to inactivation, and may thus be involved in inactivation. In addition, in our previous studies we reported that association of MS2 with Fe particles cause mild virus inactivation [25]. Capsid loosening or disruption by Fe colloids may thus have assisted in MS2 inactivation. In this case, not only Fenton process would cause the inactivation, an additional contribution may be involved via the Fe colloids.

Further studies must be conducted to obtain a better and more complete understanding of the nature of virus damage incurred during inactivation in Fenton-like systems. For example, damage to the A protein, which was not considered herein, should be quantified and taken into account. Experiments with cysteine and methionine-deficient mutants may allow verifying the importance of protein oxidation in the inactivation process. In addition, it should be investigated how the observed damage influences the individual steps in the lytic life cycle of viruses; it may inhibit the adsorption (attachment to the host), penetration (injection of genome) and genome replication processes should be considered as well. Finally, a comparison of damage incurred by the Fenton-like processes and other disinfectants may aid in understanding the efficiency of different disinfectants in virus inactivation.

Bibliography

- [1] J. Simonet and C. Gantzer. Inactivation of poliovirus 1 and F-specific RNA phages and degradation of their genomes by UV irradiation at 254 nanometers. *Applied and Environmental Microbiology*, 72(12):7671–7677, 2006.
- [2] J. Koivunen and H. Heinonen-Tanski. Inactivation of enteric microorganisms with chemical disinfectants, UV irradiation and combined chemical/UV treatments. *Water Research*, 39(8):1519–1526, 2005.
- [3] M. Cho, H. M. Chung, W. Y. Choi, and J. Y. Yoon. Different inactivation behaviors of MS2 phage and escherichia coli in TiO₂ photocatalytic disinfection. *Applied and Environmental Microbiology*, 71(1):270–275, 2005.
- [4] J. I. Nieto-Juarez, K. Pierzchała, A. Sienkiewicz, and T. Kohn. Inactivation of MS2 coliphage in Fenton and Fenton-like systems: role of transition metals, hydrogen peroxide and sunlight. *Environmental Science and Technology*, 44(9):3351–3356, 2010.
- [5] M. J. Davies. The oxidative environment and protein damage. *Biochimica Et Biophysica Acta: Proteins and Proteomics*, 1703(2):93–109, 2005.
- [6] Z. Jurasekova, A. Tinti, and A. Torreggiani. Use of Raman spectroscopy for the identification of radical-mediated damages in human serum albumin. *Analytical and Bioanalytical Chemistry*, 400(9):2921–2931, 2011.
- [7] M. J. Davies and R. J. W. Truscott. Photo-oxidation of proteins and its role in cataractogenesis. *Journal of Photochemistry and Photobiology B-Biology*, 63(1-3):114–125, 2001.
- [8] M. J. Davies. Reactive species formed on proteins exposed to singlet oxygen. *Photochemical and Photobiological Sciences*, 3(1):17–25, 2004.
- [9] K. J. A. Davies, M. E. Delsignore, and S. W. Lin. Protein damage and degradation by oxygen radicals. 2. modification of amino-acids. *Journal of Biological Chemistry*, 262(20):9902–9907, 1987.
- [10] J. Cadet, T. Douki, and J. L. Ravanat. Oxidatively generated damage to DNA and biomarkers. In S. Basu and L. Wiklund, editors, *Studies on Experimental Models. Oxidative Stress in Applied Basic Research and Clinical Practice*, chapter Part VI. In Vitro/Tissue Culture, pages 579–604. Springer Science+Business Media, 2011.
- [11] G. R. Martinez, D. Gasparutto, J. L. Ravanat, J. Cadet, M. H. G. Medeiros, and P. Di Mascio. Identification of the main oxidation products of 8-methoxy-2'-deoxyguanosine by singlet molecular oxygen. *Free Radical Biology and Medicine*, 38(11):1491–1500, 2005.

-
- [12] J. R. Wagner and J. Cadet. Oxidation reactions of cytosine DNA components by hydroxyl radical and one-electron oxidants in aerated aqueous solutions. *Accounts of Chemical Research*, 43(4):564–571, 2010.
- [13] N. Shinriki, K. Ishizaki, T. Yoshizaki, K. Miura, and T. Ueda. Mechanism of inactivation of Tobacco mosaic-virus with ozone. *Water Research*, 22(7):933–938, 1988.
- [14] Daisuke Sano, Rosa M. Pinto, Tatsuo Omura, and Albert Bosch. Detection of oxidative damages on viral capsid protein for evaluating structural integrity and infectivity of human Norovirus. *Environmental Science and Technology*, 44(2):808–812, 2010.
- [15] J. W. Li, Z. T. Xin, X. W. Wang, J. L. Zheng, and F. H. Chao. Mechanisms of inactivation of hepatitis A virus by chlorine. *Applied and Environmental Microbiology*, 68(10):4951–4955, 2002.
- [16] C. K. Kim, D. M. Gentile, and O. J. Sproul. Mechanism of ozone inactivation of bacteriophage F-2. *Applied and Environmental Microbiology*, 39(1):210–218, 1980.
- [17] S. Lee, M. Nakamura, and S. Ohgaki. Inactivation of phage Q beta by 254nm UV light and titanium dioxide photocatalyst. *Journal of Environmental Science and Health Part a: Toxic/Hazardous Substances and Environmental Engineering*, 33(8):1643–1655, 1998.
- [18] N. Kashige, Y. Kakita, Y. Nakashima, F. Miake, and K. Watanabe. Mechanism of the photocatalytic inactivation of lactobacillus casei phage PL-1 by titania thin film. *Current Microbiology*, 42(3):184–189, 2001.
- [19] K. R. Wigginton, L. Menin, J. P. Montoya, and T. Kohn. Oxidation of virus proteins during UV(254) and singlet oxygen mediated inactivation. *Environmental Science and Technology*, 44(14):5437–5443, 2010.
- [20] B. M. Pecson, L. V. Martin, and T. Kohn. Quantitative PCR for determining the infectivity of bacteriophage MS2 upon inactivation by heat, UV-B radiation, and singlet oxygen: Advantages and limitations of an enzymatic treatment to reduce false-positive results. *Applied and Environmental Microbiology*, 75(17):5544–5554, 2009.
- [21] Ernest M. Hotze, Appala Raju Badireddy, Shankararaman Chellam, and Mark R. Wiesner. Mechanisms of bacteriophage inactivation via singlet oxygen generation in UV illuminated fullerol suspensions. *Environmental Science and Technology*, 43(17):6639–6645, 2009.
- [22] B. M. Pecson, M. Ackermann, and T. Kohn. Framework for using quantitative PCR as a nonculture based method to estimate virus infectivity. *Environmental Science and Technology*, 45(6):2257–2263, 2011.

-
- [23] J. Y. Kim, C. Lee, D. C. Love, D. L. Sedlak, J. Yoon, and K. L. Nelson. Inactivation of MS2 coliphage by ferrous ion and zero-valent iron nanoparticles. *Environmental Science and Technology*, 45(16):6978–6984, 2011.
- [24] F. X. Abad, R. M. Pinto, J. M. Diez, and A. Bosch. Disinfection of human enteric viruses in water by copper and silver in combination with low-levels of chlorine. *Applied and Environmental Microbiology*, 60(7):2377–2383, 1994.
- [25] J.I. Nieto-Juarez and T. Kohn. Virus removal and inactivation by heterogeneous Fenton-like processes under sunlight and in the dark. Submitted, 2012.
- [26] J. P. Murray and S. J. Laband. Degradation of Poliovirus by adsorption on inorganic surfaces. *Applied and Environmental Microbiology*, 37(3):480–486, 1979.
- [27] J. N. Ryan, R. W. Harvey, D. Metge, M. Elimelech, T. Navigato, and A. P. Pieper. Field and laboratory investigations of inactivation of viruses (PRD1 and MS2) attached to iron oxide-coated quartz sand. *Environmental Science and Technology*, 36(11):2403–2413, 2002.
- [28] R. W. Harvey and J. N. Ryan. Use of PRDI bacteriophage in groundwater viral transport, inactivation, and attachment studies. *Fems Microbiology Ecology*, 49(1):3–16, 2004.
- [29] E. R. Stadtman. Metal ion-catalyzed oxidation of proteins - biochemical-mechanism and biological consequences. *Free Radical Biology and Medicine*, 9(4):315–325, 1990.
- [30] E. R. Stadtman and R. L. Levine. Free radical-mediated oxidation of free amino acids and amino acid residues in proteins. *Amino Acids*, 25(3-4):207–218, 2003.
- [31] E. R. Stadtman. Oxidation of free amino-acids and amino-acid-residues in proteins by radiolysis and by metal-catalyzed reactions. *Annual Review of Biochemistry*, 62:797–821, 1993.
- [32] K. Valegard, L. Liljas, K. Fridborg, and T. Unge. The 3-dimensional structure of the bacterial-virus MS2. *Nature*, 345(6270):36–41, 1990.
- [33] L. Liljas, K. Fridborg, K. Valegard, M. Bundule, and P. Pumpens. Crystal-structure of bacteriophage-FR capsids at 3.5-angstrom resolution. *Journal of Molecular Biology*, 244(3):279–290, 1994.
- [34] B. S. Berlett and E. R. Stadtman. Protein oxidation in aging, disease, and oxidative stress. *Journal of Biological Chemistry*, 272(33):20313–20316, 1997.
- [35] D. R. Dufield, G. S. Wilson, R. S. Glass, and C. Schoneich. Selective site-specific Fenton oxidation of methionine in model peptides: Evidence for a metal-bound oxidant. *Journal of Pharmaceutical Sciences*, 93(5):1122–1130, 2004.

Chapter 5

General conclusions and perspectives

Our results demonstrate that the homogeneous and heterogeneous Fenton-like processes may serve as an efficient alternative of disinfection for waterborne viruses in both natural and engineered systems. Human enteric virus can likely be inactivated by the processes studied if their morphological structures are similar to that of MS2, though this aspect remains to be experimentally confirmed.

In the case of the homogeneous Fenton system, MS2 inactivation by Cu- and Fe-catalyzed (photo-) Fenton-like reaction has been shown. Both metal ions induce considerable inactivation at low H_2O_2 and metal concentrations. Virus inactivation occurred mainly via the production of HO^\bullet radicals and either dissolved Cu in the dark or via colloidal Fe under sunlight. In the dark, ferryl species, FeO^{2+} , were the main inactivating species. Sunlight greatly enhanced virus inactivation for the Fe-catalyzed Fenton system, but not for the Cu system.

In the heterogeneous Fenton system, it has been demonstrated that MS2 adsorption onto particles slightly contributed to the inactivation for all particles with exception of hematite. Only magnetite yielded virus inactivation by dark Fenton-like process. Sunlight significantly enhanced virus inactivation for all particles containing Fe(III)-iron (hydr-)oxides. The most effective particle for MS2 inactivation was amorphous Fe(III) hydroxide, with respect to the contributions of adsorption alone and the photo-Fenton-like reaction. It remains unclear, however, how particle aging will affect reactivity toward MS2.

The nature of MS2 inactivation included both damage to the genome and the capsid protein by both Cu/ H_2O_2 and Fe/ H_2O_2 /sunlight systems. The source of metals (Fe(III)

or Cu(II)) played a role important in the virus inactivation. For Fe system the damage was more homogeneous and intensive than for the Cu system. The genome damage was via single hit and multi-hit for Cu and Fe systems, respectively. The terminal segments of the genome were most susceptible to the inactivation than that in the centre of the genome in both systems. In the capsid protein, the oxidation of amino acids Met88, Ser99, Cys101 and Lys106 on the capsid protein may contribute to inactivation in both systems as well. The composition and location of the amino acids on the MS2 capsid protein played an important role in the susceptibility of the protein to oxidation. Establishing a direct causation between the observed damage and inactivation, however, remains a challenge that needs to be addressed in future work.

Perspectives

In this work, only laboratory solutions were used to characterize MS2 inactivation by Fenton-like processes. Further studies must be conducted to completely assess the effectiveness of these AOPs, homogeneous and heterogeneous Fenton, as disinfection methods in actual natural and engineered treatment systems. In this context, the following questions should be addressed:

- What is the influence of natural organic matter (NOM) on inactivation by these Fenton-like processes?
- What is the effectiveness of commercial iron particles to cause virus inactivation over longer exposure times?
- What are the factors governing inactivation on particles-adsorbed viruses?
- How does inactivation depend on 1) the nature of iron particles, 2) time of exposure and 3) concentration of iron particles?
- How the sunlight affect on inactivation of particles-absorbed viruses?
- What would be the influence of particle size on the inactivation by heterogeneous Fenton process, to find the most efficient particle?
- What are the inactivation kinetics for other coliphages and pathogens by these processes?
- After treatment, can inactivated virus undergo re-growth?

In order to better understand the molecular mechanisms involved in virus inactivation by these processes, additional studies must be explored such as:

- Does A protein damage contribute to the inactivation?
- Which is the importance of metal-binding sites of Cu and Fe on the inactivation?
- Does the inactivation produce changes on the lytic life cycle of viruses?
- Can the findings for MS2 be generalized for other viruses?
- How do the findings for the Fenton-like processes relate to inactivation by other disinfectants?

Finally, a socio-economic evaluation for the sustainable application of these processes as a disinfection method in developing and industrialized countries must be conducted. The following questions should be focused:

- What is the economic feasibility of using Fenton-like processes as a disinfection method?
- What is the efficiency of Fenton-like processes in comparison with that of conventional disinfection methods?
- How would treatment plant have to be designed to incorporate a Fenton-type system in the dark and under sunlight?
- What maintenance services are necessary in order to maintain an efficient inactivation by these processes over longer times of handling?
- Are these materials needed for disinfection treatments easily accessible in developing countries?
- If inactivated virus undergoes re-growth, what are the necessary additional doses of residual-forming disinfectants such as chlorine after treatment by these Fenton-based processes?

Jessica Ivana NIETO JUAREZ, PhD

Chemin Auguste-Pidou 14

1007 Lausanne

Switzerland

+41 78 952 81 31

jecanj@gmail.com



1. EDUCATION

Ecole Polytechnique Fédérale de Lausanne (EPFL)
Lausanne, Switzerland, 2012

PhD of Science, Program in Environment
Laboratory of Environmental Chemistry
Thesis: "Virus inactivation by
homogeneous and heterogeneous
Fenton-like processes"
Advisor: Prof. Dr. Tamar Kohn

Concepción University (UDEC)
Concepción,, Chile, 2007

MSc of Science, Chemistry
Department of Organic Chemistry
Thesis: "Application of solar photo-
catalysis on the degradation of
antibiotics"
Advisor: Prof. Dr. Hector D. Mansilla

Environmental Sciences International Center (EULA)
Concepción, Chile, 2004

Diploma, Environmental Analysis and
Management: Environmental Impact
Study (EIS)

Engineering National University (UNI)
Lima, Peru, 2003

Diploma of Science, Chemistry
Thesis: "Elimination of organic matter in
the unhairing effluents treated by
combined biological and oxidative
system" (Thesis was done at EULA, Chile)
Advisor: Prof. Dr. Gladys Vidal

Valencia University
Valencia, Spain, 2000

Exchange student
Department of Environmental
Technology

2. PUBLICATIONS

- Nieto J.I. and Kohn T. Protein and genome damage in MS2 coliphage upon inactivation by Fenton-like systems. *In preparation*.
- Nieto J.I. and Kohn T. MS2 removal and inactivation by heterogeneous Fenton-like processes in the dark and under sunlight. *Submitted, 2012*.
- Nieto J.I., Pierzchala K., Sienkiewicz and Kohn T. Inactivation of MS2 coliphage in Fenton and Fenton-like systems: role of transition metals, hydrogen peroxide and sunlight. *Environmental Science and Technology*, 2010, 44: 3351-3356.

3. CONFERENCES

- Nieto-Juarez J.I. and Kohn T. *Virus inactivation by heterogeneous Fenton-like systems*. Presented at the 242nd ACS National Meeting, Division of Environmental Chemistry, Denver, Colorado, USA, August 28-September 01, 2011.
- Nieto-Juarez J.I. and Kohn T. *Effect of sunlight on MS2 inactivation by iron oxides and hydrogen peroxide*. Presented at the 8th IWA Leading-Edge Conference on Water and Wastewater Technologies, Amsterdam, The Netherlands, June 6-10, 2011.
- Nieto-Juarez J.I. and Kohn T. *Virus in natural waters: How to kill them?* Presented at the Journée de la Recherche ENAC, Lausanne, Switzerland, 9th June, 2010.
- Nieto-Juarez J.I. and Kohn T. *Inactivation of phage MS2 by Fenton-like system in the dark and under sunlight*. Presented at the Green days in Environmental Engineering Institute (IEE), Arolla, Switzerland, September 3-4, 2009.
- Nieto-Juarez J.I. and Kohn T. *Inactivation of MS2 by homogeneous Fenton- and Fenton-like systems: mechanistic insights*. Presented at the Meeting of the Association of Environmental Engineering and Science Professors (AEESP), Iowa, USA, July 26-29, 2009
- Kohn T. Nieto-Juarez J.I., Wigginton K.R. and Pecson B.M. *Disinfection mechanisms of viruses in water: mechanistic insight into the impact of reactive oxygen species on viral constituents*. Presented at the 15th IWA International Symposium on Health-related Water Microbiology, Naxos, Greece, May 31-June 5, 2009.
- Kohn T., Nieto-Juarez J.I. and Paz-Montoya J. *Susceptibility of different viruses to inactivation by ROS*. Presented at the Gordon Research Conference on Environmental Sciences: Water, Plymouth, USA, June 22-27, 2008.

4. PROJECTS, SCHOLARSHIP AND AWARDS

- Award of best Poster, 8th IWA Leading-Edge Conference on water and wastewater technologies, Amsterdam, The Netherlands (6-10 June 2011)
- Research assistant, doctoral project was supported by the Swiss National Science Foundation, Project N° 200021_118077 and 200020_131918, Lausanne, Switzerland (Oct 2007-Mar 2012)
- Swiss Confederation Scholarship, Research stay, Group of Electrochemical Engineering, Institute of Chemical Sciences and Engineering, EPFL (Oct 2006-Sept 2007)
- Swiss Confederation Scholarship, French language training in Fribourg (Jul 2006-Aug 2006)
- Concepcion University Scholarship, graduate research of Master (Apr 2004-Jun 2006)
- Research stay was supported by the European Project: "Reduction of environmental impacts of leather tanneries (EILT)", INCO-DC N° ERB IC18-CT98-0286, Concepcion, Chile (Oct 2000-Mar 2002)
- AECl scholarship, exchange student in the Valencia university, department of Environmental Technology, Valencia, Spain (Jan 2000-Mar 2000)

5. ADDITIONAL INFORMATION

Nationality:	Peruvian
Languages:	Fluent in Spanish (mother language) English and French (highly proficient) German (basic)
Computer skills:	Word, Excel, PowerPoint, Latex, Origin, KaleidaGraph, basics of PHREEQC, Matlab
Professional Affiliations:	American Chemical Society (ACS) International Water Association (IWA)
Spare-time activities:	Sports (swimming, cycling, hiking, fitness), cooking, photographing and traveling.